Scuola Normale Superiore

Sterile Neutrinos in 4D and 5D in Supernovæ and the Cosmo

Marco Cirelli

Advisors

Dr. Andrea Romanino
Prof. Riccardo Barbieri

Ph.D. Thesis

Autumn 2003

A Anna

Contents

Preface **iii**

Rationale **1**

1 Introduction: New Particle Physics from Astrophysics and Cosmology **3**
1.1 The Standard Model and why to go beyond . . . 3
1.1.1 The Hierarchy Problem . . . 5
1.1.2 Introduction to Extra Dimensions . . . 7
1.2 "Standard" neutrino physics and why to go beyond . . . 11
1.2.1 "What is left, what is next?" . . . 13
1.2.2 Sterile neutrinos . . . 15
1.3 The role of Supernovæ . . . 18
1.3.1 Supernova basics and neutrino signal formation . . . 18
1.3.2 The energy loss constraint . . . 21
1.3.3 Waiting for the next supernova . . . 23
1.4 The role of the Early Universe . . . 27
1.4.1 Big Bang Nucleosynthesis . . . 27
1.4.2 Large Scale Structure and Cosmic Microwave Background . . . 35

2 A (4D) sterile neutrino **38**
2.1 Active-sterile neutrino mixing formalism . . . 38
2.2 Sterile effects in cosmology . . . 41
2.2.1 Technical details . . . 41
2.2.2 Results . . . 45
2.3 Sterile effects in Supernovæ . . . 48
2.3.1 Technical details . . . 50
2.3.2 Results . . . 54

3 Neutrinos in Extra Dimensions **56**
3.1 The extra dimensional setup . . . 57
3.2 Cosmological safety (or irrelevance) . . . 58

3.3 Supernova core evolution 58
3.3.1 The feedback mechanisms 59
3.3.2 Details of the model of core evolution 60
3.4 The outcome: bounds and signals 70
3.5 Appendix: subleading invisible channels 76

4 Conclusions **77**

References **79**

Preface

During my Ph.D. course, under the guidance of Riccardo Barbieri and Andrea Romanino, I began working on fascinating subjects at the intersection of High Energy Physics, Neutrino Physics, Astrophysics and Cosmology. I partecipated in several collaborations which led to a number of published papers. In this Thesis, I present a extended collection of the work and the results which focus on sterile neutrinos, both in the form of a conventional 4D extra state and in the form of an infinite tower of additional states motivated by Extra Dimensions. With Guido Marandella, Alessandro Strumia and Francesco Vissani in [1], we completed a thorough analysis of the (4D) sterile neutrino effects in solar, reactor, atmospheric and short-/long-base line experiments, as well as in Supernovæ and in the Early Universe. The last two topics are included in this Thesis. Previously, with Giacomo Cacciapaglia, Lin Yin and Andrea Romanino [2] we revisited the bounds on neutrinos in Extra Dimensions set by Supernovæ and by Cosmology. In [3], we extended the study to include the mixing with extra dimensional fields of all neutrino flavors and we addressed the interesting modified supernova phenomenology.

Besides these works, during my Ph.D. course I studied further issues connected with extra dimensional field theories. In [4] and [5], in collaboration with Giacomo Cacciapaglia and Giampaolo Cristadoro, I computed two relevant observables in the framework of the theory proposed by R. Barbieri, L. Hall and Y. Nomura, an extension of the Standard Model to five dimensions endowed with a supersymmetric structure. In [4] we found that the production rate of the Higgs boson via gluon fusion (which is the main channel at a hadron collider) is significantly suppressed, due to cancellations among the additional (Kaluza-Klein) states of the theory. In [5] we showed that the theory is compatible with the precision measurements of muon anomalous magnetic moment, by explicitly computing all the relevant additional contributions to such a quantity and finding them small.

Thanks

My Ph.D. years in Pisa would have been useless without the direction and the support of Riccardo Barbieri, Andrea Romanino and Alessandro Strumia.
My Ph.D. years would have been much more difficult without the help and cooperation of Giacomo Cacciapaglia, Giampaolo Cristadoro, Lin Yin, Guido Marandella and Francesco Vissani.
My Ph.D. years would have been much less interesting and enjoyable without the presence of Andrea Gambacci, Pasquale Calabrese, Roberto Contino, Paolo Creminelli, Simone Gennai, Andrea Giammanco, Alberto Nicolis, Giuseppe Policastro, Giovanni Signorelli, Andrea Sportiello, Fabio Toninelli and many others, in the lively and stimulating atmosphere of Scuola Normale.

All these persons I really, really thank.

Rationale

We live in a peculiar epoch of Elementary Particle Physics: on one hand we have a theory (the Standard Model of strong and electroweak interactions) that works astonishingly well, being able to agree with data at an unprecedented level of accuracy. On the other hand, we know it cannot be the whole story, given the well known unsatisfying arbitrariness built in it and its incomplete description of the fundamental interactions. This notorious fact has given the way to a number of "Beyond the SM" constructions (SuperSymmetry, Technicolor, Grand Unification and, recently, Extra space Dimensions and Little Higgs theories) that still wait for confirmation or disproof. On the experimental side, a very successful era of precision experiments (mainly at Lep and the Tevatron) has almost come to an end, leaving us with no serious surprise or hint of discrepancy, while the next step (the LHC above all) still belongs to the future (fortunately: next and concrete).

Something vaguely similar is going on in the restricted realm of Neutrino Physics: in the latest years, experiment after experiment, every piece of evidence is finding its place in a beautiful picture, but several fundamental questions are still open. While the present generation of incredibly successful underground, reactor and accelerator experiments is almost over, the next generation (LBL, mega-ton detectors, neutrino factories...) is still at the level of development or even of imagination.

How to overcome, then, the theoretical impasse and the experimental await? One of the possible answers is: turning one's eyes to the stars and the cosmo.

Although, of course, less under control than table-top or accelerator experiments, stars (core-collapse Supernovæ in particular) and the Early Universe (whose image is imprinted in the deep space that we observe today) are powerful laboratories for particle physics, and often come with features that make them complementary or even more useful than the traditional means of probing the microscopic world.

The subject of this thesis fits in such a picture: focussing on the issue of the possible existence of sterile neutrinos, I discuss the constraints and the possible signals of their presence that come from the physics of Supernovæ and of the Early Universe.

In the first Chapter I substantiate the link between the search for New Physics and the use of supernovæ and cosmological processes. This Chapter has the character of an introductory general overview, which consists of four parts: The Standard Model and why to go beyond, "Standard" neutrino physics and why to go beyond, The role of Supernovæ, The role of the Early Universe. Each of these parts can be essentially read in an independent way from the others (or even skipped by the learned reader). The specific work of this thesis builds up on this general background and knowledge, to which I will occasionally refer in the subsequent Chapters.

In the second Chapter, based on ref.[1], I focus on the case of a single (4D) sterile neutrino. After the

presentation of the adopted four neutrino formalism, I describe the derivation of bounds and signals on its mixing parameters with the active neutrinos, considering BBN, LSS, CMB and supernovæ. Including the consolidated mixing of active neutrinos among themselves in all these contexts can lead to outputs quite different from those in the literature and to new features. As a result, I present plots of the combined excluded regions in the space of the mixing parameters.

In the third Chapter, based on refs.[2, 3], I move to the case of an infinite tower of sterile neutrinos motivated by Extra Dimensions. After the description of the 5D setup, I discuss the model of modified evolution developed for the SN inner core, first qualitatively and then in detail. I show that a careful study of the SN physics can allow a relaxation of the previous bounds in the literature by several orders of magnitude, giving also rise to an interesting modified phenomenology. For the three cases of electron, muon and tau neutrinos mixed with the extra dimensional states, I present the possible signatures of extra dimensional states in the neutrino signal from the next SN.

Chapter 1

Introduction: New Particle Physics from Astrophysics and Cosmology

1.1 The Standard Model and why to go beyond

Any honest discussion on possible extensions of the Standard Model [6] cannot evade to start from the fact that the Standard Model is a very successful theory. Besides the well known conceptual achievements (the union of three forces under the spell of the gauge invariance principle, the prediction of neutral current interactions and of the properties of the weak bosons, the thrifty introduction of CP violation...), the focus is rather on the overall agreement between the Theory and the vast set of experimental data coming from electron–positron annihilations, hadronic collisions and neutrino interactions, often measured at an accuracy level better than one part per mille. The present status of this good agreement [1,2] is well captured and depicted in fig.1.1.

The most important message of these ElectroWeak Precision Tests (EWPT) concernes possible physics beyond the Standard Model: only very delicate deviations from the SM predictions are allowed. This is a very strong constraint on theorist's imagination. However, the technical and conceptual flaws of the Standard Model have been the spurring force for particle physics of the last decades (and theorists' imagination has proved to be not too much curbed).

A short list of unsatisfactory features and drawbacks of the Standard Model should include at least the following:

1. too much arbitrariness,
2. no masses for neutrinos, and no description of neutrino oscillations,
3. incomplete unification of known forces, gravity being not included.

1. Even if one accepts the rather odd set of group representations and hypercharges, the Standard Model contains at least 18 free parameters (3 gauge couplings, 6 quark masses and 3 lepton masses, 4

[1] See however [8] (for instance) for recent comments on some of the few open discrepancies.

[2] The persisting mild discrepancy between SM prediction and experimental value of muon anomalous magnetic moment should also be mentioned in this context [9].

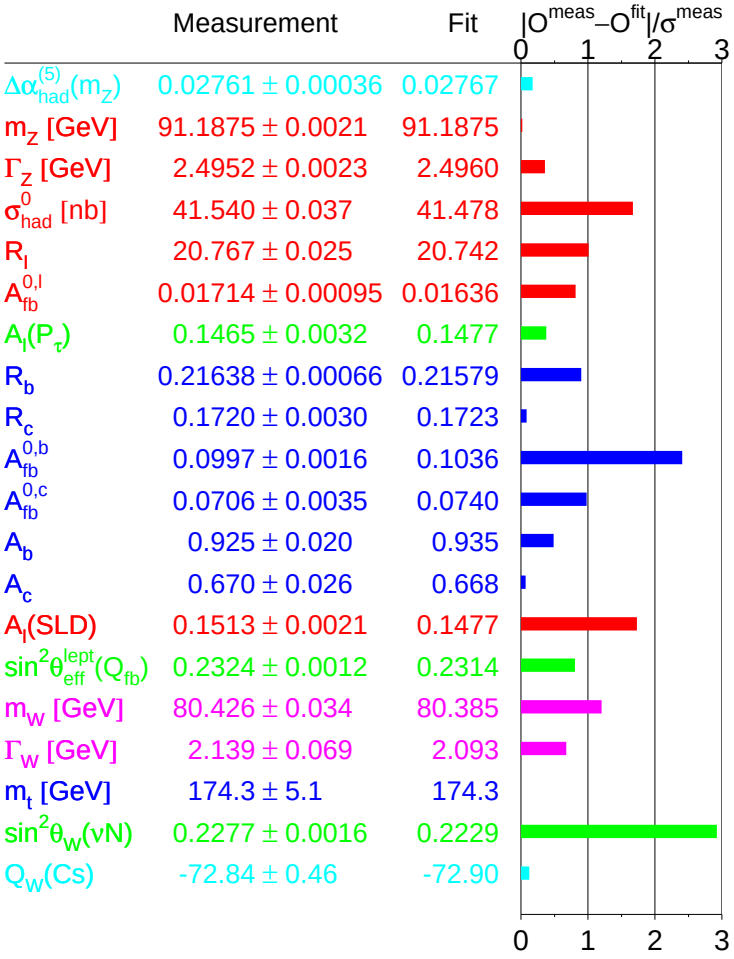

Figure 1.1: Precision Electroweak measurements and the pulls they exert on a global fit to the Standard Model [7]. Notice that the pull of the $\sin^2\theta_W$ measurements from νN interactions is considerably reduced if one takes into account a less aggressive estimation of the theoretical uncertainties (see e.g. the discussion in [10]).

Cabibbo-Kobayashi-Maskawa free elements, 2 parameters to characterize the scalar sector of theory).[3] The common feeling of this fact is that a more fundamental theory should be invoked to naturally explain the pattern. Unification theories stem from this point. They set a new high energy scale somewhere around 10^{15} GeV.

2. There is now compelling evidence that neutrinos have masses (see a short discussion in Sec.1.2) while in the minimal Standard Model these are strictly vanishing. All most popular extensions of the SM that can account for non zero neutrino masses call for a higher energy scale (should it be the mass scale suppressing higher dimensional operators that yield (Majorana) masses for left-handed neutrinos or the explicit mass for right-handed neutrino fields in the see-saw mechanism). This mass scale sits naturally close to the Unification scale and indeed small neutrino masses are addressed as the "third pillar of Unification" in [11].

3. The Standard Model is not the "Theory of Everything" since gravitational interaction is not included in the game. The unification of gravity calls for a even higher energy scale around 10^{19} GeV, at which gravitational interaction becomes comparable with gauge forces. This is called Planck mass ($M_{\rm Pl}$). String theory/M-theory is the only candidate to be the ultimate answer to this need.

1.1.1 The Hierarchy Problem

From the sketchy picture above, it seems that it is all a matter of energy scales: first we meet the well known ElectroWeak Symmetry Breaking (EWSB) scale at few·100 GeV $\div$1 TeV, then a large energy desert opens, up to the Unification scale, and above all is the Planck scale. It seems that we are simply being informed that physics is not ended at the EWSB energy and we could go and look for some New Physics at those large scales.

No, there is more: we *must* look for New Physics at *low* energy ($\lesssim$ 1 TeV) scales. Why is it so? After all the SM is a renormalizable field theory and it could be valid well above the energy scale at which it is presently tested and at which EWSB happens, if one is willing to accept (at least a portion of) the energy desert.

The compelling argument to look for New Physics at low scales is known as **hierarchy problem**. It originates in the very existence of the scalar sector of the theory coupled to the presence of higher energy scales.

The standard argument goes as follows:

a. The scalar sector of the Standard Model leaves the Higgs mass as a free parameter.

Such a sector is the most hazardous in the theory: we postulate the existence of an elementary Higgs scalar that spontaneously realizes the EWSB since we assume a tree level potential which is characterized by the negative mass parameter μ^2 and the dimensionless quartic coupling λ. The measured value of the Fermi constant fixes a combination of these parameters (essentially μ^2/λ) but the squared mass of the physical Higgs boson, proportional to μ^2, is undetermined.

b. However, the Higgs boson has to be light.

[3] The angle related to the strong CP problem is an additional free parameter.

First of all, for the obvious reason that the natural guess for the value of λ of order 1 closely ties the Higgs mass to the measured Fermi scale. More closely, the requirement of the Higgs self coupling λ not to develop a Landau pole before the high energy scales sets an overall upper bound on the Higgs mass of the order of 600 GeV [12].[4] The limit depends on the high energy scale that one aims to reach: if New Physics shows up at a scale close to the Unification scale, the Higgs is confined to be roughly under 200 GeV. Notice that this point is so even in absence of any experimental hint on Higgs mass, it simply has to do with the self-consistency of the theory itself. If one then also takes into account the indications from the experiments, the Higgs lightness appears in all its concreteness: the world famous Blue Band plot [7] teaches us that the EWPT favor a mass below 193 GeV (at 95%).

c. But the mass of the Higgs boson receives divergent contributions, quadratic in the cut-off Λ, already at one loop in perturbation theory. If the nearest cut-off at disposal is at Unification scale or even at Planck scale, the quantum corrections to Higgs mass dwarf the physical value by about 34 orders of magnitude (the Hierarchy). In other words, the tree level value is to be chosen with an accuracy of 10^{-34} compared to the Planck mass (the fine tuning), which is so unnatural... [5]

As well known, the Hierarchy Problem has been attacked along two main directions:

I. Technicolor models aim to eliminate the fundamental scalar field from the theory, replacing it with some fermion condensate: the energy scale of EWSB is then understood as the scale at which some new gauge force becomes strong.

II. Low energy SuperSymmetry relies on the existence of an additional (although broken) symmetry that can motivate the smallness of Higgs mass. In other words, low energy SuperSymmetry aims to interpose a new energy scale low enough to shield scalar masses from the harm of very high energies. This scale is related to the scale of SuSy breaking (in the observable sector). SuperSymmetric models, and in particular the Minimal SuperSymmetric Standard Model (MSSM), feature a lot of new particles (the superpartners) that enter the game with a mass comparable to that scale. In the optic of the necessity of a light touch on EWPT, this approach is very successful since the superpartner contributions decouple very fast. Unfortunately, one should also mention that a lot more parameters are introduced: in the unconstrained MSSM, for instance, we end up with 105 new ones with respect to the SM, that is certainly not what one wants in the spirit of point 1 above.

Recently, a new idea has opened a third brilliant way:

III. The only fundamental scale in nature is assumed to be the ElectroWeak Breaking scale ($\sim$ 1 TeV); it also settles the scale of gravitational interactions, the enormity of the Planck scale is only a mirage produced by the presence of **large extra (space) dimensions** accessible to gravity. From this idea, a huge quantity of different realizations and applications spurted.

[4] The unitarity bound also sets a larger upper limit of about 1 TeV.

[5] Actually, even choosing a much lower cut off of order a few TeV, as low as allowed by EWPT themselves, the unnaturalness and the fine tuning are still large enough to be a serious concern [13]. Rooted in the EWPT, this is dubbed the Lep Paradox, or Little Hierarchy Problem. Since in what follows I will be mainly interested in the framework of Large Extra Dimensions as a solution to the old good Hierarchy Problem, I do not address this even more interesting issue (and the possible solutions to it) here.

Actually, one can forget all arguments given above and realize that the stronger motivation to study Extra Dimensions comes from turning upside-down the energy scale presented so far. Indeed, we believe that gravity, sooner or later, must be quantized and string/M-theory is the only known candidate to do the job. "By chance", string/M-theory features Extra Dimensions (and SuperSymmetry) as corner stones of mathematical consistency. In string theory the extra six-dimensional space is usually thought as squeezed in a manifold of tiny volume, the compactification scale being of the order of the inverse Planck mass. In this case the low energy world (in which we remain interested) would definitely appear as four-dimensional. However, as we will see, this belief can be questioned and the study of low energy theories with Extra Dimensions (and possibly with SuSy) receive further motivation.

1.1.2 Introduction to Extra Dimensions

Motivated by the discussion above, we are willing to assume that one or more extra space dimensions exist.[6] However, we do not experience more than 3 spatial dimensions in our everyday life and in current physical investigation. Thus the first issue in the physics of Extra Dimensions is of course how to hide them. Two main streams have emerged since the beginning:

- (Flat) Compactified Extra Dimensions;
  depending on which fields experience the extra space one can also distinguish:
  - Gravitational Extra Dimensions (only the graviton [7] in extra dimensions)
  - Universal Extra Dimensions (also SM fields in extra dimensions)
- Warped Extra Dimensions.

The additional space is named "bulk". In the bulk it can be embedded a hyper-surface (often a (3+1)-dimensional space) called "brane", on which some fields are possibly confined by some mechanism.

1.1.2.a Compact Extra Dimensions

Each extra dimension is assumed to be compactified on a compact manifold (e.g. a circle), the size (radius R) of which is the crucial parameter. If the size of the extra dimensions is enough microscopic, the space-time is effectively four dimensional at distances that largely exceed it. Equivalently: experiments probing energies much lower than the compactification scale ($1/R$) will see no hint of their presence. A more precise statement on the maximum size allowed depends of course on what physics is extended into the extra space and on which experiments can probe it, as we will see later.

In general, the physics of Extra Dimensions is effectively described from a 4-dimensional point of view in terms of Kaluza-Klein fields. As a reference, let us consider the case of one extra dimension y, so that the complete set of coordinates in (4+1)-dimensional space time is $x^M = (x^\mu, y)$, $M = (0, 1, 2, 3, 5)$, $\mu = (0, 1, 2, 3)$. Every field allowed in the extra dimension is a function of all 5 coordinates: $\Phi(x^\mu, y)$.

[6] For general reviews on Extra Dimensions see [14].

[7] ...and possibly some SM gauge singlet, see Chapter 3.

The compactification implies that the points $y = 0$ and $y = 2\pi R$ are identified so that the wave function of the field is periodic and can be expanded in Fourier series

$$\Phi(x^\mu, y) = \sum_{n\in\mathbb{Z}} e^{in\frac{y}{R}} \phi_n(x^\mu) \tag{1.1}$$

where $\Phi_n(x^\mu)$ are an infinite tower of 4-dimensional (Kaluza-Klein, KK) fields. The kinetic lagrangian term for a 5D massless scalar, for instance, reads

$$\int d^4x\ dy \left(\partial_M \Phi^*\ \partial^M \Phi\right) = \int d^4x\ dy \left(\partial_\mu \Phi^*\ \partial^\mu \Phi + \partial_5 \Phi^*\ \partial^5 \Phi\right) = \int d^4x \sum_{n\in\mathbb{Z}} \left(\partial_\mu \phi_n^*\ \partial^\mu \phi_n - \frac{n^2}{R^2}\phi_n^* \phi_n\right) \tag{1.2}$$

Each KK mode ϕ_n, therefore, can be interpreted as a separate particle with mass $m_n = |n|/R$. At low energies, only massless modes are relevant, while at energies $\sim 1/R$ heavy modes will be produced in collision and take part in physical processes.

Gravitational Extra Dimensions

This framework of Extra Dimensions (the first that was investigated [15]) blossomed from the simple observation that the behavior of gravitational interaction is not known at distances in the sub-mm range[8]. This opens the possibility that the graviton can experience a certain number δ of extra space dimensions of size up to $\sim 100\ \mu$m.

The general set-up is very simple: all Standard Model fields are (somehow) confined on a 4D brane while the graviton is free to propagate in all the $4 + \delta$ dimensions. The extra ones are compactified on circles of radii R_i.

The Hierarchy Problem is solved (as mentioned in 1.1.1) thanks to the volume of the extra space: the only fundamental scale is $M_* \sim$ TeV while the hugeness of the Planck mass is produced by

$$M_{Pl}^2 = \prod_{i=1}^{\delta} (2\pi R_i M_*)\ M_*^2\,. \tag{1.3}$$

This formula is simply obtained from the consistency of the Gauss law in 4D and in $4+\delta$ dimensions. The Newton potential at distances smaller than the compactification radius is modified and goes with r like $1/r^{1+\delta}$ instead of $1/r$.

A lot of different physical processes have to be considered in order to guarantee the experimental viability of such a scenario. Schematically, relevant constraints or confirmations can come from (besides of course the detection of a modification of Newton law at small distances):

- collider physics [17, 19, 20], via the phenomenon of graviton production and virtual exchange or even, since the gravity scale is lowered to TeV, black hole production;
- astrophysics [17, 162], since the cooling of Supernovae must not be unacceptably accelerated by KK graviton emissions; this turns out to be one of the most stringent constraints in the case

[8] See [16] for the latest results.

that all extra dimensions have the same size (at least 3 extra dimensions are needed), but can be relaxed if the radii are allowed to be different;

- cosmology [17, 162], from the fact that relic KK gravitons must not be so numerous to over-close the universe and from the fact that KK gravitons can "come back" from the bulk and decay giving an unobserved distorsion of the photon spectrum; again these severe limits can be eased in models with enough extra dimensions or with a non degenerate structure of radii.

Moreover, one can investigate the modifications induced by KK gravitons in rare decays [17], ultra high energy cosmic ray physics [21], other astrophysical issues such as the additional heating of neutron stars [17], other cosmological points including Big Bang Nucleosynthesis [162] and so on.

In short, one can state that all phenomenological tests are passed, with the fundamental scale still fixed at $M_* \sim$ TeV (to solve the Hierarchy), at least paying the price of some uncomfortable flexibility in the constructions.

Probably the most important criticism to the Compact Extra Dimensions picture is related to the determination and stabilization of the compactification radii. In a sense, one introduces a new unmotivated hierarchy between the fundamental scale $M_* \sim$ TeV and the compactification scale of the extra dimensions ($\sim 10^{-3}$ eV when $R \sim 100$ μm). Although the embedding in some string theory can support certain choices (see [18]) [9,10], the need for a more fundamental theory that can predict such structures is still alive.

Universal Extra Dimensions

In these realizations of theories with extra dimensions also the fields of the Standard Model (or MSSM) propagate in the bulk.[11] Many possible variations on this theme have been implemented, particularly regarding the choice of the fields allowed in the bulk (all SM/MSSM fields, only gauge bosons with all or some matter fermions confined on a brane, only Higgs bosons...) but I argue that some general aspects can be outlined:

- the size of the extra dimensions have to be much smaller than the case where only gravity is higher dimensional, since of course ElectroWeak interactions are probed at much smaller distances; the typical compactification energy must indeed be larger than $\sim$ few $\cdot 100$ GeV $\div 1$ TeV, corresponding to radii smaller than $\sim 10^{-17}$ cm; [12]

- the focus here is often not on a solution of the Hierarchy Problem but rather more on possible beneficial effects with respect to other problems of the Standard Model or MSSM (flavour

[9] The stabilization of the radii (seen as dynamical scalar fields) at large values requires very flat potentials, for which SuperSymmetry can help. One more time, SuperSymmetry (which fortunately is part of string theory) should better enter the game.

[10] Applying string theory to cosmology ("brane gas cosmology"), one can even aim to explain why 3+1 dimensions are allowed to expand while others remain compactified, and even also to set a non trivial morphology for the extra dimensions, see [22].

[11] For just some examples see [23, 24, 25, 26, 27].

[12] Of course hybrid models are possible, where some large extra dimensions are accessible to gravity and some smaller ones to the SM fields [28].

physics, ElectroWeak Symmetry Breaking, SuperSymmetry Breaking, neutrino masses, unification...); gravitational interactions are not of interest here, as in usual ElectroWeak physics;

- the models usually need only one extra dimension, that is often compactified on $\mathbb{S}^1/\mathbb{Z}_2$; this structure is called an orbifold: a $\mathbb{Z}_2$ symmetry is introduced under which $y \to -y$ and all 5D fields are either even or odd;

- the chosen "reference model" (SM, 2HDSM, MSSM, NMSSM...) is usually reproduced by the lower modes of the KK fields (the zero or sometimes the first modes).

1.1.2.b Warped Extra Dimensions

An alternative scenario [30, 31] that does not suffer of the residual hierarchy (between the fundamental and compactification scale) highlighted above, can be built with a single extra dimension accessible to the graviton, provided that the metric of the space time distinguishes between the four traditional coordinates and the additional one. Indeed, the 4-dimensional metric is multiplied by a "warp" factor, a rapidly changing (exponential) function of the extra coordinate:

$$ds^2 = e^{-2k|y|}\eta_{\mu\nu}dx^\mu dx^\nu + dy^2 \tag{1.4}$$

where k is a free factor for the moment. The additional dimension is contained between two branes located at $y = 0$ and $y = \pi r_c$. This metric is a solution of Einstein equations provided that the tension on each brane is opposite in sign and equal to $24M_\star^3 k$ (where $M_\star$ is the only fundamental scale of the theory, which we assume to be of order of 10^{19} GeV) and the bulk is endowed with a negative cosmological constant, thus corresponding to a slice of Anti-de Sitter space. The value of the cosmological constant is fine tuned to the value $\lambda = -24M_\star^3 k^2$.

The Hierarchy Problem is solved thanks to the exponential factor in the metric. Indeed, any mass parameter (or energy scale) m_0 in the fundamental theory will generate a physical mass $m = e^{-\pi k r_c}\, m_0$ in the 4D theory; in particular, the 5-dimensional fundamental scale $M_\star$ produces the TeV scale of ElectroWeak interactions if only $kr_c \approx 50$. On the other hand, the old (4-dimensional) Planck mass is produced from $M_\star$ with only a slight dependance on the extra space: $M_{Pl} = (M_\star^3/k)(1 - e^{-2\pi k r_c})$.

The message is that one can generate the Hierarchy and keep the extra space concealed at the same time, without introducing very large or very small numbers: it holds $M_\star \sim k \sim 50/r_c$. The picture is perfectly consistent with $r_c \to \infty$ [32], therefore opening the way to infinite, non-compact extra dimensions.[13]

As apparent, the field of extra dimensions has been very active and developed several different directions. My main focus in Chapter 3 will be on the Gravitational Extra Dimensional scenario.

[13] Notice that in this case the focus is no more on the Hierarchy Problem.

1.2 "Standard" neutrino physics and why to go beyond

It is customary, in neutrino physics, to speak of "neutrino anomalies". These, indeed, have been the driving force of the field in the latest decades and continue to be so. Some of them (the solar neutrino anomaly, the atmospheric anomaly) have actually turned into "evidences", namely of neutrino oscillations, of which they have provided us with a remarkably consistent picture. Some others of them (LSND, NuTeV...) are instead still there and could be hints to some refinement of the picture or to some new phenomenon. Some others again (17 KeV neutrino, 17 eV neutrino, Karmen...) simply belong to the forgotten past. On the other hand, of course, other new anomalies may appear in the future, especially as the measurements of the oscillation parameters get more stringent.

In the following I shortly present the status of the established physics of neutrino oscillations, as it cleanly revealed itself in solar, atmospheric and reactor experiments in the recent years. An extensive review of the physics of neutrino oscillations is of course beyond my purpose and can be found elsewhere [33, 34]. I restrict instead to quote the bare results, pursuing a double aim: (1) to portray the astonishing improvement in the field achieved in the last few years; (2) to set the stage to take into consideration possible extensions of the present status. This I do when I move to a short discussion of some open tasks and puzzles, on the experimental and on the theoretical sides. In the last portion I focus on the single issue of sterile neutrinos, brought into attention by some of the present day experimental anomalies and theoretical speculations.

The huge harvest of data from experiments that cover a time interval of decades (Homestake, Sage, Gallex, GNO, SuperKamiokande and SNO) allows to explain the disappearance on Earth of solar ν_e in terms of $\nu_e \to \nu_{\mu,\tau}$ oscillations. This is corroborated by the evidence of the disappearance of reactor $\bar{\nu}_e$ in the KamLAND detector, which can be explained in terms of $\bar{\nu}_e \to \bar{\nu}_\mu$ oscillations. A quite different physics underlies the two setups (enormous baseline, relevance of matter effects, astrophysics vs medium baseline, no matter effects, terrestrial physics); nevertheless the two beautifully combine (see fig. 1.2) to identify the oscillation parameters of the LMA MSW solution

$$\Delta m^2_{\rm sun} \simeq 7.1\ 10^{-5}\,{\rm eV}^2 \qquad \theta_{\rm sun} \simeq 32^o. \tag{1.5}$$

The systematics connected with the author of the fit [39, 40] moves the central values of about $\delta(\Delta m^2_{\rm sun}) \sim 0.1\ 10^{-5}\,{\rm eV}^2$, $\delta(\theta_{\rm sun}) \sim 2^o$. The allowed intervals at 1σ (as apparent from fig. 1.2 and the like) typically span $\Delta m^2_{\rm sun} \in (6.0 \to 8.5)\,10^{-5}\,{\rm eV}^2$, $\theta_{\rm sun} \in (29^o \to 35^o)$.

The data from SuperKamiokande, MACRO and Soudan2 allow to interpret the disappearance of atmospheric ν_μ and $\bar{\nu}_\mu$ in terms of $\nu_\mu \to \nu_\tau$ oscillations. The disappearance of ν_μ in the K2K accelerator experiment comes as a confirmation (see fig. 1.3) so to determine the oscillation parameters [41, 42]

$$\Delta m^2_{\rm atm} \simeq 2.6\ 10^{-3}\,{\rm eV}^2 \qquad \theta_{\rm atm} \simeq 45^o. \tag{1.6}$$

with typical allowed intervals $\Delta m^2_{\rm atm} \in (2.0 \to 3.0)\ 10^{-3}\,{\rm eV}^2$, $\theta_{\rm atm} > 39^o$.

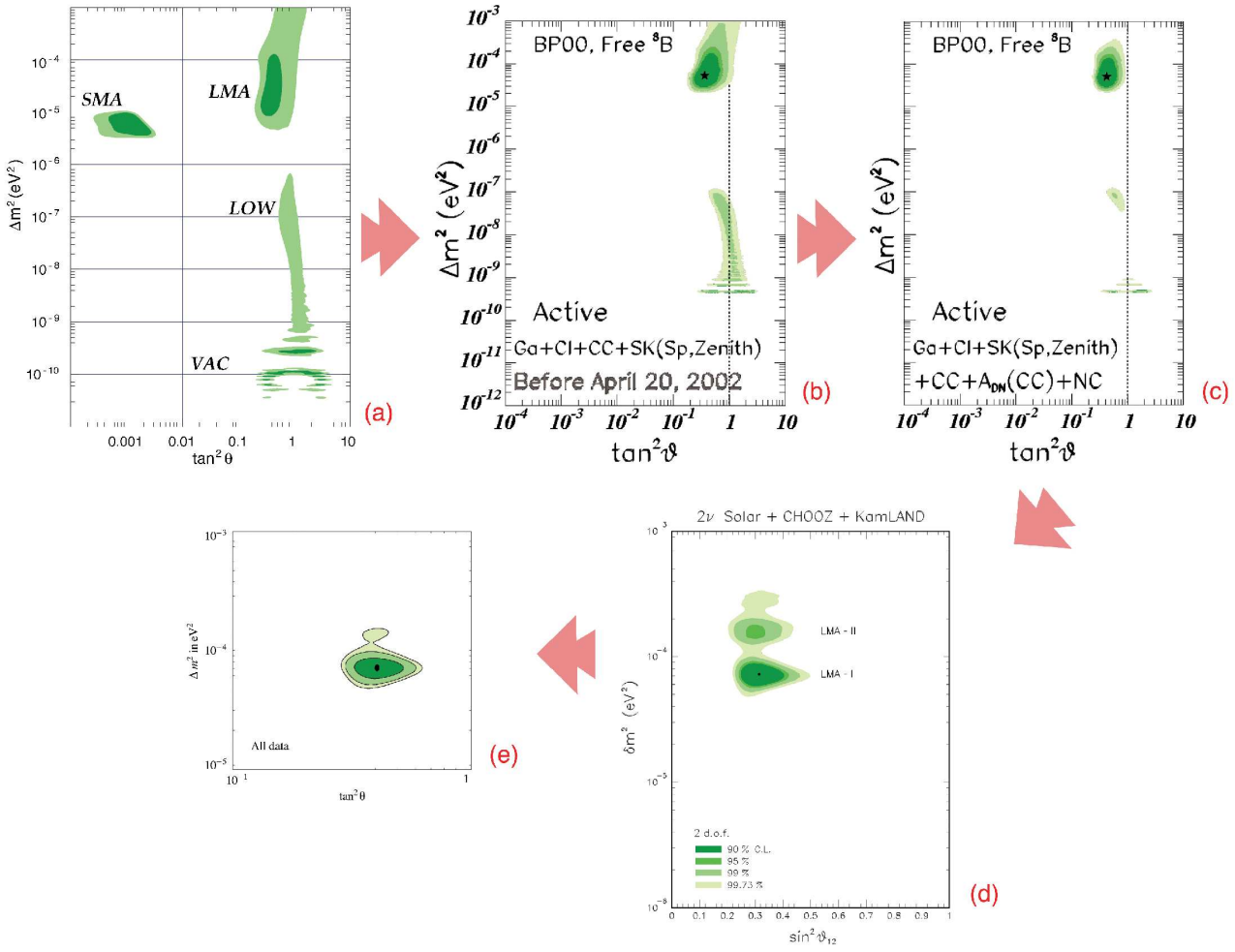

Figure 1.2: Allowed regions in the oscillation parameter plane from global analysis of solar (and reactor) neutrino data, at several different stages during the latest three years. The figure does not aim to present rigorously the results but instead to convey a sense of the progress in the field. On purpose, the different panels are taken (and adapted) from different authors, whose method of analysis and whose results may vary. The contours do not always have the same statistical significance. The time line and the references are as follows:

Panel	Date	Stage	Reference
a	February 2000	early data	[35]
b	July 2001	after SNO CC	[36]
c	after 20 April 2002	+ SNO NC	[36]
d	December 2002	+ Kamland	[37]
e	September 2003	+ salted SNO	[38]

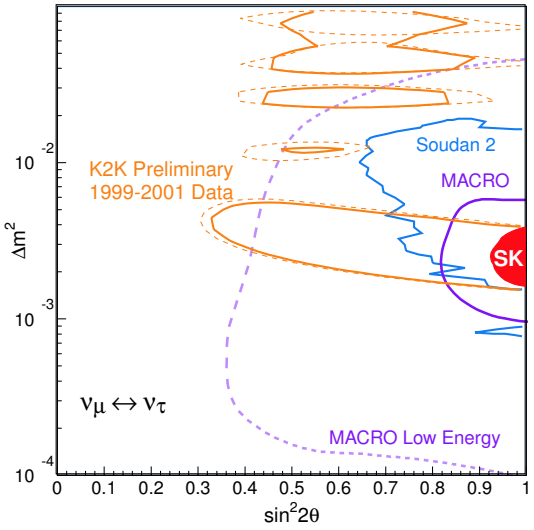

Figure 1.3: Allowed regions in the atmospheric oscillation parameter plane. From [43].

Given the evidences above, the absence of disappearance of reactor $\bar{\nu}_e$ in the Chooz experiment allows to put constraints on the remaining mixing angle. In a full 3 ν analysis one gets [44] at 3σ

$$\theta_{13} < 13^o. \tag{1.7}$$

In summary, what is "standard" in neutrino physics today? [45]

- three neutrinos
- massive, but light ($m \lesssim 1\,\mathrm{eV}$)
- split by two hierarchically different gaps $\Delta m^2_{23} \equiv \Delta m^2_{\mathrm{atm}} \gg \Delta m^2_{\mathrm{sun}} \equiv \Delta m^2_{12}$
- largely or largely/maximally ($\theta_{\mathrm{sun}} \equiv \theta_{12}$, $\theta_{\mathrm{atm}} \equiv \theta_{23}$) mixed two by two.

1.2.1 "What is left, what is next?"

The fact that a consistent "standard" picture of neutrino oscillations has been unveiled does not mean that the exploration is over. On the contrary, there are unknown spots to be defined and there are vast lands to be yet discovered. Let us lay down a possible roadmap:

1. perform better measurements on the already known parameters and properties;
2. determine the unknown parameters and properties;
3. find a solution of the LSND anomaly;

4. give a theoretical framework of the whole picture;

5. exploit neutrinos as diagnostic tools;

6. probe exotic possibilities.

1. In the context of solar (and reactor) neutrinos, a better determination of the parameters Δm^2_{12} and θ_{12} is generically important and will be achieved with the upcoming results from KamLAND, SNO and Borexino. In order to perform some kind of consistency check on the LMA MSW solution, it would be also important to detect directly some of its other predicted effects: a day/night asymmetry of order few % at SNO and SK and the raising of the spectrum at low energies (upturn). Moreover, although the LMA MSW solution has been singled out as the dominant effect [46], there could be additional processes in operation (spin-flavor precession [47], non standard neutrino interactions [48]...; or simply a possible effect of θ_{13} in a full three neutrino oscillation scenario [44]) that would be tightly constrained by more precise measurements. And also: solar data concern neutrinos, while reactor (KamLAND) data are relative to antineutrinos. If the current perfect agreement in the oscillation parameters extracted in the two sectors should break under better measurements, that would probably be a signal for some new physics at work, if not CPT violation. Finally, one should not forget that the investigation still has to dip into the low energy part of the spectrum of solar neutrino (below a few MeV, more than 99% of the total solar flux).

In the context of atmospheric neutrinos, the main refinement concerns the oscillations of the electron flavor, guided either by the Δm^2_{12}-θ_{12} parameters or by a non vanishing θ_{13} or by both [49]. Moreover, also in the case of atmospheric neutrinos, secondary effects could still be allowed (decoherence [41]).

Summarizing, the near future of solar(-reactor) and atmospheric oscillations, since the gross features have been by now pinned down, is a physics of sub-leading effects, which is nevertheless very important and can be very fruitful.

2. The standard list of the parameters and properties yet to be determined includes: the third mixing angle θ_{13}, the absolute neutrino mass scale, the kind of spectrum (hierarchical or degenerate), $sign(\Delta m^2_{23})$ (direct or inverted hierarchy), the nature of the neutrinos (Majorana or Dirac) and the CP violating phases. On most of these point the intermediate/far future projects (β decay experiments, Long Base Line beams, Superbeams, Neutrino Factories) seem to have more promising capacities (see for instance the review [50]).

3. The LSND experiment found a signal [51] for $\bar{\nu}_\mu \to \bar{\nu}_e$ oscillations in the appearance of $\bar{\nu}_e$ in an originally $\bar{\nu}_\mu$ beam. The best fit point is located at $\sin^2\theta_{LSND} = 3\ 10^{-3}$, $\Delta m^2_{LSND} = 1.2\,\mathrm{eV}^2$ (the whole allowed region is represented in fig. 1.4). An early evidence of $\nu_\mu \to \nu_e$ conversion [52] is now reabsorbed. Being the suggested LSND mass gap incompatible with the solar and atmospheric ones, the first possibility that comes to mind is the introduction of an additional state, necessarily sterile not to contradict the Lep bound on the number of active neutrinos $N_\nu^{\mathrm{active}} = 2.984 \pm 0.008$ [53]. We will come back on this point later on.

However, a couple of other possibilities can be investigated. The first involves a violation of CPT symmetry: it can be that the antineutrino spectrum probed by LSND differs from the neutrino spectrum

to which solar experiments are solely sensitive (and atmospheric experiments mainly sensitive) [54]. However, this solution is now very hardly compatible with KamLAND or atmospheric data [55, 56]. The second possibility contemplates exotic $\Delta L = 2$ decays of the μ^- of the beam which could account for the detected $\bar{\nu}_e$ as a contamination [57]. The adoption of this possibility makes difficult to explain why Karmen, which operated under very similar conditions, did not catch the effect.[14]

Ultimately, the MiniBooNE experiment [61] will cover the whole LSND suggested region. Although MiniBooNE was designed to run in the $\nu_\mu \to \nu_e$ channel first and in the $\bar{\nu}_\mu \to \bar{\nu}_e$ channel then, the second stage is quite far in time, if possible at all. It will be interesting to see whether a confirmation or a rejection of the LSND evidence will be achieved. In the second case, the CPT violating possibility runs the risk of not being directly checked.

4. Even when all the mixing and oscillation parameters will be nailed down, the question remains of how to justify their values. This is something more than just adding a few new parameters to the list of the arbitrary numbers of the SM, as already discussed in 1.1. The additional deep questions are: why are the neutrino masses so small compared to the charged lepton and quark ones? Why is the lepton mixing large with respect to the small quark mixing? In short: what do we see out of the celebrated window on New High Energy Physics that the massive and oscillating neutrinos have opened for us?

5. A satisfying understanding of the physics of neutrino oscillations can allow us to turn the logic upside down and start exploiting neutrinos as probes of unknown environments. This has been discussed since long for the case of the Sun [62]. The case of supernovæ is also very important (see a brief discussion in 1.3.3). Moreover, neutrinos from the radioactive decays in the Earth interior can give clues on the composition[15] of the core, crust and mantle (see for instance [64]). It has even been proposed to exploit high energy neutrinos fluxes (from the cosmic rays, from a future SN or even from an accelerator) to take tomographic images of the Earth interior [65]. Finally, the atmospheric neutrinos could give relevant informations on the fluxes of cosmic rays, once the oscillations are completely under control.

6. At any given step in the present and future understanding of the picture of neutrino physics, the search for exotic modifications or additions should never go out of the to-do list. Most of them have already been mentioned: non standard neutrino interactions [48], anomalous neutrino magnetic moments, effects of Lorentz violation [66], and, of course, the existence of extra, sterile neutrinos.

1.2.2 Sterile neutrinos

A sterile neutrino is defined as a fermionic state that is neutral under all SM forces (electromagnetic, weak and strong). It can have a non negligible role, however, through the mixing with active (electron, muon and tau) neutrinos [67].

[14] A few more proposals: (i) one can even consider 3+1 neutrinos together with CPT violation [58]; (ii) or one can introduce 2 additional sterile neutrinos, although it is not certain that this improves the situation [59]; (iii) or: can one speculate on a varying mass term for the neutrinos (motivated by interaction with dark (sterile) fields) that generates a large mass gap in the experiments in which the neutrino beam travels through rock (LSND) while vanishing in cases (Bugey, Chooz) in which the neutrino beam does not [60]?

[15] Or even the age? [63]

Originally introduced by Pontecorvo [68] in 1967 [16], more recently the hypothesis of the existence of one (or more) sterile neutrino has played the role of "emergency exit" from several puzzling situations in particle physics, astronomy and cosmology. For instance, sterile neutrinos have been invoked to account for the origin of the pulsar kicks [69], to constitute a Dark Matter candidate [70], to explain (via their decay) the diffuse ionization of the Milky Way [71], to help the r-process nucleosynthesis in the environment of exploding stars [72], to interpret the slightly too low Argon production in the Homestake experiment [73] etc. Above all, the (maybe, partial) conversion into sterile neutrinos has been a viable candidate for the explanation of the solar and atmospheric anomalies jointly with the LSND evidence, in the so called (2+2) mass pattern (briefly discussed in Section 2.1), until the active-active oscillations were definitively established.

On the other hand, it is true that there is no shortage of possible candidates to the role of sterile neutrinos: slightly beyond the context of the SM, the right handed neutrino is the natural candidate, to complete the lepton sector in similarity (symmetry?) with the quark one. In this case, actually, three states (one per family) would be natural. More broadly, several (GUT-/string-/ED- inspired) SM gauge singlets line up awaiting for consideration.

However, a point must be stressed: in all these cases there is no good reason for them to be light. Or, even, there are good reasons to hope them to be heavy. The case of the tower of naturally light sterile neutrinos motivated by the presence of fermion states in the bulk of large extra dimensions [17] (which we will address thoroughly in Chapter 3) represents an exception. However, it requires to explain the largeness of the compactification scale in some other way (as discussed in 1.1.2). Pragmatically, I will not enter these issue any more and I will simply restrict to consider light sterile neutrinos.

The relatively more solid motivation today for the introduction of a sterile neutrino consists, as mentioned, in the LSND controversial results on muon antineutrino disappearance [51]. The (3+1) sterile neutrino explanation assumes that the $\bar{\nu}_\mu \to \bar{\nu}_e$ oscillation proceeds through $\bar{\nu}_\mu \to \bar{\nu}_\mathrm{s} \to \bar{\nu}_e$. The large LSND mass scale Δm^2_{LSND} separates the three active states (split by the solar and atmospheric gaps) from the additional sterile state. The effective angle of the LSND oscillation can be expressed in terms of the two active-sterile angles θ_{es}, $\theta_{\mu s}$ as

$$\sin^2 2\theta_{LSND} = \frac{1}{4} \sin^2 2\theta_{es} \sin^2 2\theta_{\mu s} \tag{1.8}$$

However, each one of those two angles is constrained by several other experiments that found no evidence of electron or muon neutrino disappearance. Moreover, the $\bar{\nu}_\mu \to \bar{\nu}_e$ oscillations are directly excluded by KARMEN in a fraction of the parameter space. As a result [55, 74], a large portion of the area indicated by the LSND experiment is ruled out and only a few islands (with poor statistical quality) still survive, see fig. 1.4.

In this sense, the LSND motivation for the introduction of sterile neutrinos is already somehow shaking.

[16] Essentially referring to right handed neutrinos.

[17] In absence of explicit mass terms, see e.g. [159].

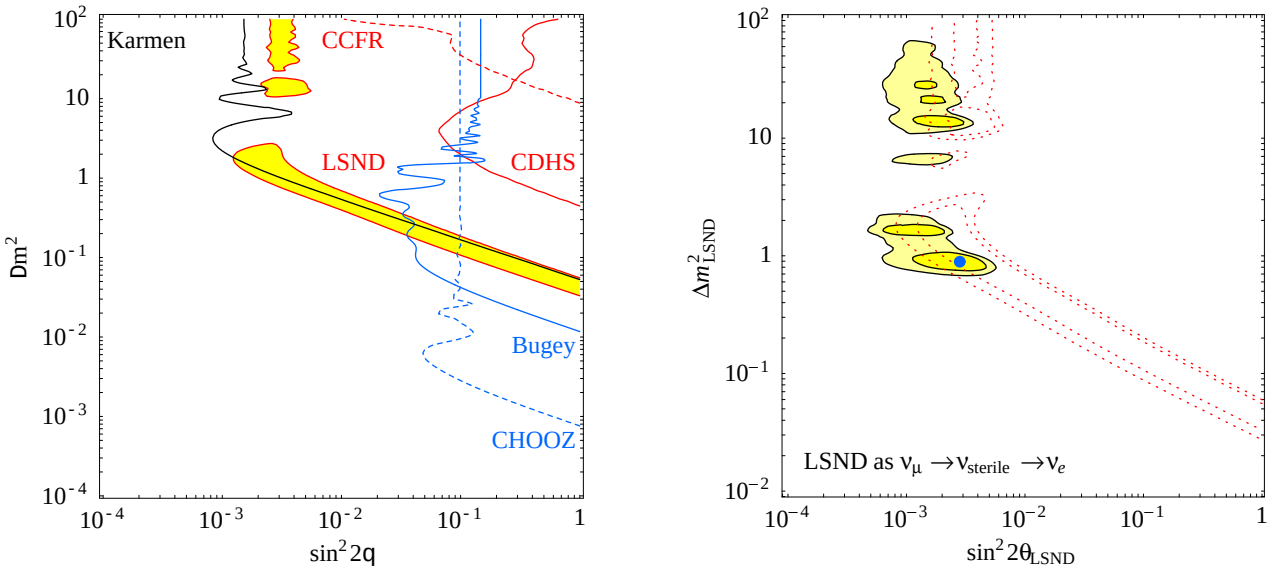

Figure 1.4: On the left, the excluded regions (at 90% cl) from Karmen and other experiments, together with (shaded) the LSND suggested region. The mixing angle on the horizontal axis is different for the different experiments. The combination of these data leaves the surviving regions for the LSND signal depicted on the right panel. From [55].

On the other hand, particle physics presented several examples of ad hoc postulated particles that only fitted in the picture later on: even the (left handed) electron neutrino itself, to save the conservation of energy in beta reactions. Nevertheless, it would not be fair to argue that the motivations for sterile neutrinos today are as compelling, so that, instead of embracing any positive instigation, I prefer to keep as a stimulus to discuss (light) sterile neutrinos the questions: why not? and, if yes, to what extent?

1.3 The role of Supernovæ

Supernovæ can be powerful and important laboratories for Particle Physics, and particularly for neutrino physics. The fundamental reasons for this basic fact are simply listed:

- SNe are abundant sources of neutrinos, since this is the main channel into which most of their enormous energy is emitted; as a consequence, neutrinos play a crucial role in the evolution of the SN phenomenon;
- given the characteristic temperatures of the SN environment, the typical energy of the emitted neutrinos ($\sim 10 \div 20\,\mathrm{MeV}$) is such that they can be easily detected on Earth;
- SNe are so far away that neutrinos must travel over distances so large that they have plenty of time (or space) to experience and fully develop the consequences of several "exotic" effects (oscillations, non-conventional very feable interactions, decay...), if any is present;
- SN cores are so extremely dense that neutrinos remain trapped and undergo matter effects that cannot be relevant anywhere else.

On the other hand, it is true that the physics of supernovæ is very complicated and demanding, and could pose a threat on their possible usefulness as "clean experiments". Nevertheless, it has been shown several times that the basic features are robust enough to be used as uncontrovertible criteria, sometimes, maybe, requiring a sensible compromise between detailness and usefulness in the treatment of SN physics.

In turn, with a reversion of prospective, one can think of using the neutrinos as probes of the supernova environment itself. Carrying, in particular, undelayed information about the inner region of the exploding star, they could help understanding this very complicated process.

In this double-faced sense, the combined study of supernova and neutrino physics has proven to be very fruitful in the past years and promises to be very important as well in the future. In the following I will briefly sketch the basic features of the SN phenomenon, focussing in particular on the aspects that allow to obtain constraints on the underlying ν physics.

1.3.1 Supernova basics and neutrino signal formation

For our purposes, it will be sufficient to sketch the standard picture of the supernova phenomenon [75, 76] in terms of three main phases: (i) the gravitational collapse, (ii) the (delayed) explosion and (iii) the cooling phase.

(i) The collapse begins when the iron core of the star, accreting matter from the outer layers but no more capable of nuclear burning, reaches the Chandrasekhar limit: the electrons cannot compensate the gravitational pressure any more. During a fraction of a second the radius of the core gets reduced and its density increased by several orders of magnitude ($10^9\,\mathrm{g\,cm^{-3}} \to \mathrm{few} \cdot 10^{14}\,\mathrm{g\,cm^{-3}}$). The capture reaction $pe^- \to n\nu_e$ leads to the neutronization of matter and produces a large number of very energetic electron neutrinos, that remain trapped when densities of order $10^{12}\,\mathrm{g\,cm^{-3}}$ are reached.

(ii) The collapse abruptely stops when nuclear densities ($\sim 3 \cdot 10^{14}\,\mathrm{g\,cm^{-3}}$) are reached: the falling material bounces on the surface of the inner core and turns the implosion of the core in an explosion of the outer layers. However, the outward propagating shock wave loses energy on the way, slows down and would eventually recollapse. In the meantime, the cooling phase is beginning: the neutrinos contained in the inner core start to diffuse out. They hit and push the stalling matter from below so that their energy deposition is believed to be essential for the actual explosion (delayed explosion picture). Unfortunately, the current computer simulations that include standard physics and assume spherical symmetry do not generally succeed in reproducing an explosion [77]. It could simply be due to the excessive simplifications adopted or it could even be a hint for the need of new physics. This does not necessarily mean that something is missing in our general understanding. The problem is likely to originate from the complexity of the system to be modeled and the variety of the physics involved. It may just be necessary to turn to full 3D simulations able to account for non-spherically symmetric effects. Convection is likely to be important in this context, since it may boost the neutrino luminosity [18]. Moreover, the neutrino energy deposition in what was the prompt shock is likely to be just one of the several effects giving rise to the explosion [79] and the outcome critically depends on a number of poorly known variables like the progenitor structure, the equation of state, the details of neutrino transport, etc. Also note that a purely neutrino driven explosion is not obviously reconciliable with the indications of a non-spherical mechanism [80].

(iii) The cooling phase is the stage in which neutrino interact more with the star environment, so let us focus on it a bit more closely. The process consists in the diffusion of the very energetic ($E \sim 100\,\mathrm{MeV}$) neutrinos out of the dense and hot inner core of the star (with mass $\sim M_\odot \simeq 2 \cdot 10^{33}\,\mathrm{g}$, radius $\sim 10\,\mathrm{km}$, density $\sim$ few $\cdot\, 10^{14}\,\mathrm{g\,cm^{-3}}$). The beta reactions effectively act as a continuous pumping of energy and lepton number from the core matter into the neutrinos, that carry them away. The evolution can be completely described in terms of a few dynamic variables, to be followed in the core during the evolution: the temperature T, the matter density ρ and the leptonic fractions $Y_{L_{e,\mu,\tau}} = Y_{\nu_{e,\mu,\tau}} + Y_{e,\mu,\tau}$, where Y_x is the net number fraction per baryon of the species x: $Y_x = (n_x - n_{\bar{x}})/n_B$. At the beginning, $T \sim 10 - 40\,\mathrm{MeV}$ and $Y_{L_e} \sim 0.35$ (with some characteristic initial profile produced during the collapse phase). In such conditions ν_e are highly degenerate, with a large chemical potential. On the contrary, $Y_{L_{\mu,\tau}} = 0$, since these flavours are produced in pairs. The mean free path of a $200\,\mathrm{MeV}$ neutrino is $\lambda \sim 10\,\mathrm{cm}$. This determines the time scale for neutrino diffusion and emission: $t_{\mathrm{diff}} \sim 3R^2/\lambda \sim 10\,\mathrm{sec}$ for a neutrino at a depth $R = 10\,\mathrm{km}$ in the inner core. Neutrinos carry out of the core almost all the energy and the (electron) lepton number and leave, at the end of the process, a cold, deleptonized proto-neutron star.

Coming out from the inner SN core, the emitted neutrinos have to go through several stages before they constitute the signal that can be detected on Earth. First is the flavor and energy redistribution that takes place up to the neutrino spheres, defined as the regions after which neutrinos are not trapped anymore and stream freely (roughly at $\rho \sim 10^{12}\,\mathrm{g\,cm^{-3}}$): in short, every outgoing very energetic neutrino experiences several interactions and degradates its energy that goes redistributed into many lower

[18] However, whether such effects do provide a solution of the SN problem is still an open issue [78].

energy neutrinos ($\sim 10\,\mathrm{MeV}$). A detailed examination of this phase would require a careful study of the evolution of the mantle; see e.g. [81]. What one can reasonably do in first approximation, instead, is to assume that the energy E emitted from the inner core ends almost equiparted in neutrinos and antineutrinos of all flavours, once the portion carried by the lepton number excesses has been subtracted; also, the (positive) lepton number L_e (and possibly $L_{\mu,\tau}$) are assumed to be separately conserved in the reprocessing. With these ingredients one can determine the neutrino and antineutrino number fluxes in each flavour: $n_{\bar{\nu}_j} \simeq \frac{1}{\langle E_{\bar{\nu}_j}\rangle}\left(E - \sum_i \langle E_{\nu_i}\rangle L_i\right) / \left(3 + \sum_i \langle E_{\nu_i}\rangle / \langle E_{\bar{\nu}_i}\rangle\right)$, $n_{\nu_j} \simeq L_j + n_{\bar{\nu}_j}$, where $i, j = e, \mu, \tau$. As for the average energies, typical values are given by $\langle E_{\nu_e}\rangle \approx 13\,\mathrm{MeV}$, $\langle E_{\bar{\nu}_e}\rangle \approx 16\,\mathrm{MeV}$ and $\langle E_{\nu_{\mu,\tau},\bar{\nu}_{\mu,\tau}}\rangle \approx 23\,\mathrm{MeV}$.[19] Their difference is due to the fact that neutrinos of different families do not experience the same interactions with matter and therefore are set free at different depths in the star environment, characterized by different temperatures: non-electron neutrinos lack charged current interactions and therefore stream freely from a deeper, hotter region; electron neutrinos and antineutrinos, instead, interact with protons and neutrons also via charged current processes, the neutrinos mainly feeling the presence of the more abundant neutrons and therefore being trapped the most. As a bottom line, the typical percentage composition of the neutrino flux that comes out of the neutrino spheres in standard conditions is depicted in fig.1.5

Concerning the spectral shape, the accurate results of simulations are usually empirically approximated by a so called "pinched" Fermi-Dirac spectrum for each flavor $\alpha = \nu_e, \bar{\nu}_e, \overset{(-)}{\nu}_{\mu,\tau}$

$$f(E,t) \propto \frac{E_\nu^2}{e^{E_\nu/T - \eta_\alpha} + 1} \tag{1.9}$$

where the pinching parameter η_α is in principle variable in time (decreasing) and takes the typical values $\eta_{\nu_e} \sim 5 - 3$, $\eta_{\bar{\nu}_e} \sim 2.5 - 2$, $\eta_{\overset{(-)}{\nu}_{\mu,\tau}} \sim 0 - 2$ [75].

Next, neutrinos and antineutrinos undergo the matter flavor oscillations in the peripheric low-density region of the star and the vacuum flavor oscillations in the journey from the supernova to Earth. The first transition at very high densities is produced by the small matter potential difference between tau and muon neutrinos, which is due to the mass difference of the corresponding leptons. This transition is found to be completely adiabatic and switches the $\overset{(-)}{\nu}_\mu$, $\overset{(-)}{\nu}_\tau$ flavour eigenstates to the states rotated by the angle θ_{23}, labelled $\overset{(-)}{\nu}_{\mu'}$ and $\overset{(-)}{\nu}_{\tau'}$. At lower densities, two more resonances are met, due to the charged current contribution to the electron matter potential. In the case of normal hierarchy, these resonances are both active in the neutrino sector. The ν_e–$\nu_{\mu'}$ resonance turns out to be adiabatic for LMA values while for the ν_e–$\nu_{\tau'}$ we consider a level crossing probability P_H, which can vary from 0 to 1 depending on the value of θ_{13}. For a more detailed analysis, I refer the reader to [83, 84]. Finally, neglecting terms proportional to $\sin\theta_{13}$, the neutrino and antineutrino fluxes F reaching the Earth's

[19] Recent results based on numeric simulations of the mantle evolution, however, point out [82] that the mean energies of muon and tau neutrino and antineutrino can be closer to the electron antineutrino's, at the level of less than $1.2\,\langle E_{\bar{\nu}_e}\rangle$ during the core cooling phase and that the equipartition of energy may not be present. I will consider this possibility later in the analysis. Nevertheless, the standard picture outlined above is effective in giving a qualitative understanding of the neutrino flux composition.

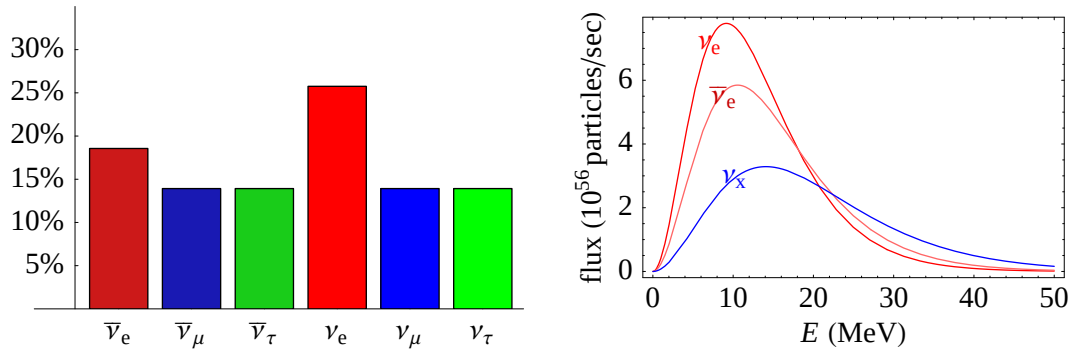

Figure 1.5: Typical indicative neutrino flux composition at the exit of neutrino-spheres (left panel) and typical energy spectra (right panel).

surface are related to the neutrino sphere fluxes F^0 by the simple relations

$$F_e = P_H s_{12}^2 F_e^0 + c_{12}^2 F_\mu^0 + (1-P_H) s_{12}^2 F_\tau^0 \tag{1.10a}$$
$$F_\mu = \left(P_H c_{12}^2 c_{23}^2 + (1-P_H) s_{23}^2\right) F_e^0 + s_{12}^2 c_{23}^2 F_\mu^0 + \left(P_H s_{23}^2 + (1-P_H) c_{12}^2 c_{23}^2\right) F_\tau^0 \tag{1.10b}$$
$$F_\tau = \left(P_H c_{12}^2 s_{23}^2 + (1-P_H) c_{23}^2\right) F_e^0 + s_{12}^2 s_{23}^2 F_\mu^0 + \left(P_H c_{23}^2 + (1-P_H) c_{12}^2 s_{23}^2\right) F_\tau^0 \tag{1.10c}$$

$$F_{\bar{e}} = c_{12}^2 F_{\bar{e}}^0 + s_{12}^2 F_{\bar{\tau}}^0 \tag{1.11a}$$
$$F_{\bar{\mu}} = s_{12}^2 c_{23}^2 F_{\bar{e}}^0 + s_{23}^2 F_{\bar{\mu}}^0 + c_{12}^2 c_{23}^2 F_{\bar{\tau}}^0 \tag{1.11b}$$
$$F_{\bar{\tau}} = s_{12}^2 s_{23}^2 F_{\bar{e}}^0 + c_{23}^2 F_{\bar{\mu}}^0 + c_{12}^2 s_{23}^2 F_{\bar{\tau}}^0 \tag{1.11c}$$

where s_{ij} and c_{ij} are the sine and cosine of the angle θ_{ij}.

In standard conditions, the typical percentual composition of the neutrino flux reaching the Earth surface after this complicated flavor reshuffle is depicted for instance as the first columns of fig. 3.9.

Finally, in order to predict the actual signal in the detectors, one should also consider matter-induced oscillations inside the Earth. This effect can significantly change the expected signal, but of course depends on the geographical position of the detectors at the time of arrival of the signal. For a given path in the Earth, it is not difficult to include the matter effect (see [83, 84]).

1.3.2 The energy loss constraint

Although the details can be complicated, some robust key features of the picture above can be highlighted:

- first, the total energy emitted in neutrinos roughly corresponds to the gravitational energy of the progenitor star (estimated in $\sim$ few $\cdot\, 10^{53}$ erg for a typical star);

- second, the overall timescale of neutrino emission is predicted to be a few tens of seconds, since it is determined by the conditions of neutrino trapping.

Remarkably enough, these key features are confirmed by SN1987a, the single supernova event in which we could detect the neutrino signal (namely: about 20 $\bar{\nu}_e$) so far [85]. As a consequence, any loss in a channel that is alternative to (active) neutrinos must neither drain a too large portion of the total energy nor shorten the neutrino emission too much. This energy loss constraint, even though so simple, proves to be a stringent one for several kinds of modification that one is willing to introduce in the standard supernova evolution. Considering the low statistics of the SN1987a signal, usually a reasonable constraint is set by considering a reduction of more than, say, 70% of the final $\bar{\nu}_e$ flux in the detectors (IMB and K2), with respect to the standard case, as unacceptable.

The dangerous loss of energy (and, therefore, of neutrino events at detection) could occur at different stages and sites. Namely

- in the SN core (the production region of neutrinos, think for instance of competitor carriers of energy that could be parallely produced in the core, like axions, KK gravitons, KK neutrinos...),
- in the SN mantle that neutrinos have to cross (think for instance of resonant oscillations into sterile states, of non standard neutrino interactions...),
- during the travel of neutrinos in the interstellar space towards detection on Earth (think for instance of vacuum oscillations into sterile states, of exotic neutrino decays...)
- even during the crossing of Earth matter, via resonant oscillations, just before the detection of the neutrinos in an underground laboratory.

All different effects (and their possible interplay and pile-up) have to be considered in order to reliably estimate the resulting constraints.

Other declinations or specifications of the energy loss constraint provide alternative sources of bounds (besides the direct detection of SN1987a neutrinos), often considered in the literature. They include

- *r-process nucleosynthesis*: a fraction of the heavy elements in nature is supposed to be synthetized in the region surrounding the core of the exploding stars, via rapid neutron capture (the so-called "r-process"), provided that the electron fraction $Y_e < 0.5$; since a modification of neutrino fluxes (e.g. due to flavor oscillation among active states or to conversion into sterile states) would affect Y_e, the request of a successful r-process nucleosynthesis can be used to set limits;
- *re-heating of the shock*: in the delayed-shock/neutrino-driven picture of SN explosion, the flux of neutrinos and antineutrinos from the early stages of the cooling phase are responsible for the actual explosion of the star, pushing from below the stalling shock wave; since electron neutrinos (and antineutrinos) are the most effective in this (interacting with charged and neutral currents with baryonic matter), a cut of their flux would prevent this mechanism from working.

In the following, however, I will only consider the bound from direct observation, which can be considered strong enough. Indeed, although the r-process bound can be a severe one, I believe it cannot be considered as compelling as desired (for instance, alternative sites for effective nucleosynthesis have been recently proposed). On the same step, since the details and the nature itself of the neutrino-driven explosion mechanism are still to be fully understood, I prefer not to consider it here as a robust constraint, not mentioning that it would require a demanding understanding and simulation of the evolution of the SN mantle.

1.3.3 Waiting for the next supernova

Given all the discussion above, it is evident that the day of the next (galactic[20]) explosion of a supernova will be a great day for neutrino physics. So, while we wait, a few questions can be addressed: Can we reasonably expect such a SN event in the near future? Will we be able to fully detect its neutrino signal? Which features of the signal are generically more rich in information? [21]

The answer to the first question is (statistically) easy. Observing SN rates in other nearby galaxies a (slightly discouraging) estimate of 2 ± 1 events/century in the Milky Way can be inferred. However, here a tricky point is the determination of which kind of galaxy is more similar to ours. On the other hand, turning to a historical approach, i.e. looking at the observed and recorded SNe in the latest centuries, and extrapolating to include regions of the galaxy that are obscurated by dust, the estimate does not change much: $3 \div 4$ events/century [86]. From experiments, of course, we only have loose upper bounds on the galactic SN rate: since the Baksan detector has only seen the SN1987A event in 17.6 years of actual lifetime, no more than 13 events/century can be expected [87]. And since SuperKamiokande did not detect any significant background of relic $\bar{\nu}_e$ (above a threshold of 18 MeV) from all past SNe, less than ~ 30 events/century can occur [88]. However, these bounds could soon become more stringent [89].

The answer to the second question is definitely more encouraging: at the present neutrino detectors (mainly designed for solar neutrinos, like SK, SNO or KamLAND, or more aimed to SN ν detection (and therefore more long-lasting and optimized) like LVD, Baksan...) the collected number of events will be large enough to allow a satisfying analysis of the signal, and the situation brightly improves if some of the future "second generation" detectors will be running at the time of the explosion. To support the optimism, in Table 1.2 we show the indicative number of events expected at several experiments, divided by neutrino flavor.

The dominant signal consists of course of $\bar{\nu}_e$, easily detected through the inverse beta decay reaction on water/scintillator protons: compared to the mere $\sim$ 20 events of SN1987a the improvement is evident. This reaction benefits of a relatively low threshold (1.8 MeV) that does not cut much of the characteristic spectrum.

[20] The location of the exploding star needs to be galactic otherwise the neutrino flux will be too low to allow a sufficient statistics at present or near-future detectors; however we could even accept an event in the Large Magellanic Cloud, a satellite galaxy of the Milky Way, where the SN1987a was.

[21] I thank Francesco Vissani for a careful reading of this Section and for useful comments and suggestions.

ES on electrons	$\nu e^- \to \nu e^-$	(a)
CC on protons	$\bar{\nu}_e p \to e^+ n$	(b)
CC on deuterium	$\nu_e d \to e^- pp$	(c1)
	$\bar{\nu}_e d \to e^+ nn$	(c2)
NC on deuterium	$\nu d \to \nu np$	(d)
CC on Argon	$\nu_e\, ^{40}\mathrm{Ar} \to ^{40}\mathrm{K}^* e^-$	(e)
CC on organic nuclei	$\nu_e\, ^{12}\mathrm{C}, \to e^- X$	(f1a)
	$\nu_e\, ^{16}\mathrm{O} \to e^- X$	(f1b)
	$\bar{\nu}_e\, ^{12}\mathrm{C} \to e^+ X$	(f2a)
	$\bar{\nu}_e\, ^{16}\mathrm{O} \to e^+ X$	(f2b)
NC on organic nuclei	$\nu\, ^{12}\mathrm{C} \to \nu\, ^{12}\mathrm{C}^*(\to \gamma)$	(g1)
	$\nu\, ^{16}\mathrm{O} \to \nu\, ^{16}\mathrm{O}^*(\to \mathrm{X} + \gamma' s)$	(g2)
NC on high-Z nuclei	$\nu\,\mathrm{Ca,Na,Pb} \to nX$	(h)
ES on protons	$\nu p \to \nu p$	(i) [90]
ES on Ne (or other noble gas)	$\nu\,\mathrm{Ne} \to \nu\,\mathrm{Ne}^*(\to \gamma)$	(l)

Table 1.1: Most of the considered reactions for the detection of SN neutrinos. ν stands for neutrinos and antineutrinos of all flavors. See the references in the caption of Table 1.2. Caveat: several reactions look similar in principle but can be very different from the experimental point of view (tagging of the reaction products, of the recoils, experimental cleanness, backgrounds...). In particular, a relevant issue is the energy thresholds, which can be very different. Part of these considerations are taken into account in the making of Table 1.2.

The ν_e will be more difficult to efficiently detect and recognize; the main tool consists of the elastic scattering on electrons, which also allows to reconstruct the arrival direction of the neutrino and therefore to point at the SN; in SNO's heavy water, the deuterium dissociation in two protons is a promising channel, characterized by a low threshold and recently tested with solar neutrinos.

The flux of $\overset{(-)}{\nu}_{\mu,\tau}$ can be inferred by deduction from the events that are caused by neutrinos and antineutrinos of all flavors, since the production of μ and τ leptons is of course under threshold in the range of SN neutrino energies. Striking is the possibility of collecting a lot of information from neutrino-proton elastic scattering in a scintillator detector like KamLAND or Borexino, able to tag the recoiling proton (thanks to its low threshold, not enjoyed by Čerenkov water detectors). However, for this to work, given the low recoil energy of the proton, the background must be well under control. The numbers reported in Table 1.2 are perhaps on the optimistic side.

A general remark is in order: since any detector or principle of detection is more sensible to different features of the neutrino signal, it is of course important to combine all the different observations. This for instance also helps in the identification of the SN direction, via triangulation. For the same generic need of redundance, also the large telescopes designed for high energy neutrinos (Amanda-IceCube and the sea projects [101], [102], [103]) or even non-underground detectors aimed to accelerator beams (MiniBooNE [104]) can have a role.

What features will we look for in such an abundant neutrino signal from the next event, then? One can schematically list:

	water		heavy water	scintillator		liquid Ar	liquid Ne	high-Z
existing:	SK		SNO	LVD	KamLAND/			
future:		UNO			Borexino	Icarus/ LANNDD	CLEAN	OMNIS
total	∼7600	$\sim 10^5$	∼1100 (H_2O + D_2O)	∼ 320	∼500(1100 with (i))/ ∼100	∼110/ thousands	∼400	∼ 1000
$\bar{\nu}_e$	(b) (96%)		(b) (40% H_2O) (c2) (18% D_2O) (d) (4% D_2O)	(b) (93%)		(a)	(l)	
	7350	10^5	**680**	300	400/80	4/tens	30	
ν_e	(a) (1.5%) (f1) (0.7%)		(a) (2.3%) (c1) (10%) (d) (4%)	(a) (1.5 %) (f1a)		(e)	(l)	
	150	1500	180	5	15/5	90/3000	30	
$\overset{(-)}{\nu}_{\mu,\tau}$	(a) (0.9%)		(d) (20%)	(g1) (3.5%)		(a)	(l)	(h)
	70	1000	**220**	10	45(**670** with (i))/20	4/1000	330	880

Table 1.2: Indicative number of collected events expected at several neutrino detectors (existing, in construction or projected), in case of a SN ∼10 Kpc away from Earth. The most interesting numbers at existing detectors are given in bold face. The letters in parenthesis refer to the relevant reaction among those listed in Table 1.1, with an approximate percentage of the total events it is responsible for. The numbers are only an indication and not all the possible reactions are considered. Icarus data refer to the 1.2 Kton set-up; in smaller or larger configurations, the numbers can vary accordingly. The set of references includes: [91], [92], [93], [90], [94], [95], [96], [97], [98], [99], [100].

- the time structure of the signal, as produced by the SN core and deep layers. For instance, SN models predict a first sudden burst of ν_e followed by the cooling-phase neutrinos of all flavors which last tens of seconds; this structure has not been observed yet and can carry precious hints about the early evolution of the deep layers of the star, namely the shock wave, or even on exotic neutrino properties [105]. Moreover, the time evolution of the cooling-phase neutrinos itself will allow a better understanding of the physics of neutrino transport. Besides that, exotic modifications of the core evolution can have an imprint on the time structure, even preserving the overall time scale and total energy emission; we will see an example of this case in Chapter 3.

- the flavor composition of the flux, as determined by the core emission itself or by the subsequent redistribution. For instance, we will see an example in Chapter 3 of distorted flux composition signaling exotic phenomena at work.

- the spectra of each of the different flavors, which are probably the richest source of insight on neutrino properties. Just to quote some possibilities, the game of flavor oscillations (matter (star and/or Earth) and vacuum) among active neutrinos is responsible for the overall hardening or softening of the original spectra and for peculiar energy-dependent features. From the analysis of

the spectra some of the values of the oscillation parameters could possibly be inferred, for instance θ_{13}, sign(Δm^2_{23})... [93, 106, 107, 108, 109]. Moreover, the modifications in the SN mantle due to the passing shock wave can modify the oscillation game, allowing maybe to obtain information on the shock wave itself from the neutrino spectra [110]. On the other hand, the oscillations into invisible states (e.g. sterile neutrinos) can lead to characteristic shapes of the spectra. We will address this issue more closely in Chapter 2.

1.4 The role of the Early Universe

The Early Universe can be a powerful laboratory for Particle Physics, and particularly for neutrino physics [111]. The fundamental reasons for this basic fact are simply listed:

- (light) neutrinos are very abundant (namely "as abundant as photons") for a long period of the evolution of the universe, keeping thermal equilibrium until $T \sim$ few MeV;
- in a Friedman-Robertson-Walker standard cosmology, the total energy density is a crucial parameter that sets the expansion rate of the universe; since that energy is predominantly stored in the relativistic species, namely electrons, positrons, photons and all species of neutrinos, for $T \simeq 100\,\mathrm{MeV} \to 1\,\mathrm{MeV}$, it is evident that the relative abundance of neutrinos (e.g. increased by the presence of additional states) can make a real difference and reveal some of their properties;
- the early plasma is so dense that neutrinos are initially trapped and undergo peculiar matter effects while the density decreases as a consequence of the expansion;
- the detailed balance of the different species of neutrinos among themselves can also be important for processes that distinguish flavor: for instance, the ν_e density affects the $n \to p$ conversion and therefore is imprinted in the primordial ratio of n/p that we read today (see below).

We have access to several different windows during the history of the Universe. Actually, this dispersion in time and, moreover, the diversification of the adopted investigation techniques are bonus features that allow some important cross tests. The overall consistent picture of the evolution of the Universe that comes out is a wonderful success of modern cosmology that must not be underestimated.

On the other hand, it is true that cosmological constraints are often based on untested assumptions and plagued by systematic uncertainties that we cannot resolve. Moreover, it often happens that a given observable is sensitive to several independent cosmological parameters, so that the determination of one of them depends on the values adopted for the others ("priors") and degeneracies are almost the rule, considering also the poor number of observables. In other words, the obvious fact that we have only one Universe at disposal and we cannot tune its parameters one at a time is our main limit. Nevertheless, the sensitivity of many cosmological processes to neutrino properties (masses, oscillation parameters...) is nowadays competitive with direct measurements and even offers better prospective of improvements in the near future, making the study of quantitative neutrino cosmology worthwhile. In the following I will briefly review the basic features of the main cosmological tools that are more relevant for neutrino physics.

1.4.1 Big Bang Nucleosynthesis

The earliest window ($T \sim 10 \div 0.1\,\mathrm{MeV}$, time $\sim 0.01 \div 100\,\mathrm{sec}$) of our interest on the history of the Universe is open on primordial (Big Bang) Nucleosynthesis (BBN), during which most of the light elements were produced by chains of nuclear reactions. Of particular interest are its predictions for Deuterium (D), Lithium (^{7}Li) and the ^{3}He and ^{4}He isotopes of Helium, whose primordial abundance

we can infer via astronomical observation in some of the most ancient and untouched environments in the universe (young galaxies, pristine clouds...).

In this Section I will qualitatively review the basic points of BBN [115] and how it compares with observations, while in Section 2.2.1 I will set up the complete formalism that is necessary in order to obtain precise predictions and to include the modifications due to the presence of an extra sterile neutrino. Any detail that is missing in this qualitative Section should be found there.

1.4.1.a The tale

The all-important quantity for the outcome of primordial nucleosynthesis is the ratio of neutron to protons n/p. This is rather obvious since these are the building blocks of the nuclei that are going to be formed and since essentially all neutrons are incorporated into some light element in the process, so that the neutron abundance at the moment that the synthesis begins essentially fixes the proportions of all the products. Among these, the ^{4}He constitutes by far the largest fraction in mass ($\sim 25\%$) (the abundances of the other nuclei (D, ^{7}Li and ^{3}He) are of the order of 10^{-5}, 10^{-10} and 10^{-5} in mass respectively), so that for purposes of illustration one can focus mainly on this quantity.

Let us follow, therefore, the qualitative evolution of n/p step by step as time elapses (or temperature decreases). The relative population of neutrons and protons is determined by the weak interactions

$$n \longleftrightarrow p + e^- + \bar{\nu}_e \tag{1.12a}$$

$$n + \nu_e \longleftrightarrow p + e^- \tag{1.12b}$$

$$n + e^+ \longleftrightarrow p + \bar{\nu}_e. \tag{1.12c}$$

At very high temperatures ($T \gg$ MeV) the two directions proceed at the same pace so that, essentially, $n/p \simeq 1$. More precisely: as long as the rates for these interactions, that are proportional to the temperature, are fast in comparison with the expansion of the universe, there are conditions of chemical equilibrium, i.e. by definition $\mu_n + \mu_{\nu_e} = \mu_p + \mu_e$; the number density of the non-relativistic species n and p are of course given by $N_{p,n} = g_{p,n}\left(\frac{M_{p,n}T}{2\pi}\right)^{3/2}\exp\left(\frac{\mu_{p,n}-M_{p,n}}{T}\right)$ so that, neglecting the electron and neutrino chemical potentials (an approximation which can be questioned if a large lepton asymmetry is present, see below)

$$n/p = \exp\left(-\frac{\Delta M}{T}\right) \tag{1.13}$$

with $\Delta M = M_n - M_p = 1.293\,\mathrm{MeV}$. While $T \gg$ MeV, $n/p \simeq 1$; as T decreases by means of the expansion, the ratio slightly decreases, accurately following eq. (1.13).

At $T \sim$ few MeV, the decoupling of the 3 neutrino species occurs. This means that the elastic scattering reactions $e^+e^- \leftrightarrow \nu\bar{\nu}$, $e\nu \leftrightarrow e\nu$ that are mainly responsible for the neutrinos to keep thermal equilibrium with the rest of the bath (consisting of γ, e^+, e^- and nucleons) are no more able to keep the pace of expansion (however, the weak interactions in eq. (1.12) can still be considered going on). In formulæ:

$$\Gamma_{\mathrm{es}}/H \lesssim 1\ , \tag{1.14}$$

which is easily interpreted as "the mean free path $\lambda \propto 1/\Gamma$ for a typical interacting particle becomes larger than the scale of the horizon H^{-1}". The Hubble parameter H is given by

$$H \simeq \sqrt{\frac{8\pi^3}{90}} g_*^{1/2} \frac{T^2}{M_{Pl}} \simeq 1.66\ g_*^{1/2} \frac{T^2}{M_{Pl}}. \tag{1.15}$$

where the parameter g_* counts the effectively massless degrees of freedom that contribute to the total energy density $\rho = \frac{\pi^2}{30} g_* T^4$

$$g_* = \sum_{i=bosons} g_i \left(\frac{T_i}{T}\right)^4 + \frac{7}{8} \sum_{i=fermions} g_i \left(\frac{T_i}{T}\right)^4 \tag{1.16}$$

For $T >$ MeV, $g_* = 2 + \frac{7}{8}4 + \frac{7}{8} N_\nu 2 \left(\frac{T_\nu}{T}\right)^4 = 10.75$, ($\gamma$, $e^\pm$, $N_\nu = 3$ with $T_\nu \equiv T$). The elastic scattering reactions rate is roughly $\Gamma_{\rm es} \simeq 0.2\ G_F T^5$. A detailed analysis gives the typical values

$$T_{{\rm decoupl},\nu_\mu,\nu_\tau,\bar\nu_\mu,\bar\nu_\tau} \simeq 5\,{\rm MeV} \qquad T_{{\rm decoupl},\nu_e,\bar\nu_e} \simeq 3\,{\rm MeV}, \tag{1.17}$$

the difference being due to the lack of charged current interactions for the non electron species. From this point on, it is useful to assign to the neutrinos a temperature T_ν; in first approximation, it evolves (redshifts) independently from the (photon) temperature T.

Slightly later on, for $T \lesssim 1\,{\rm MeV}$, the $e^\pm$ pairs annihilate, transferring their entropy to the thermal bath but not (in first approximation) to the decoupled neutrinos. The temperature T is raised with respect to the neutrino temperature by a factor $(11/4)^{1/3}$: $T_\nu = \left(\frac{4}{11}\right)^{1/3} T$. However, neither the neutrino decoupling nor the $e^\pm$ annihilation are instantaneous processes: the $\nu_e, \bar\nu_e$ are not completely decoupled at the time the annihilations begin and therefore they get actually a bit heated. Also, more energetic neutrinos decouple later so that they are more affected by the heating: distortions in the neutrino spectra arise. The careful inclusion of these effects in the formalism is straightforward although a bit involved, see the discussion in Chapter 2. Usually, it is easier (and equivalent) to keep conventionally T_ν at its decoupling value while augmenting the effective number of (active) neutrinos that contribute to the total energy density from $N_\nu = 3$ to a value which turns out to be roughly 3.04.

At $T_{\rm fo} \sim 0.7\,{\rm MeV}$, also the reactions eqs. (1.12) that interconvert neutrons and protons are no more able to keep track of the expansion, i.e. the so called "neutrino freeze out" occurs. In formulæ, analogously to what above,

$$\Gamma_{\rm weak}/H \lesssim 1 \Rightarrow T_{\rm fo} \simeq 0.7\,{\rm MeV} \tag{1.18}$$

where now roughly $\Gamma_{\rm weak} \simeq 2.1\ G_F T^5$ and the correct value of g_* is complicated by the ongoing annihilations and will in general be an interpolating number between $g_*(T >$ MeV$) = 10.75$ and $g_*(T \ll$ MeV$) = 3.38$ (γ, $N_\nu = 3.04$ with $T_\nu = \left(\frac{4}{11}\right)^{1/3} T$). The n/p ratio freezes at the value of

$$n/p = \exp\left(-\frac{\Delta M}{T_{\rm fo}}\right) \simeq \frac{1}{6}. \tag{1.19}$$

Neutrinos, from this point on, are out of the game.

However, the true beginning of nucleosynthesis still has to wait. Indeed, the coagulation of the nucleons is impeded for a while by the large number of photons, that immediately dissociate the would-be nuclei. A rough estimate of the temperature at which a nuclear species of mass number A becomes stable is given by

$$T_{\rm nucl} \simeq \frac{B_A/(A-1)}{\ln(\eta^{-1}) + 1.5\ln(m_N/T)} \tag{1.20}$$

where B_A is its nuclear binding energy. As apparent, the crucial parameter here is the baryon to photon ratio η; its very small value $\eta \sim 10^{-10}$ suppresses the value of $T_{\rm nucl}$ with respect to the naive intuition $T_{\rm nucl} \sim B_A$. The first building block to be cooked must be the Deuterium, after which all other elements feverishly are created. For Deuterium, one finds $T_{\rm nucl} = 0.07\,{\rm MeV}$ so nucleosynthesis begins only after this temperature is reached ("Deuterium bottleneck"). In this stalling phase, as the temperature continues to decrease, n/p slowly decreases by effect of occasional weak interactions, essentially dominated by the decay of the free neutrons. As a result

$$n/p\rfloor_{T=T_{\rm nucl,\,D}} \simeq \frac{1}{7}\,. \tag{1.21}$$

The last step is simply to determine the amount of ^{4}He that can be baked with that quantity of neutrons and protons. Straightforwardly, its mass fraction over the total mass of the nucleons is

$$Y_P \simeq \frac{4n_{^4{\rm He}}m_N}{(n_p+n_n)m_N} = \frac{4(n_n/2)}{n_p+n_n} = \frac{2\,(n/p)\rfloor_{T=T_{\rm nucl,\,D}}}{1+\,(n/p)\rfloor_{T=T_{\rm nucl,\,D}}} \simeq 25\% \tag{1.22}$$

As apparent, even this qualitative picture yields a remarkably sensible prediction for Y_P.

Let us summarize the crucial inputs of the discussion above. Put simple, one can think of BBN as a "2-inputs" $\rightarrow$ "4-outputs" black-box theory (and essentially this is how the publicly available codes [117] are effectively used). The outputs are of course the predicted abundances of ^{4}He, D, ^{7}Li and ^{3}He; many others are predicted, but the first two of these are the most useful for comparison with observations, as described below. The two crucial input parameters [22] are:

- η ($= n_B/n_\gamma$, baryon to photon ratio), that sets the nucleation temperature for Deuterium at which the actual nucleosynthesis begins; the larger η is, the sooner the synthesis begins and therefore, for instance, the more ^{4}He is produced, since more neutrons have survived;

- g_* as defined in eq. (1.16), that counts the effectively massless degrees of freedom that contribute to the total energy density; the more energy density is present, the faster the expansion, so that the freeze out (and the decoupling) occur at slightly higher temperatures, allowing more neutrons to survive and therefore, for instance, more ^{4}He to be produced.

[22] Of course many other internal parameters must be set (nuclear reaction rates, neutron lifetime...) but these are determined elsewhere and are tuned to their latest state-of-the-art values periodically (see e.g. [118]).

It is customary to parameterize deviations from the standard energy density content in terms of a deviation ΔN_ν in the effective number of neutrinos:

$$g_* = \text{eq. (1.16)} + \frac{7}{8}\,\Delta N_\nu\, 2\left(\frac{T_\nu}{T}\right)^4 \tag{1.23}$$

In other words, any additional particle or any additional effect is expressed in terms of the corresponding (fractional) amount of relativistic massless fermions that would produce the same final result.

Standard BBN (SBBN) is defined as $N_\nu \equiv 3$ (i.e. $\Delta N_\nu \equiv 0$): this corresponds to the situation within the SM in the approximation of instantaneous neutrino decoupling. The deviations from this value (which define *non-standard* BBN) can have different sources, which are not usually simple to disentangle.[23] Actually, we have already met an example of deviations from SBBN: relaxing the hypothesis of instantaneous neutrino decoupling and carefully including the partial neutrino reheating from $e^\pm$ annihilations, the related spectral distortions and finite temperature QED small effects one gets $\Delta N_\nu \simeq 0.04$, as anticipated above [120]. The deviations due to any exotic phenomenon go on top of this. Among those deviations, we are particularly interested in the following ones: a ΔN_ν can be due (i) to the actual presence of extra relativistic degrees of freedom (e.g. KK gravitons, sterile neutrinos...), or (ii) to the existence of distortions of neutrino and antineutrino spectra from a Fermi-Dirac distribution with zero chemical potential, or, on the contrary, (iii) to the presence of a chemical potential in the thermal spectrum for neutrinos or antineutrinos, corresponding to a primordial lepton asymmetry (*degenerate* BBN). Of course, two ΔN_ν can be engineered to cancel each other, drastically reducing the information that can be extracted from measurements. For instance, a very large lepton asymmetry can hide the effect of an additional sterile neutrino. Having said that this extreme possibility exists, in Chapter 2 we will stick to *non*-degenerate BBN and we will adopt an approximation to avoid following spectral distortions (see the discussion there).

The sensitivity of (non-standard) BBN predictions to the values of the parameters η and ΔN_ν is expressed by the following fit formulæ [121, 119]

$$Y_p \simeq 0.248 + 0.0096 \ln \frac{\eta}{6.15\ 10^{-10}} + 0.013\ \Delta N_\nu^{(^4\mathrm{He})}, \tag{1.24}$$

$$Y_\mathrm{D} \simeq (2.75 \pm 0.13)\ 10^{-5}\ \frac{1 + 0.11\ \Delta N_\nu^{(\mathrm{D})}}{(\eta/6.15\ 10^{-10})^{1.6}}. \tag{1.25}$$

1.4.1.b Comparison with observation

^{4}He: The abundance of ^{4}He is measured (looking at the intensity of its recombination lines) in clouds of ionized hydrogen (H II regions) in Blue Compact Galaxies (BCG), very young galaxies with a high star formation rate. These are among the least chemically evolved systems in the universe, a fact that guarantees the primordiality of almost all the present Helium. More precisely, a small quantity

[23] Moreover, some observables can be sensitive to ΔN_ν's produced by certain causes and not to others. This is the reason why in eq. (1.24) and eq. (1.25) below one has to distinguish between the effective ΔN_ν for ^{4}He and D production. For a detailed discussion see for instance [119] and references therein.

of additional ^{4}He has certainly been produced by stellar burning, but this is positively correlated with the abundance of other elements of stellar origin ("metals": C, N, O) in the same region. Therefore, performing an extrapolation to zero metallicity, the truly primordial abundance of ^{4}He can be inferred.

At present, a long lasting disagreement among the results obtained by different groups is still alive. Although the adopted techniques are essentially the same, the considered sets of H II regions and of BCGs overlap only partially and, above all, the correct treatment of the systematic uncertainties is under debate. For the sake of illustration, fig. 1.6 is an (incomplete) list of the most recent experimental results.[24] A conservative estimate must therefore be

$$Y_P \equiv Y_{^4\mathrm{He}} = 0.238 \pm 0.007\,. \tag{1.26}$$

D: Since it is believed that there are no astrophysical processes able to produce Deuterium, the measurement of its abundance is of particular importance. In particular, given its strong inverse dependance on the value of η, it can be used as a powerful "baryometer", alternative to the (now better) determination from CMB (see below).[25] Primordial Deuterium abundance is mainly measured looking at its isotopic shifted Lyman-α absorption lines in the light from very far quasars. The present (conservative) estimate is affected by a large uncertainty:

$$Y_{\mathrm{D}} = (2.8 \pm 0.5)\ 10^{-5}\,. \tag{1.27}$$

^{7}Li and ^{3}He: Primordial Lithium abundance is mainly measured in selected hot, metal-poor stars in the halo of our galaxy, that almost certainly have not burnt it in significant quantities. A conservative estimate can be considered $Y_{^7\mathrm{Li}} = (1.23 \pm 0.15)\,10^{-10}$ [113]. The primordial abundance of ^{3}He, instead, is difficult to estimate, since the only available sites are chemically evolved regions in our galaxy or in the solar system, and is therefore commonly not included in the comparisons with BBN predictions. The estimate gives $Y_{^3\mathrm{He}} < (1.9 \pm 0.6)\,10^{-5}$ [113].

A picture of the present condition of Standard BBN is expressed by fig.1.7. The solid colored lines are the abundances predicted by the theory as a function of $\eta \times 10^{10}$ (with their uncertainty). On the vertical axis, the measured abundances with their errors determine intervals whose intersection with the solid lines identifies correspondent allowed intervals of η. The region of their overlapping is given by the blue blurred band, indicating the acceptable consistency and overall success of the theory for $2.6 < \eta < 6.2$; however, it is true that the agreement is much less satisfactory if the more stringent estimates of the errors are used.

Actually, the best determination of η comes nowadays from the CMB anisotropy measurements by WMAP (combined with other CMB experiments, Large Scale Structure and Lyα data) [133]:

[24] Unfortunately, no other competitive method seems to be presently available. In [131, 132] the possibility is discussed to determine the primordial He abundance from the details of the CMB spectrum, based on the fact that the He atoms start recombining before the last scattering time, subtracting free electrons to the matter fluid that is still coupled with CMB photons. However, although [132] is surprisingly more optimistic, it looks like this method cannot measure Y_P more precisely than a 5%, even with future(-istic) CMB experiments.

[25] However, since Deuterium is easily destroyed in stars, strictly speaking one can be confident only of an upper bound on η.

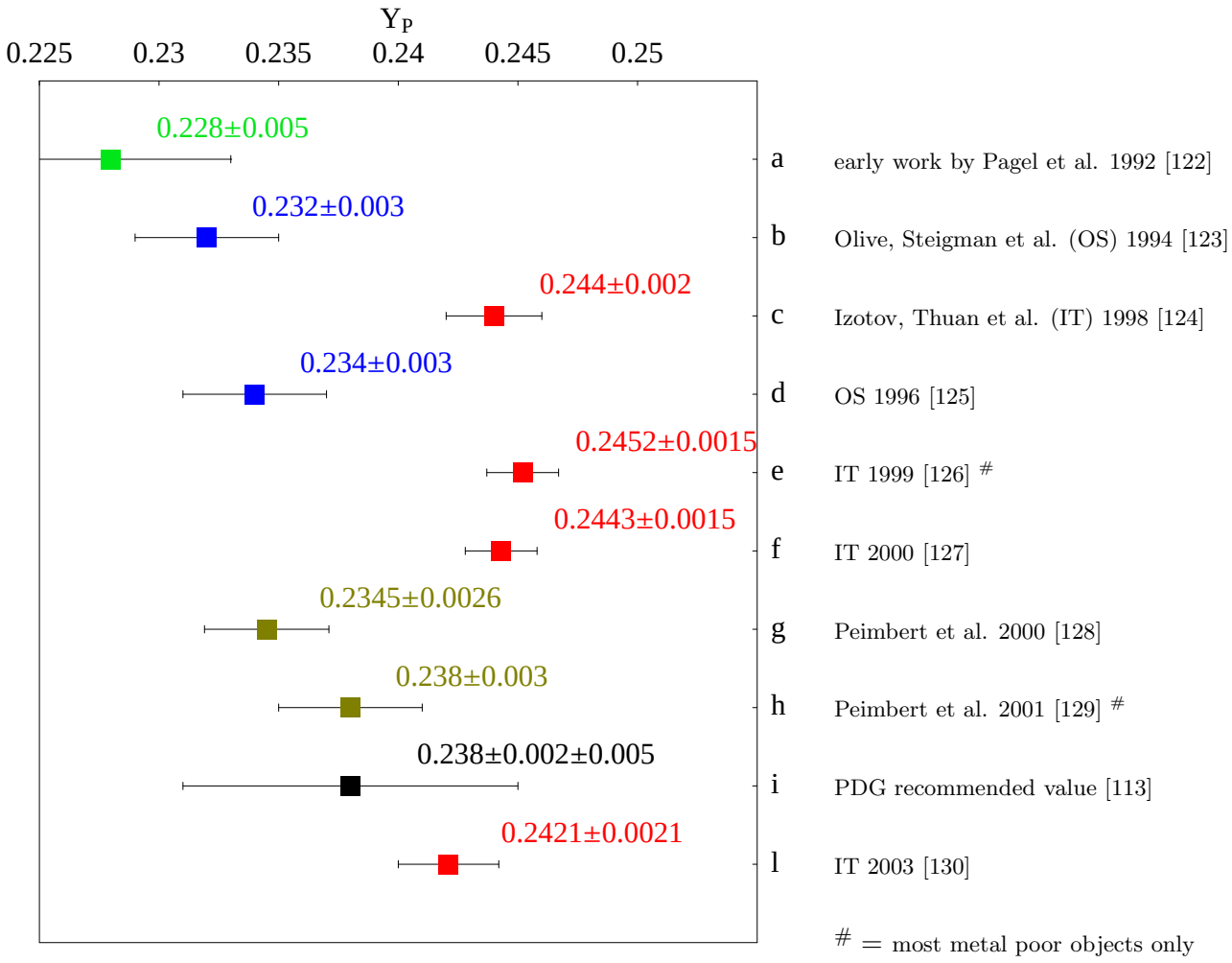

Figure 1.6: Some recent experimental results in the determination of Y_P. The bars correspond to the claimed 1σ errors. The PDG recommended value adds an estimate of the systematic uncertainties (± 0.005).

$$\eta = 6.1^{+0.3}_{-0.2}\ 10^{-10} \tag{1.28}$$

at 68% CL. The good agreement of the determination of η from BBN consistency and from CMB (that probe different epochs and use completely independent techniques) is to be considered as one of the best successes of recent cosmology. On the other hand, it is evident that the tension between the D and the ^{4}He (and ^{7}Li) measurements is exacerbated. In other words, the use (as plausible) of the η from CMB as an input for Standard BBN leads to a slightly high prediction for the ^{4}He primordial abundance. This fact has even been interpreted by some authors as evidence for the need of a non-Standard BBN.

Running the BBN codes with η from CMB and with N_ν as a free parameter and comparing the results with the observed primordial abundances, several authors have found bounds on N_ν. A summary

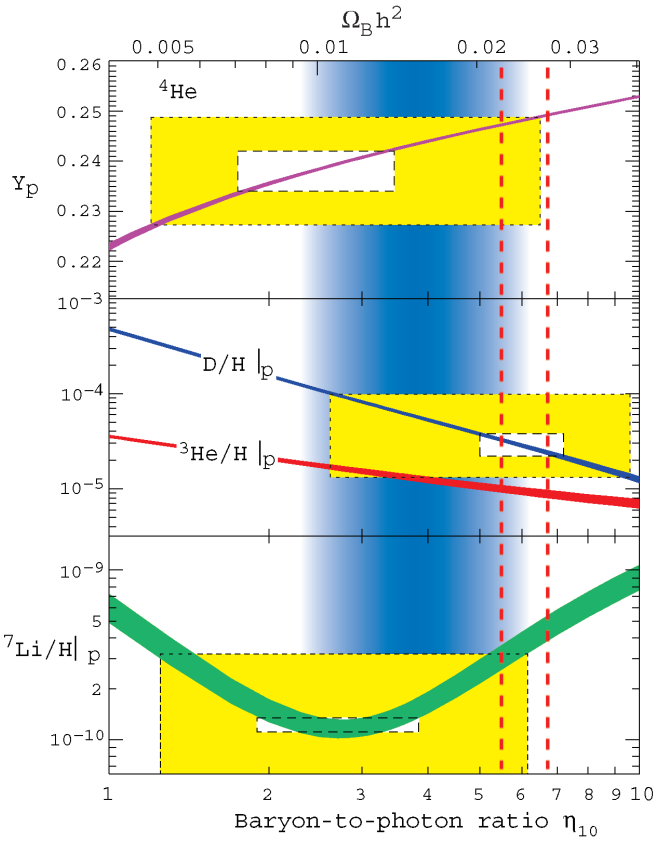

Figure 1.7: The primordial abundances of ^{4}He, D, ^{3}He and ^{7}Li as predicted by the standard BBN model compared to observations. Smaller (white) boxes correspond to 2σ errors; larger (yellow shaded) boxes correspond to more conservative estimates of the statistical and systematic errors. The WMAP value of η is also reported as red vertical dashed lines. Adapted from [113].

$N_\nu = 2.2 \rightarrow 3.1$ (IT values for ^{4}He) $N_\nu = 1.0 \rightarrow 3.4$ (PDG value for ^{4}He)	[119]
$N_\nu = 2.3 \rightarrow 3.0$	[144]
$N_\nu < 3.4$	[145]
$N_\nu = 1.7 \rightarrow 3.0$	[142]
$N_\nu = 2.5 \pm 0.4$	[146]

Table 1.3: Bounds on the effective number of neutrinos from BBN. Intervals are at 2σ, except 3σ [119].

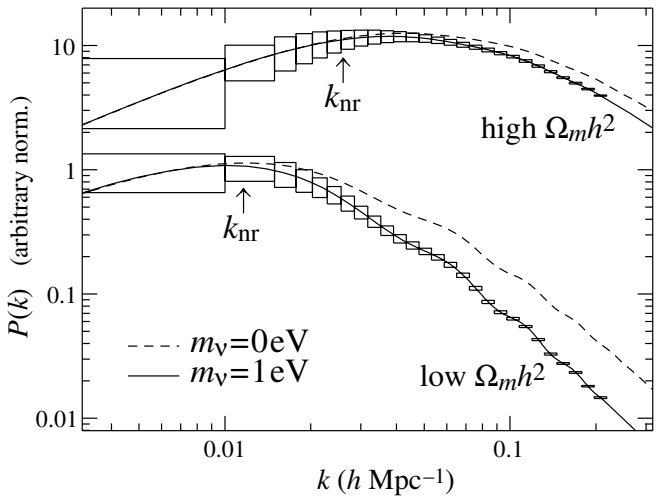

Figure 1.8: Sensitivity of the LSS power spectrum suppression to neutrino mass. From [134].

of the latest results is in Table 1.3.

As can be checked using eq. (1.24) and eq. (1.25), compared with eq. (1.26) and eq. (1.27), all those results can be roughly summed up in

$$N_\nu^{^4\mathrm{He}} \simeq 2.4 \pm 0.7\,, \tag{1.29}$$

$$N_\nu^{\mathrm{D}} \simeq 3 \pm 2\,. \tag{1.30}$$

1.4.2 Large Scale Structure and Cosmic Microwave Background

Neutrinos can also be studied looking at the distribution of galaxies. The connection lies at the time of the formation of the anisotropies in the primordial plasma that were the seeds for the formation of the Large Scale Structures (which took place much time later). The point is that the neutrinos, relativistically traveling through the plasma (from which they are decoupled) until their mass is of the order of the temperature, have the effect of smoothing the anisotropies, i.e. they cause a suppression in the power spectrum of the galaxies that is measured today. Qualitatively, light neutrinos travel relativistically for a long period and therefore delay the formation of structures characterized by a scale smaller than that of the horizon at the time they become non-relativistic. The more massive the neutrinos are, the earlier they become non-relativistic, the smaller the scale of the horizon is at that time, inside which the perturbations are smoothed, the more suppressed are the large momenta of the LSS power spectrum. The effect is well visible in fig. 1.8.

In formulæ, the effect is usually expressed in terms of the quantity Ω_ν, which is related to the sum of the neutrino masses [114]

$$\Omega_\nu h^2 = \frac{\mathrm{Tr}[m \cdot \rho]}{93.5\,\mathrm{eV}} \tag{1.31}$$

where m is the 4×4 neutrino mass matrix and ρ is the 4×4 neutrino density matrix, better discussed in 2.2.1. In a standard case, the numerator corresponds to $\sum m_{\nu_i}$. Ω_ν is related to the suppression

$\sum m_{\nu_i} < 1.8\,\mathrm{eV}$	$\Omega_\nu h^2 < 2.0\,10^{-2}$	$n = 1$	2dF coll. [137], pre WMAP
$\sum m_{\nu_i} < 2.2\,\mathrm{eV}$	$\Omega_\nu h^2 < 2.4\,10^{-2}$	running n	
$\sum m_{\nu_i} < 2.47\,\mathrm{eV}$	$\Omega_\nu h^2 < 2.6\,10^{-2}$	$n = 1$	[138], pre WMAP
$\sum m_{\nu_i} < 0.71\,\mathrm{eV}$	$\Omega_\nu h^2 < 0.76\,10^{-2}$		WMAP coll. [133]
$\sum m_{\nu_i} < 1.7\,\mathrm{eV}$	$\Omega_\nu h^2 < 1.8\,10^{-2}$	weak priors on b	SDSS coll. [139]
$\sum m_{\nu_i} < 0.75\,\mathrm{eV}$	$\Omega_\nu h^2 < 0.8\,10^{-2}$	free b	[140], SDSS+2dF+WMAP
$\sum m_{\nu_i} < 0.66\,\mathrm{eV}$	$\Omega_\nu h^2 < 0.7\,10^{-2}$	prior on b	

Table 1.4: Bounds (at 2σ) on neutrino masses or Ω_ν from recent sets of experiments.

of the power spectrum at momenta larger than $k_{\rm nr} = 0.03 \left(\frac{m_\nu}{1\,\mathrm{eV}}\right)^{1/2} \Omega_{\rm m}^{1/2} h\,\mathrm{Mpc}^{-1}$ (corresponding to the scale of the size of the horizon when a neutrino of mass m_ν become non-relativistic) by $\frac{\Delta P}{P} = -8\frac{\Omega_\nu}{\Omega_{\rm m}}$. In general, the determination of Ω_ν depends on priors and on normalisations, possibly fixed by the CMB spectrum; examples are $\Omega_{\rm m}$ and the bias parameter b that comes in the relation between the power spectra [135]. A partial collection of the latest results is in Table 1.4. As a rule of thumb, the present bound and the future expected sensitivity [136] can be summed in

$$\text{present}: \qquad \Omega_\nu h^2 \lesssim 10^{-2} \tag{1.32}$$

$$\text{future}: \qquad \Omega_\nu h^2 \lesssim 10^{-3} \tag{1.33}$$

For completeness, one should mention that other similar methods exist to constraint the sum of neutrino masses. One is the so called *Lyman-α forest technique*. Looking at the light of distant quasars, one observe a series of deep lines corresponding to the absorption at the Lyman-α frequency by the

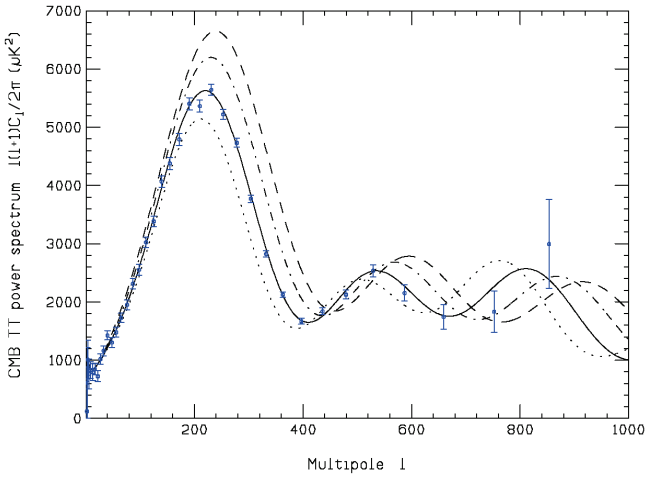

Figure 1.9: The effect of additional (effective) neutrinos on the CMB spectrum. The solid line corresponds to the best-fit to the WMAP data ($N_\nu = 2.75$). With all other parameters and the overall normalization of the primordial spectrum fixed, the spectra for $N_\nu = 1$, $N_\nu = 5$ and $N_\nu = 7$ are the dotted, dot-dashed and dashed lines, respectively. From [142].

hydrogen atoms in the clouds crossed by the light, that gets redshifted as it moves towards us. From the deepness of the lines, the reconstruction of the large scale structures along the line of sight is possible, and then the analysis of the power spectrum. From this technique, a (now overcome) constraint of $\sum m_{\nu_i} < 5.5\,\mathrm{eV}$ is obtained [141].

Finally, neutrinos can be studied via the CMB spectrum too, which is sensitive to the total energy density in relativistic species

$$\rho = \rho_\gamma \left[1 + \frac{7}{8} \left(\frac{4}{11} \right)^{4/3} N_\nu^{\mathrm{CMB}} \right]. \tag{1.34}$$

More degrees of freedom (neutrinos) imply a faster expansion (as also discussed in 2.2.1) which translates in more power in the acoustic peaks of the microwave radiation. Without entering in the details, a plot like fig. 1.9 gives an idea of the magnitude of the effect.

Global fits at the moment imply [143]

$$N_\nu^{\mathrm{CMB}} \approx 3 \pm 2 \tag{1.35}$$

somewhat depending on which priors and on which data are included in the fit. Future data might start discriminating 3 from 4 neutrinos.

Chapter 2

A (4D) sterile neutrino

Specific effects of an extra sterile neutrino on cosmological and astrophysical processes have already been studied in the past (see the references below). However, the discussion has usually been limited to restricted cases (ν_e-sterile mixing only, absence of active-active mixing, small mixing angle regime, degenerate active-sterile Δm^2...) and/or it did not address in an unified way all the different probes.

In this Chapter, I present an analysis which relaxes these simplifying assumptions and studies the more general 4-neutrino context, in all the broad range of allowed active-sterile mass gaps and for all possible active-sterile mixing angles. Moreover, it takes into account several relevant sources of constraints and (possible) signals in astrophysics and cosmology.

This Chapter, based on ref. [1], is organized as follows: in Section 2.1 I describe the non-standard parameterization of active/sterile mixing that is choosen (because probably more convenient and intuitive than standard parameterizations) and describe the qualitatively different kinds of spectra on which I will focus. In Section 2.2 I present the study of sterile effects in cosmology, comparing the relative sensitivities of two BBN probes (the ^{4}Helium and Deuterium abundances), of Cosmic Microwave Background radiation (CMB) and of Large Scale Structures (LSS). In section 2.3 I discuss sterile oscillations in SN1987a and future supernovæ. [1]

Each Section contains a 'Results' Subsection, which can be read skipping the other more technical parts. From a computational point of view, exploring 4ν oscillations is $3 \div 4$ orders of magnitude more demanding than usual 2 or 3ν fits and therefore requires significant improvements of usual techniques. Subsections entitled 'Technical details' describe how this was achieved.

2.1 Active-sterile neutrino mixing formalism

A generic 4×4 Majorana neutrino mass matrix is described by 4 masses, 6 mixing angles and 6 CP-violating phases; 3 of them affect oscillations.

In absence of sterile neutrinos, U denotes the usual 3×3 mixing matrix that relates neutrino flavour

[1] Ref. [1] completes the thorough analysis with the discussion of sterile oscillations in solar (and reactor) and atmospheric neutrinos, in cosmic/astrophysical relic neutrinos and in short- and long-baseline beams. There one also finds summary plots that superimpose the bounds and signals from all the different probes. We prefer not to attribute a precise probabilistic meaning to cosmological bounds by performing global

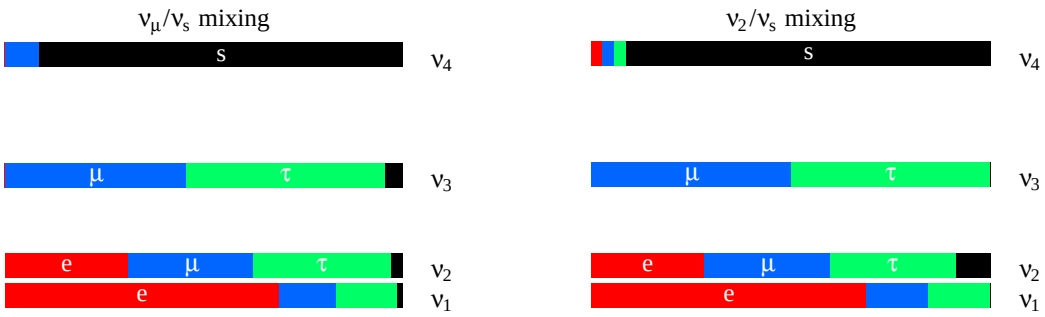

Figure 2.1: **Basic kinds of four neutrino mass spectra**. *Left: sterile mixing with a flavour eigenstate (ν_μ in the picture). Right: sterile mixing with a mass eigenstate (ν_2 in the picture).*

eigenstates $\nu_{e,\mu,\tau}$ to neutrino mass eigenstates $\nu_{1,2,3}$ as $\nu_\ell = U_{\ell i}\nu_i$ ($i = \{1,2,3\}$, $\ell = \{e,\mu,\tau\}$). The extra sterile neutrino can mix with one arbitrary combination of active neutrinos,

$$\vec{n}\cdot\vec{\nu} = n_e\nu_e + n_\mu\nu_\mu + n_\tau\nu_\tau = n_1\nu_1 + n_2\nu_2 + n_3\nu_3 \tag{2.1}$$

The mixing of the sterile neutrino is therefore fully described by a complex unit 3-versor $\vec{n}$ (containing two CP-violating phases) and by one mixing angle θ_s. With this parameterization the 4 neutrino mass eigenstates are

$$\begin{cases} \nu_4 = \nu_s \ \cos\theta_s + n_\ell\nu_\ell \ \sin\theta_s \\ \nu_i = U^*_{\ell i}[\delta_{\ell\ell'} - n^*_\ell n_{\ell'}(1-\cos\theta_s)]\nu_{\ell'} - \sin\theta_s n^*_\ell U^*_{\ell i}\nu_s \end{cases} \tag{2.2}$$

i.e. the 4×4 neutrino mixing matrix V as that relates flavour to mass eigenstates as $\nu_{e,\mu,\tau,s} = V\cdot\nu_{1,2,3,4}$ is

$$V = \begin{pmatrix} 1-(1-\cos\theta_s)\vec{n}^*\otimes\vec{n} & \sin\theta_s\vec{n}^* \\ -\sin\theta_s\vec{n} & \cos\theta_s \end{pmatrix} \times \begin{pmatrix} U & 0 \\ 0 & 1 \end{pmatrix}. \tag{2.3}$$

In order to understand what happens in the generic case, it is convenient to focus on two different kinds of limiting cases, pictorially exemplified in fig. 2.1

- **Mixing with a flavour eigenstate** (fig. 2.1a): $\vec{n}\cdot\vec{\nu} = \nu_\ell$ ($\ell = e$ or μ or τ). The sterile neutrino oscillates into a well defined flavour at 3 different Δm^2 (which cannot all be smaller than the observed splittings $\Delta m^2_{\rm sun,atm}$).
- **Mixing with a mass eigenstate** (fig. 2.1b): $\vec{n}\cdot\vec{\nu} = \nu_i$ ($i = 1$ or 2 or 3). The sterile neutrino oscillates at a single Δm^2 into a neutrino of mixed flavour ν_ℓ.

Such a parametrization of sterile mixing, in eq. (2.2) or eq. (2.3), makes physics more transparent than other frequently used choices[2].

[2]When studying sterile mixing with a flavour eigenstate our expression is directly related to the 'standard' parameter-

The oscillation probabilities among active neutrinos in the limit where the active/sterile mass splitting dominates, and active/active mass splittings can be neglected, are

$$P(\nu_\ell \to \nu_{\ell'}) = P(\bar{\nu}_\ell \to \bar{\nu}_{\ell'}) = \begin{cases} 1 - 4|V_{\ell 4}^2|(1 - |V_{\ell 4}^2|)\sin^2(\Delta m_{41}^2 L/4E_\nu) & \text{for } \ell = \ell' \\ 4|V_{\ell 4}^2||V_{\ell' 4}^2|\sin^2(\Delta m_{41}^2 L/4E_\nu) & \text{for } \ell \neq \ell' \end{cases} \tag{2.4}$$

and in our parametrization $V_{\ell 4} = n_\ell \sin\theta_{\rm s}$ (see eq. (2.2)).

Older papers studied active/sterile mixing in 2 neutrino approximations. In such a case $\theta_{\rm s} = \pi/2$ gives no oscillation effect. On the contrary, in the full 4 neutrino case $\theta_{\rm s} = \pi/2$ swaps the sterile neutrino with one active neutrino. (e.g. ν_μ in fig. 2.1a or ν_2 in fig. 2.1b, if $\theta_{\rm s}$ were there increased up to $\pi/2$) affecting solar and atmospheric oscillations in an obvious way. Therefore large active/sterile mixing is excluded by experiments for all values of $\Delta m_{4i}^2 \equiv m_4^2 - m_i^2$ (with one exception: the sterile neutrino mixes with a mass eigenstate ν_i and is quasi-degenerate to it. This structure arises naturally in certain models).

In order to explore a more interesting slice of parameter space when considering sterile mixing with a mass eigenstate ν_i for $\theta_{\rm s} > \pi/4$ let us modify the spectrum of neutrino masses and replace (m_i^2, m_4^2) with $(2m_i^2 - m_4^2, m_i^2)$. In such a way, the mostly active state always keeps the same squared mass (fixed to its experimental value), so that in the limit $\theta_{\rm s} = \pi/2$ the sterile neutrino gives no effect rather than giving an already excluded effect. Physically, in the $\nu_{\rm s}/\nu_i$ plots that will be presented the mostly sterile neutrino is heavier (lighter) than the mass eigenstate to which it mixes when $\theta_{\rm s} < \pi/4$ ($\theta_{\rm s} > \pi/4$). When studying mixing with a flavour eigenstate one cannot modify the spectra at $\theta_{\rm s} > \pi/4$ in order to obtain some other experimentally allowed configuration, so that the plots are restricted to $\theta_{\rm s} < \pi/4$.

The '$2 + 2$' neutrino mixing pattern, namely two neutrino couples separated by a mass splitting much larger than $\Delta m_{\rm sun,atm}^2$ is not considered here. In fact this spectrum does not reduce to active-only oscillations in any limiting case so that sterile effects are always sizable, and present experiments already exclude this possibility [147]. When the separation among the two couples is comparable to $\Delta m_{\rm sun,atm}^2$, '$2 + 2$' is no longer a special case qualitatively different from '$3 + 1$'.

Finally, I assume $\theta_{13} = 0$. Using $\theta_{13} \sim 0.2$, the maximal value allowed by present experiments, leads to minor (in some cases) or no (in other cases) modifications, not discussed. Measuring θ_{13} and discovering sterile effects will likely be two independent issues (however both could first manifest as disappearance of reactor $\bar{\nu}_e$).

---

ization

$$V = R_{34}R_{24}R_{14} \cdot U_{23}U_{13}U_{12}$$

where R_{ij} represents a rotation in the ij plane by angle θ_{ij} and U_{ij} a complex rotation in the ij plane. θ_{14} or U_{e4} gives rise to $\nu_e/\nu_{\rm s}$ mixing, θ_{24} or $U_{\mu 4}$ to $\nu_\mu/\nu_{\rm s}$ mixing, and θ_{34} or $U_{\tau 4}$ to $\nu_\tau/\nu_{\rm s}$ mixing.

The above 'standard' parameterization becomes unconvenient when studying mixing with a mass eigenstate. In such a case our parameterization is directly related to the alternative 'standard' parameterization appropriate for this case,

$$V = U_{23}U_{13}U_{12} \cdot R_{34}R_{24}R_{14}$$

Now θ_{i4} gives rise to $\nu_i/\nu_{\rm s}$ mixing. The parameterization adopted here is convenient because it remains simple in both cases.

2.2 Sterile effects in cosmology

In this Section the effects of the additional sterile neutrino in cosmology are discussed [148].

Its production via oscillations from the active states occurs roughly at the time of BBN, for any interesting range of its mass.[3] This is a rather robust phenomenon: it is difficult to modify cosmology in order to avoid production of sterile neutrinos while keeping the success of BBN. For example, as already commented, neutrino asymmetries/chemical potentials much larger (8 orders of magnitude) than the one in baryons can inhibit sterile production and introduce extra unknown parameters in nucleosynthesis, voiding all bounds and predictions. I stick here to a more plausible cosmology, and neglect them.

What is done is the following: for each choice of the active-sterile oscillation parameters Δm^2, θ_s, in each of the six limiting cases $\nu_s/\nu_\alpha(\alpha = e, \mu, \tau)$ or $\nu_s/\nu_i(i = 1, 2, 3)$ (expressed by the versor $\vec{n}$ in a specified basis), the evolution with temperature of the e, μ, τ and sterile neutrino densities is followed and the computation of how the cosmological observables get modified is done.

Concerning BBN, I consider the modifications to the values of Y_P and $Y_{\rm D}$, which can be directly compared to the their measured values; however, for ease of presentation and for the present unclear situation in the BBN measurements, their values are converted into effective numbers of neutrinos, $N_\nu^{^4{\rm He}}$ and $N_\nu^{\rm D}$, univocally defined by the inversion of eq. (1.24) and eq. (1.25). Nevertheless, it should be stressed that these parameters somewhat hide the richer information that comes from the reconstruction of the time (temperature) evolution: the precise association of a set of oscillation parameters ($\vec{n}$, Δm^2, θ_s) with an effective N_ν can only be done this way.

Concerning the later probes, the final neutrino densities are as well translated in terms of effective N_ν by eq. (1.34) for CMB, while the relevant observable for LSS is Ω_ν as defined in eq. (1.31).

2.2.1 Technical details

In the spirit of the qualitative discussion developed in Section 1.4.1 (of which this Section is the technical counterpart), what we want to follow closely is the time evolution of n/p. With this quantity in hand, a set of nuclear reaction equations will then allow to determine the relative abundances of the different nuclei.

The time evolution of n/p is **(a)** governed by the rates of the weak reactions in eqs. (1.12), that of course depend on the electron neutrino and antineutrino densities in the environment; **(b)** sensitive to the expansion rate H of the universe, which is in turn determined by the total energy density ρ and therefore by the abundance of neutrinos of all flavors that enter in the count of g_*. A sterile neutrino can enter the game through these two avenues.

What we need first of all, therefore, is the time evolution of the densities of the active and the sterile neutrinos. These are described in terms of 4×4 matrices ρ and $\bar{\rho}$ (written in the flavor basis, i.e. with entries $\rho_{\rm ee}$, $\rho_{\rm e\mu}$, $\rho_{\rm e\tau}$, $\rho_{\rm es}$, $\rho_{\mu\rm e}$ and so on; the densities are intended as relative to the photon one, so that $\rho \in (0, 1)$). The kinetic equations for such matrices must take into account (i) the vacuum

[3] I conservatively assume the initial abundance (at $T \gg$ MeV) of the sterile neutrino to be vanishing. This is a excellent approximation considering that the expansion dilutes any preceding abundance.

oscillations (active-active and active-sterile), (ii) the matter effects in the primordial plasma, (iii) the $\nu e \leftrightarrow \nu e$ scattering reactions and the $\nu\nu \leftrightarrow ee$ annihilation reactions.

An important remark is in order: in general, the ρ's are functions of the neutrino momentum (or energy); let us make use of the standard assumption [149]

$$\rho_{\alpha\beta}(E_\nu) = f(E_\nu)\,\rho_{\alpha\beta}(\langle E_\nu\rangle) \qquad f(E) = \frac{1}{e^{E/T}+1} \tag{2.5}$$

and consider $\rho_{\alpha\beta}(\langle E_\nu\rangle)$ (from now on: $\rho_{\alpha\beta}$) as the variables of interest. In other words, an average is made a priori over the neutrino energy spectra using a Fermi-Dirac distribution (with vanishing chemical potential). This means that neutrino spectral distortions, pre-existing or generated by oscillations, are neglected.

Moreover, the absence of lepton asymmetries is assumed, which implies the decoupling of the neutrino and antineutrino evolution, that proceed identically.[4] From now on, we focus for definiteness on the neutrino sector.

With this simplifications, the kinetic equations for the 4×4 density matrix read [112, 150]

$$\frac{d\rho}{dt} \equiv \frac{dT}{dt}\frac{d\rho}{dT} = -i\,[\mathcal{H}_m, \rho] - \{\Gamma, (\rho - \rho^{\rm eq})\} \tag{2.6}$$

$\mathcal{H}_m$ is the Hamiltonian in matter, composed by the vacuum Hamiltonian in the flavor basis and the matter potentials V_α for each flavor: they consist in the thermal masses [151] for the neutrinos in the primordial plasma. The usual MSW potential is in this case subdominant because the plasma is charge symmetric.

$$\mathcal{H}_m = \frac{1}{2E_\nu}\left[V\,\mathrm{diag}(m_1^2, m_2^2, m_3^2, m_4^2)\,V^\dagger + E_\nu \mathrm{diag}(V_e, V_\mu, V_\tau, 0)\right] \tag{2.7}$$

$$V_e = -\frac{199\sqrt{2}\pi^2}{180}\frac{\zeta(4)}{\zeta(3)} G_{\rm F}\frac{T}{M_W^2}\left(T^4 + \frac{1}{2}T_\nu^4\cos\theta_W \rho_{ee}\right) \tag{2.8a}$$

$$V_\mu = -\frac{199\sqrt{2}\pi^2}{180}\frac{\zeta(4)}{\zeta(3)} G_{\rm F}\frac{T T_\nu^4}{M_W^2}\left(\frac{1}{2}T_\nu^4\cos\theta_W \rho_{\mu\mu}\right) \tag{2.8b}$$

$$V_\tau = -\frac{199\sqrt{2}\pi^2}{180}\frac{\zeta(4)}{\zeta(3)} G_{\rm F}\frac{T T_\nu^4}{M_W^2}\left(\frac{1}{2}T_\nu^4\cos\theta_W \rho_{\tau\tau}\right) \tag{2.8c}$$

$$V_s = 0 \tag{2.8d}$$

As for the reaction part, we use the standard 'anticommutator' approximation: the reactions tend to thermalize neutrinos, driving their matrix density to its thermal equilibrium value, $\rho^{\rm eq} = \mathrm{diag}(1,1,1,0)$. A detailed comparison with the full equations [112] reveals that they are accurately mimicked by inserting the following values of the damping coefficients.

$$\Gamma_{\rm tot} \approx 3.6\; G_{\rm F}^2\; T^5 \quad \text{for } \nu_e \qquad \text{and} \qquad \Gamma_{\rm tot} \approx 2.5\; G_{\rm F}^2\; T^5 \quad \text{for } \nu_{\mu,\tau} \tag{2.9}$$

[4] In the peculiar conditions of the early universe, the matter effects are equal for neutrinos and antineutrinos, see below.

because all scatterings damp the coherent interference between different flavours. In the equations for the diagonal components of ρ, insert the annihilation rate

$$\Gamma_{\rm tot} \approx 0.5\, G_{\rm F}^2\, T^5 \quad \text{for } \nu_e \qquad \text{and} \qquad \Gamma_{\rm tot} \approx 0.3\, G_{\rm F}^2\, T^5 \quad \text{for } \nu_{\mu,\tau} \tag{2.10}$$

since annihilations are needed to change the number of neutrinos.

The determination of $\frac{dT}{dt}$ is quite involved, since we need to keep track of the several phenomena that go on in the range $T \sim 1\,\text{MeV}$ which is under examination. In particular, we want to include the possible extra degrees of freedom (the sterile neutrinos) that are produced by the oscillations and we do not want to neglect the heating due to e^+e^- annihilations. The result (details are given below) is the equation

$$\begin{aligned}\frac{dT}{dt} =& H(T,\rho_\nu)\frac{1}{T\mathcal{S}^{1/3}}\left(\frac{\partial}{\partial T}\left(\frac{1}{T\mathcal{S}^{1/3}}\right)\right)^{-1} + \\ &- \frac{\dot\rho_\nu T}{4}\left(\rho_\nu\left(1+\frac{T}{3\mathcal{S}}\frac{\partial\mathcal{S}}{\partial T}\right)+\frac{8}{7}\left(\frac{11}{4}\right)^{4/3}\mathcal{S}^{-4/3}\left(1+\frac{\mathcal{R}}{2}+\frac{T}{8}\frac{\partial\mathcal{R}}{\partial T}\right)\right)^{-1}\end{aligned} \tag{2.11}$$

with H as determined by eqs. (2.12), (2.13), with $\mathcal{R}\left(\frac{m_e}{T}\right)$, $\mathcal{S}\left(\frac{m_e}{T}\right)$ as defined in eq. (2.14) and eq. (2.15) and $\rho_\nu = \rho_{\rm ee} + \rho_{\mu\mu} + \rho_{\tau\tau} + \rho_{\rm ss}$. [5]

Notice that ρ_ν introduced here must not be confused with the commonly employed N_ν: while N_ν is an effective quantity which incorporates any possible effect translated in terms of neutrinos, ρ_ν is simply a shorthand for the sum of the neutrino populations; while N_ν is a time independent quantity, ρ_ν varies with time (or temperature).

Eq. (2.11), in principle, is to be solved together with the kinetic equations for the neutrino densities. The second term, however, turns out to be small [150] and can be safely neglected. We are left with a system of 16 coupled equations in the variables $\rho_{\alpha\beta}$ for $\alpha,\beta = e,\mu,\tau,s$ which must be solved in the range of temperature of interest ($T \sim$ few MeV $\to <$ 0.1 MeV). Once that is done, we obtain in particular the four neutrino populations $\rho_{\rm ee}, \rho_{\mu\mu}, \rho_{\tau\tau}, \rho_{\rm ss}$ as functions of the temperature.

Details of the derivation of eq. (2.11) [114, 152]:
The Friedman equation for the scale parameter a, neglecting curvature, is $\frac{\dot a^2}{a^2} = \left(\frac{8\pi G_N}{3}\rho_{tot}\right)$. By definition of $H = \frac{\dot a}{a}$

$$H = \left(\frac{8\pi G_N}{3}\rho_{tot}\right)^{1/2}. \tag{2.12}$$

The total energy density is given by $\rho_{tot} = \rho_\gamma + \rho_{\nu_e,\bar\nu_e} + \rho_{\nu_\mu,\bar\nu_\mu} + \rho_{\nu_\tau,\bar\nu_\tau} + \rho_{\nu_{\rm s},\bar\nu_{\rm s}} + \rho_{e^+} + \rho_{e^-}$ where ($g_\gamma = 2$, $g_\nu = 2$) $\rho_\gamma = \int \frac{d^3q}{(2\pi)^3} g_\gamma q \frac{1}{e^{q/T}-1} = \frac{\pi^2}{30}2T^4$, $\rho_{\nu_i,\bar\nu_i} = \rho_{ii}\int \frac{d^3q}{(2\pi)^3} g_\nu q \frac{1}{e^{q/T_\nu}+1} = \rho_{ii}\frac{7}{8}\frac{\pi^2}{30}2T_\nu^4$ but for e^+e^- we leave ($g_e = 2$) $\rho_{e^+} = \rho_{e^-} = \int \frac{d^3q}{(2\pi)^3} g_e E(q) \frac{1}{e^{E(q)/T}+1}$ with $E(q) = \sqrt{q^2+m_e^2}$ (recall that $T_{e^+e^-} \equiv T$, when e^+e^- are in the bath):

$$\rho_{tot} = \frac{\pi^2}{30}T^4\left(2 + \frac{7}{4}\rho_\nu\left(\frac{T_\nu}{T}\right)^4 + \mathcal{R}\left(\frac{m_e}{T}\right)\right) \tag{2.13}$$

[5] Notice that, neglecting the production of new degrees of freedom ($\dot\rho_\nu = 0$) and setting $T_\nu = T$ (valid for $T \gg$ MeV, where $\mathcal{S} = 11/4$) one gets the usual relation $\dot T = -HT$.

with $\rho_\nu = \rho_{ee} + \rho_{\mu\mu} + \rho_{\tau\tau} + \rho_{ss}$ and

$$\mathcal{R}(x) = \frac{60}{\pi^4}\int dy y^2 \sqrt{y^2+x^2}\frac{1}{e^{\sqrt{y^2+x^2}}+1} \tag{2.14}$$

At $T \sim$ MeV neutrinos decouple and T_ν redshifts independently. At $T \sim 1\,\mathrm{MeV}$ the e^+e^- annihilations heat the γ bath (ie increase T, or better temporarily reduce the cooling of T due to redshift) so that $T_\nu \neq T$. What is the relation of T_ν with T? The entropy for γ and e^+e^- (not including the neutrinos) is by definition $s = \frac{a^3}{T}\left(\rho_\gamma + \rho_{e^+} + \rho_{e^-} + P_\gamma + P_{e^+} + P_{e^-}\right)$. For relativistic bosons (or even fermions, actually) $P_\gamma = \rho_\gamma/3$, while for e^+e^- we leave $\rho_{e^+} = \rho_{e^-} = \int \frac{d^3q}{(2\pi)^3} g_e E(q) \frac{1}{e^{E(q)/T}+1}$, $P_{e^+} = P_{e^-} = \int \frac{d^3q}{(2\pi)^3} g_e \frac{q^2}{3\sqrt{q^2+m_e^2}} \frac{1}{e^{E(q)/T}+1}$. Thus $s = (aT)^3 \frac{4\pi^2}{45}\mathcal{S}\left(\frac{m_e}{T}\right)$, with

$$\mathcal{S}(x) = 1 + \frac{45}{2\pi^4}\int dy y^2 \left(\sqrt{y^2+x^2} + \frac{y^2}{3\sqrt{y^2+x^2}}\right)\frac{1}{e^{\sqrt{y^2+x^2}}+1}. \tag{2.15}$$

On the other hand, before the e^+e^- annihilation (i.e. at $T \gg 1\,\mathrm{MeV}$) the entropy for γ and e^+e^- reads $s' = \frac{a^3}{T}\frac{4}{3}\left(\rho_\gamma + \rho_{e^+} + \rho_{e^-}\right)$ where now $\rho_{e^+} = \rho_{e^-} = \frac{7}{8}\frac{\pi^3}{30}2T^4$. At $T \gg 1\,\mathrm{MeV}$, $T_\nu = T$ therefore $s' = (aT_\nu)^3 \frac{11\pi^2}{45}$. Since entropy is conserved ($s' = s$)

$$\left(\frac{T_\nu}{T}\right)^3 = \frac{4}{11}\mathcal{S}\left(\frac{m_e}{T}\right). \tag{2.16}$$

This gives T_ν for every value of T.[6]

Now, a change in T can be due to the expansion or to the creation of new degrees of freedom (e.g. sterile neutrinos):

$$\frac{dT}{dt} = \left(\frac{\partial T}{\partial a}\right)_{\rho_\nu}\dot{a} + \left(\frac{\partial T}{\partial \rho_\nu}\right)_a \dot{\rho_\nu} \tag{2.17}$$

To determine $\left(\frac{\partial T}{\partial a}\right)_{\rho_\nu}$ the conservation of (γ and e^+e^-) entropy $s = (aT)^3\frac{4\pi^2}{45}\mathcal{S}(m_e/T)$ is exploited: at fixed ρ_ν the entropy is a constant; thus $\left(\frac{\partial T}{\partial a}\right)_{\rho_\nu}\dot{a} = \frac{\dot{a}}{a}\frac{1}{T\mathcal{S}^{1/3}}\left(\frac{\partial}{\partial T}\left(\frac{1}{T\mathcal{S}^{1/3}}\right)\right)^{-1}$ where $\mathcal{S} = \mathcal{S}\left(\frac{m_e}{T}\right)$. To obtain $\left(\frac{\partial T}{\partial \rho_\nu}\right)_a$ one uses the conservation of the total energy density (eq. (2.13)). At fixed a, the total energy density is a constant during the production of new degrees of freedom. Thus $\left(\frac{\partial T}{\partial \rho_\nu}\right)_a \dot{\rho_\nu} = -\frac{\dot{\rho_\nu} T}{4}\left(\rho_\nu\left(1 + \frac{T}{3\mathcal{S}}\frac{\partial \mathcal{S}}{\partial T}\right) + \frac{8}{7}\left(\frac{11}{4}\right)^{4/3}\mathcal{S}^{-4/3}\left(1 + \frac{\mathcal{R}}{2} + \frac{T}{8}\frac{\partial \mathcal{R}}{\partial T}\right)\right)^{-1}$ where again $\mathcal{S} = \mathcal{S}\left(\frac{m_e}{T}\right)$ and $\mathcal{R} = \mathcal{R}\left(\frac{m_e}{T}\right)$.

Having determined the neutrino evolution we can study the relative n/p abundance. It evolves according to

$$\dot{r} \equiv \frac{dT}{dt}\frac{dr}{dT} = \Gamma_{p\to n}(1-r) - r\Gamma_{n\to p} \qquad r = \frac{n_n}{n_n + n_p} \tag{2.18}$$

where, again, the quantity $\frac{dT}{dt}$ is governed by eq. (2.11). $\Gamma_{p\to n}$ is the total rate for all the $p \to n$ reactions (presented in eq. (1.12)) and $\Gamma_{n\to p}$ for the inverse processes. In general, they are given by the expressions [112, 153]

[6] An extension of this formalism is necessary to take into account also the non-instantaneous decoupling of the neutrinos, which causes their partial heating. Moreover, since neutrinos are differently heated depending on their momentum, spectrum distortions (which we continue to neglect tout court) arise. Both these effects have a small impact for our purposes.

$$\Gamma_{p\to n} = \frac{1}{\tau_n m_e^5 l_0}\left(\int_0^\infty dE_\nu E_\nu^2 E_e p_e f_e(E_e)\left[1-f_{\nu_e}(E_\nu)\right]|_{E_e=E_\nu+\Delta M}\right.$$
$$+\int_{m_e}^\infty dE_e E_\nu^2 E_e p_e f_{\bar\nu_e}(E_\nu)\left[1-f_{\bar e}(E_e)\right]|_{E_\nu=E_e+\Delta M}$$
$$\left.+\int_{m_e}^{\Delta M} dE_e E_\nu^2 E_e p_e f_{\bar\nu_e}(E_\nu) f_e(E_e)\,|_{E_\nu+E_e=\Delta M}\right), \tag{2.19}$$

$$\Gamma_{n\to p} = \frac{1}{\tau_n m_e^5 l_0}\left(\int_0^\infty dE_\nu E_\nu^2 E_e p_e f_{\nu_e}(E_\nu)\left[1-f_e(E_e)\right]|_{E_e=E_\nu+\Delta M}\right.$$
$$+\int_{m_e}^\infty dE_e E_\nu^2 E_e p_e f_{\bar e}(E_e)\left[1-f_{\bar\nu_e}(E_\nu)\right]|_{E_\nu=E_e+\Delta M}$$
$$\left.+\int_{m_e}^{\Delta M} dE_e E_\nu^2 E_e p_e\left[1-f_{\bar\nu_e}(E_\nu)\right]\left[1-f_e(E_e)\right]|_{E_\nu+E_e=\Delta M}\right) \tag{2.20}$$

in terms of the neutron lifetime τ_n, of the coefficient $l_0 = 1.633$ and $\Delta M = m_n - m_p$. Although quite lengthy, these equations allow to straightforwardly compute the rates and the role of the electron neutrino (and antineutrino) distribution ($f_{\nu_e}(E_\nu) \equiv \rho_{ee}(E_\nu)$, $f_{\bar\nu_e}(E_\nu) \equiv \rho_{\bar e\bar e}(E_\nu)$ in the notation above) is explicitly shown. As above, we assume and make the average over the Fermi-Dirac neutrino distribution.

At this point, it is apparent how the production of sterile neutrinos affects n/p by (a) modifying the $\Gamma_{p\to n}, \Gamma_{n\to p}$ rates directly, if the $\nu_e, \bar\nu_e$ population is depleted by oscillations; (b) entering in ρ_ν and thus increasing the Hubble parameter H.

With the value of n/p in hand, finally a network of Boltzmann equations describes how electroweak, strong and electromagnetic processes control the evolution of the various nuclei: p, n, D, T, ^{3}He, ^{4}He,... Rather than discussing here the various important features of these equations, we just state (without explanation) the approximation we use. At a sufficiently low temperature $T^* \sim 0.08\,\mathrm{MeV}$ almost all neutrons wind up in ^{4}He, so that its mass abundance is given by $Y_p \simeq 2r(T^*)$ with T^* obtained solving

$$180H = \Gamma_{\mathrm{DD}\to p\mathrm{T}}(\Gamma_{pn\to \mathrm{D}\gamma}/\Gamma_{D\gamma\to pn})^2. \tag{2.21}$$

The precise numerical value is fixed in such a way that in the SM case our simplified code precisely agrees with state of the art codes (that include thermal, radiative and other corrections corrections, smaller than the present experimental uncertainty). We use the CMB determination of η (eq. (1.28)). The Deuterium abundance is obtained with a similar technique.

For the purposes of the CMB and LSS bounds, the neutrino densities ρ_{ee}, $\rho_{\mu\mu}$, $\rho_{\tau\tau}$, ρ_{ss} at the time of recombination and today are needed. These are simply given by the final outputs (i.e. for $T \ll 0.1\,\mathrm{MeV}$) of the kinetic equations described above.

2.2.2 Results

As previously discussed, we plot the effective numbers N_ν of neutrinos defined in terms of the physical observables (the ^{4}He and D abundances and the energy density at recombination) from eq. (1.24),

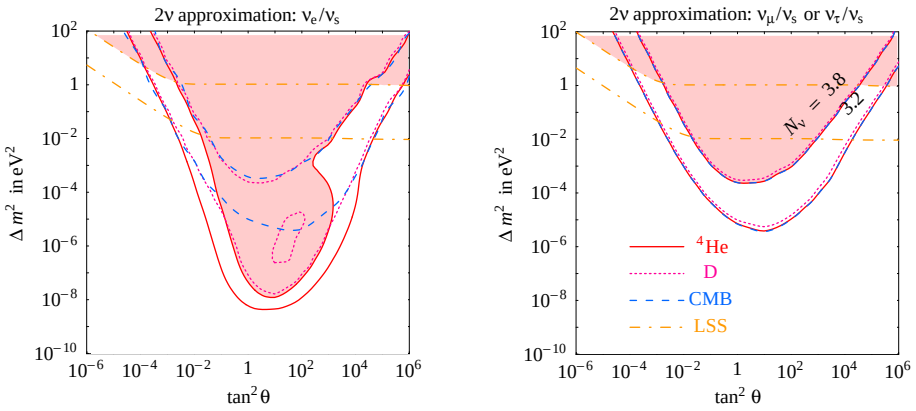

Figure 2.2: Isocurves of the effective number of neutrinos produced by 2 neutrino oscillations in the cases ν_e/ν_s (left plot, panel (a)) and $\nu_{\mu,\tau}/\nu_s$ (right plot, panel (b)). Solar and atmospheric oscillations are included in the 3 neutrino plots of fig. 2.3, where the meaning of the various isolines is precisely explained.

eq. (1.25) and eq. (1.34). We also plot the value of the present energy density in neutrinos Ω_ν (eq. (1.31)), probed by observations of Large Scale Structure together with CMB constraints.

The plots have the following meaning: shaded regions have $N_\nu^{^4\mathrm{He}} > 3.8$ or $\Omega_\nu h^2 > 10^{-2}$ and are therefore 'disfavoured' or 'excluded' (depending on how conservatively one estimates systematic uncertainties) within minimal cosmology. The other lines indicate the sensitivity that future experiments might reach. More precisely we plot contour-lines corresponding to $N_\nu = 3.2$ and 3.8 and to $\Omega_\nu h^2 = 10^{-2}$ and 10^{-3}.

To start, in fig. 2.2 we show the effects produced by 2 neutrino mixing: ν_s/ν_e in fig. 2.2a and ν_s/ν_μ or ν_s/ν_τ mixing in fig. 2.2b.[7] The red dashed line shows the total number of neutrinos, N_ν^{CMB}: it is equal in the two cases and is not affected by oscillations with $\Delta m^2 \lesssim 10^{-5}\,\mathrm{eV}^2$ that are too slow and start only after neutrino decoupling, when the total number of neutrinos remains frozen.[8] Neutrinos can still change flavour. The difference between fig. 2.2a and fig. 2.2b is due to the fact that only electron neutrinos are involved in the reactions that control the n/p ratio. Therefore ν_s/ν_e oscillations that occur after neutrino freeze-out and that do not affect the total number of neutrinos (ν_s are created by depleting ν_e) affect n/p and consequently the ^{4}He abundance[9] (continuous line) and, to a lesser extent, the D abundance. This happens down to $\Delta m^2 \sim 10^{-8}\,\mathrm{eV}^2$: oscillations with smaller values occur after decoupling of electroweak scatterings, when the relative n/p abundancy can only be affected by neutron decay.

[7] Previous papers studied the ^{4}He abundancy and we agree with their results. We however use as a variable $\tan^2\theta$ rather than $\sin^2 2\theta$, so that we unify in a unique plot the non-resonant ($0 < \theta < \pi/4$) and the resonant ($\pi/4 < \theta < \pi/2$) case.

[8] To be precise we should say 'the total entropy in neutrinos per comoving volume remains constant'. For simplicity we will adopt loose abbreviations.

[9] These region are strongly disfavoured because it has a value corresponding to $N_\nu^{^4\mathrm{He}} > 4$.

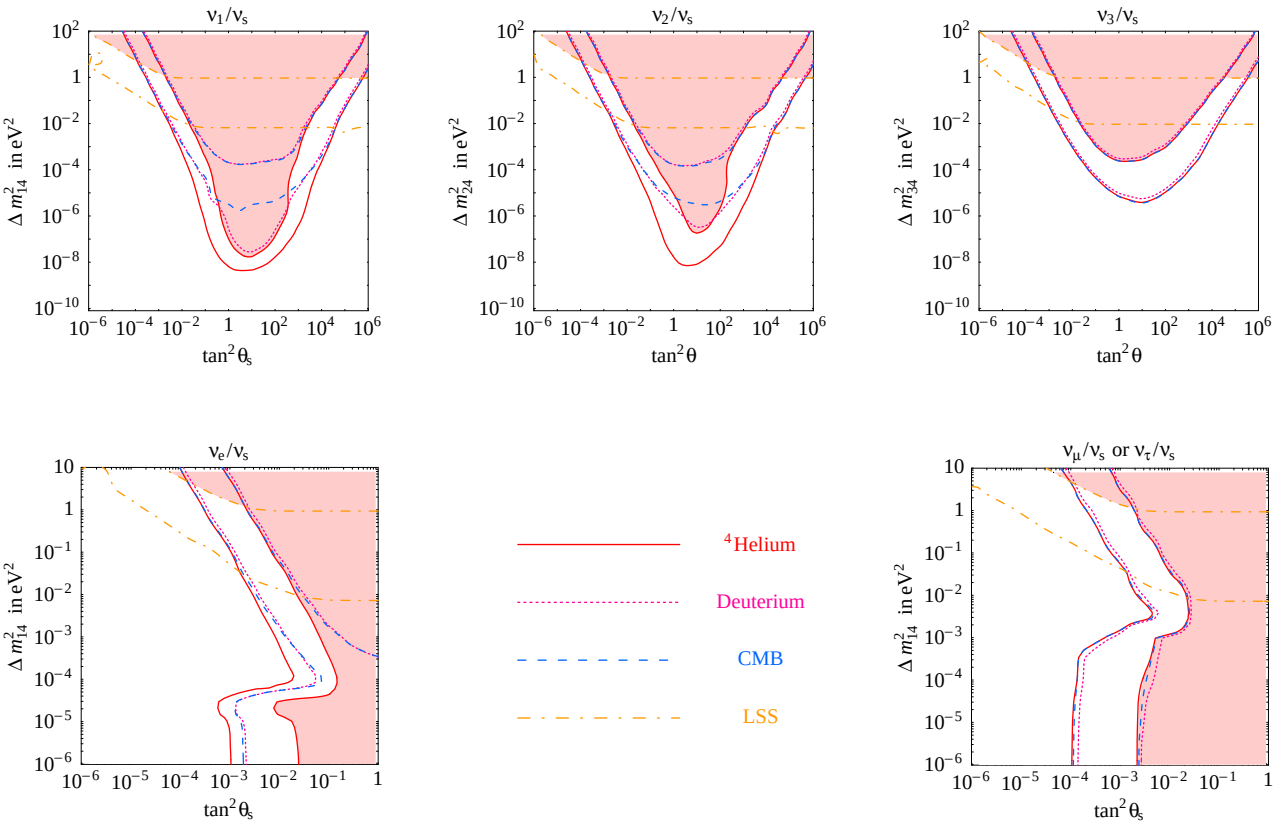

Figure 2.3: Cosmological effects of sterile neutrino oscillations. The panels are named (a), (b), (c) in first line and (d), (e) in the second line. We compare four different signals. The continuous red line refers to the ^{4}He abundance (we shaded as 'disfavoured' regions where its value corresponds to $N_\nu > 3.8$), the purple dotted line to the deuterium abundance, and the dashed blue line to the effective number of neutrinos at recombination. We plotted isolines of these three signals corresponding to an effective number of neutrinos $N_\nu = 3.2$ and 3.8. The precise meaning of the parameter N_ν in the three cases is explained in the text. The upper (lower) dot-dashed orange lines corresponds to $\Omega_\nu h^2 = 10^{-2}$ (10^{-3}), where Ω_ν is the present energy density in neutrinos.

Effects are larger at $\theta > \pi/4$ (i.e. $\tan\theta > 1$) because this corresponds to having a mostly sterile state lighter than the mostly active state, giving rise to MSW resonances in neutrinos and anti-neutrinos . In the past years it has been debated about whether a neutrino asymmetry and/or large inhomogeneity develop as a consequence of non-linear effects, and this issue has not yet been fully clarified. Our Boltzmann equations assume that both these effects can be neglected. At $\tan\theta > 1$ the bound from Ω_ν holds even for very small mixing, $\theta \simeq \pi/2$ just because these region correspond to heavy active neutrinos.

We now discuss how the above picture changes taking into account oscillations among active neutrinos. Our results are shown in fig. 2.3: the upper row refers to sterile mixing with mass eigenstates $\nu_{1,2,3}$ and the lower row to mixing with flavour eigenstates ν_e and $\nu_{\mu,\tau}$.

An inspection of the upper row shows that their main features can be understood in terms of the (unrealistic) results in the case of 2 neutrino mixing, fig. 2.2. Having assumed $\theta_{13} = 0$, the 4 ν sterile mixing with ν_3 gives no new effect with respect to the 2 ν sterile mixing with $\nu_{\mu,\tau}$. Due to solar and atmospheric oscillations ν_e depletion due to oscillations into sterile neutrinos now happens in all cases and becomes milder, because no longer confined to ν_e but shared among all active neutrinos. Fig. 2.3b shows the effects of $\nu_{\rm s}/\nu_2$ mixing (this kind of neutrino spectrum is plotted in fig. 2.1b): since ν_2 contains some ν_e component, electron neutrinos are in part directly affected. Fig. 2.3a shows the effects of $\nu_{\rm s}/\nu_1$ mixing: ν_e depletion effects are largest in this last case because ν_1 is the neutrino eigenstate with the largest ν_e component. In summary: depletion gets transferred to all neutrinos and diluited.

Mixing with flavour eigenstates is qualitatively different, for the general reasons explained in section 2.1. We can see the effects of the solar (atmospheric) mass splitting as bumps in fig. 2.3d (fig. 2.3e) where cosmological effects of $\nu_{\rm s}/\nu_e$ ($\nu_{\rm s}/\nu_{\mu,\tau}$) mixing are computed. In the case of $\nu_{\rm s}/\nu_e$ mixing $N_\nu^{\rm D}, N_\nu^{\rm CMB} = 4$ is reached only if the sterile neutrino has a large enough Δm^2: the solar $\Delta m^2_{\rm sun} \approx 0.7\ 10^{-4}\,{\rm eV}^2$ alone is not sufficient as clear from the 2ν limit plotted in fig. 2.2a. Fig. 2.2b shows that in the case of $\nu_{\rm s}/\nu_{\mu,\tau}$ mixing a $\Delta m^2 \sim \Delta m^2_{\rm atm} \approx 2\ 10^{-3}\,{\rm eV}^2$ is large enough to reach $N_\nu \approx 4$ for any value of the sterile mass.

Finally, notice that the LSS bound shows an "upturn" at small values of the mixing angle, simply due to the fact that sterile neutrinos with those mixing parameters are less efficiently produced. This detail was missing in previous analysis [145, 55], since of course its recognition requires the knowledge of the time (temperature) evolution of the sterile neutrino densities that we performed.

2.3 Sterile effects in Supernovæ

The study of the (light) sterile neutrinos effects in the SN environment [156] presents a few striking features, especially if compared with the more familiar case of the Sun:

- the matter density spans a huge interval, starting from the nuclear density ($\rho \simeq 10^{14}\,{\rm g\,cm^{-3}}$) of the stiff inner core and decreasing in the mantle: active-sterile matter effects exist for all the mass range that we need to consider in the light of the cosmological upper bound (about 10 eV)

obtained in the previous Section. However, given the typical SN neutrino energy ($\sim 10\,\mathrm{MeV}$), they take place outside of the core and outside of the neutrino-spheres (roughly defined as the regions after which neutrinos freely stream, $\rho \ll 10^{12}\,\mathrm{g\,cm^{-3}}$). [10]

- the neutrino production region, on the other hand, lies within the neutrinospheres; this somehow simplify the picture with respect to the case of the Sun, allowing to decouple spatially the production and the oscillation regions.

- Supernovæ produce not only ν_e but all kinds of active neutrinos and antineutrinos, roughly in similar amounts. They mix and convert among themselves and with the sterile neutrino, so that the prediction of the flux of a specific flavor reaching Earth requires to control the other flavors too. Present experiments most accurately can study the $\bar{\nu}_e$ since, in the energy range of solar and SN neutrinos, $m_e \ll E_\nu \ll m_p$, the $\bar{\nu}_e p \to \bar{e} n$ process allows to easily detect $\bar{\nu}_e$ and to measure their energy spectrum. Detecting other neutrinos (e.g. via νe scattering or deuterium dissociation) is possible but less effective, although future projects have the power to improve this point drastically (see the discussion in 1.3.3). In the following, we will mainly focus on the $\bar{\nu}_e$ flux reaching Earth.

- the spectra of the neutrinos emitted from the neutrinospheres have a shape close to the thermal distribution, in first approximation; while this implies a less rich fine structure in energy of the signal, it nevertheless allows an easy detection of possible spectral distortions.

- the peculiar composition of the inner part of the mantle (deleptonized matter) is the origin of a peculiar shape of the matter potentials experienced by the neutrinos. Namely, the electron neutrino potential changes its sign in the deep region of the mantle, and it does so in a very steep manner. This is a robust feature, although the details can vary as we comment below. It implies that the sterile state always meets a "sharp" resonance with the electron antineutrinos in the deep region of the mantle.

- unlike the Sun, an exploding SN is of course a changing environment (neutrino light-curve evolution, passage of the shock wave...); including the time dependance in the neutrino fluxes and in the matter density profile turns out to be too much demanding and probably useless, given the poor knowledge of the details. We choose instead to focus on a typical static configuration, which includes all the characteristic features of the SN cooling phase.

- SN are very distant objects, so that in principle they can be a useful tool to probe vacuum oscillations with Δm^2 as low as $10^{-18}\,\mathrm{eV}^2$ (a precise value depend on the supernova and on its distance from the earth: different supernovæ could probe different ranges).

In the following Section I present a detailed discussion of the general procedure that allows to study bounds and signals of sterile neutrinos in supernovæ. In the subsequent one I present an example of its application.

[10] The resonances with the sterile state would enter in the neutrino-spheres (in the inner core) for $\Delta m^2 \gtrsim 10^5\,\mathrm{eV}^2$ ($\gtrsim 10^7\,\mathrm{eV}^2$ respectively).

2.3.1 Technical details

We need to follow the fate of the neutrinos produced in the center of the SN along their travel through the star matter, the vacuum and the Earth; they experience matter enhanced and vacuum oscillations, both among active neutrinos and with the sterile neutrino; ultimately, they are collected with some specific efficiency in the detectors on Earth. We need therefore to extend the discussion presented in 1.3.1 to the present case of four neutrinos.

For the reasons discussed above, we focus on antineutrinos.

The fluxes of matter eigenstates leaving the star and reaching the Earth surface ($\mathcal{F}_1$, $\mathcal{F}_2$, $\mathcal{F}_3$, $\mathcal{F}_4$) are related to the initial fluxes coming out of the neutrino-sphere(s) ($F^0_{\bar\nu_e}$, $F^0_{\bar\nu_\mu}$, $F^0_{\bar\nu_\tau}$, $F^0_{\bar\nu_s}$) by

$$\begin{pmatrix} \mathcal{F}_1 \\ \mathcal{F}_2 \\ \mathcal{F}_3 \\ \mathcal{F}_4 \end{pmatrix} = \mathcal{P} \begin{pmatrix} F^0_{\bar\nu_e} \\ F^0_{\bar\nu_\mu} \\ F^0_{\bar\nu_\tau} \\ F^0_{\bar\nu_s} \end{pmatrix} \tag{2.22}$$

where $\mathcal{P}$ contains complicated combinations of all the crossing probabilities at the several resonances met in the star's mantle. In turn, the fluxes on Earth surface of neutrinos of definite flavor ($F_{\bar\nu_e}$, $F_{\bar\nu_\mu}$, $F_{\bar\nu_\tau}$, $F_{\bar\nu_s}$) are obtained from the matter eigenstates fluxes projecting with the mixing matrix V

$$\begin{pmatrix} F_{\bar\nu_e} \\ F_{\bar\nu_\mu} \\ F_{\bar\nu_\tau} \\ F_{\bar\nu_s} \end{pmatrix} = \mathcal{S} \begin{pmatrix} \mathcal{F}_1 \\ \mathcal{F}_2 \\ \mathcal{F}_3 \\ \mathcal{F}_4 \end{pmatrix} \qquad \mathcal{S}_{\alpha i} = |V_{\alpha i}|^2 \tag{2.23}$$

Concerning the initial fluxes, we adopt a Fermi-Dirac spectrum for each flavor $\alpha = \nu_e, \bar\nu_e, \nu_x$

$$f_\alpha(E,t) = \frac{120}{7\pi^4} \frac{L_\alpha}{T_\alpha^4} \frac{E_\nu^2}{e^{E_\nu/T}+1}. \tag{2.24}$$

Based on the recent results of [82], we adopt typical energies for the different species that are close to each other ($T_{\nu_e} \simeq 12\,\mathrm{MeV}$, $T_{\bar\nu_e} \simeq 14\,\mathrm{MeV}$, $T_{\nu_x} \simeq 14\,\mathrm{MeV}$) and neutrino luminosities ($L_{\nu_e}, L_{\nu_e}, L_{\nu_e}$) $\simeq (30,30,20) \times 10^{51}\,\mathrm{erg\,sec^{-1}}$. The initial flux of sterile neutrinos is assumed to be vanishing, as a consequence of the fact that matter oscillations only take place out of the neutrinosphere.[11]

[11] To be precise, shortly after the collapse the electron neutrino matter potential in the very center of the core is positive, due to the contribution of the trapped neutrinos themselves. This configuration lasts for a short transient period, until the neutrino diffusion depletes their abundance and carries the potential to negative values, where it stays. A small fraction of the electron (anti)neutrinos produced in the deep core could then oscillate into sterile states and constitute a non vanishing flux injected in the mantle.

Neutrinos traveling in the SN matter experience the MSW potentials

$$V_e = \sqrt{2} G_{\rm F} n_B \left(\frac{3}{2} Y_e - \frac{1}{2} \right) \tag{2.25a}$$

$$V_\mu = \sqrt{2} G_{\rm F} n_B \left(\frac{Y_e}{2} - \frac{1}{2} \right) \tag{2.25b}$$

$$V_\tau = V_\mu + V_{\mu\tau} \tag{2.25c}$$

$$V_s = 0 \tag{2.25d}$$

where n_B is the baryon number density (in particular $n_B = \frac{\rho}{m_N}$ where $m_N \simeq 939\,\text{MeV}$ is the nucleon mass[12]) and Y_e is the net electron fraction per baryon $Y_e = (N_{e^-} - N_{e^+})/n_B$. Antineutrinos, of course, experience the same potentials with opposite sign.

The difference $V_{\mu\tau}$ in the ν_μ and ν_τ potentials, which appears at one loop level due to the different masses of the muon and tau leptons [163], reads

$$V_{\mu\tau} = \frac{3}{2\pi^2} G_{\rm F}^2 m_\tau^2 \left[2(n_p + n_n) \ln \left(\frac{M_W}{m_\tau} \right) - n_p - \frac{2}{3} n_n \right] \tag{2.26}$$

The effect is not irrelevant in the inner dense regions: for densities above $\rho \sim 10^8\,\text{g}\,\text{cm}^{-3}$, the $\mu\tau$ vacuum mixing is suppressed.

A crucial point concerns the characteristic of the matter density and of the electron fraction in the mantle of the star. We adopt the profiles represented in fig. 2.4 and we modelize them with analytic functions that preserve their peculiarities.[13] Namely, the density profile decreases according to a power law r^{-4} out of the $\sim 10\,\text{km}$ inner core (where instead it has a roughly constant, nuclear density value). The Y_e profile is inevitably dictated by the deleptonization process: behind the shock wave which has passed in the mantle matter, the electron capture on the newly liberated protons is rapid, driving Y_e to low values ($\sim 0.2 \div 0.3$). In the outer region, where the density is sensibly lower, the efficiency of the capture is much lower, so that Y_e essentially does not move from its usual value ~ 0.5. The data refer to $\sim$0.3 sec after bounce for a typical star of ~ 11 solar masses. The subsequent evolution is supposed to move the wave of the Y_e profile slightly outwards, maintaining, however, its characteristic shape. The slight dependance on the progenitor mass, in turn, is not really relevant [155].

In summary, although the profiles that we adopt come from a specific computation and refer to a specific instant in time, we believe that they incorporate well the peculiar features that are important for our purposes. A more refined treatment of this point (later times behavior of the profiles, fine structures connected with the passage of the shock wave...) would of course require to obtain first a complete simulation of the SN evolution, including the explosion, which is still not the case.

As a consequence of the steep passage of the Y_e profile across 1/3, the potential for the electron (anti)neutrinos is characterized by a change of sign that occurs in the deep region of the mantle. On

[12] For the very high densities closer to the core, m_N should be replaced by a (quite different) effective nucleon mass. We can neglect this refinement in the regions of our interest.

[13] I thank Adam Burrows (and Stan Woosley) for having provided me with the raw data, and for useful discussions and clarifications.

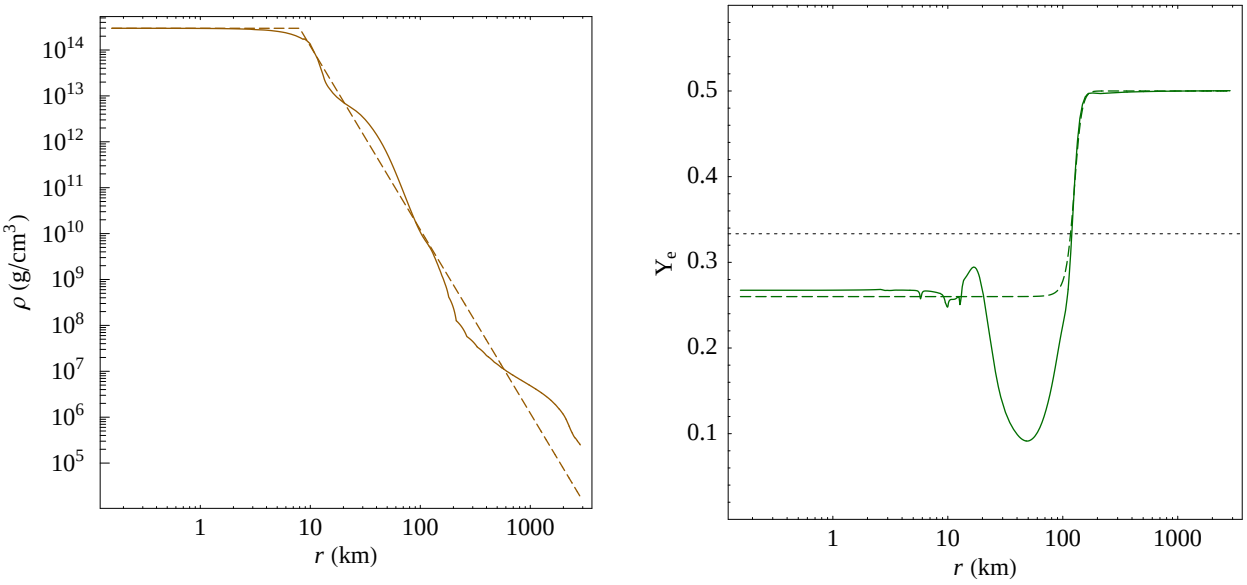

Figure 2.4: Density ρ and electron fraction Y_e profiles from the data of [154] (solid lines) and the analytic modelization that we adopt (dashed line). The horizontal dotted line $Y_e = 1/3$ corresponds to the change of sign of the V_e potential.

the other hand, the matter potentials for muon and tau (anti)neutrinos follow a smooth decrease. Both are represented in fig. 2.5.

The knowledge of the matter potentials allows to draw the pattern of the eigenstates that is qualitatively depicted in fig. 2.5, in the specific case of small ν_e/s mixing, for the sake of illustration. It is apparent how the (mainly) sterile state (the black line) always crosses the first eigenstate in the region corresponding to the sign change of the electron potential. The matter effects are completely dominant over the active-active mixing in that region, so that the eigenstate is almost totally constituted of the electron flavor. On the other hand, the crossing of the (mainly) sterile line with the other eigenstates occurs in a region determined by the Δm^2 under consideration. The flavor composition of these states is less sensitive, but not insensitive, to the matter effects: in the inner regions, not far enough from the $\mu\tau$ resonance, the $\mu\tau$ matter effects still plays a role so that the states are dominantly of muon or tau flavor; at lower densities there is no difference in the V_μ and V_τ potentials so that the two states are maximally mixed according to the atmospheric angle, and of course contaminated by the electron flavor according to the solar (and θ_{13}) angle. Below $\Delta m^2_{\rm atm}$ ($\Delta m^2_{\rm sun}$) it does not meet the second (third) eigenstate at all.

Besides the previous ones, active-active resonances occur in the SN mantle. The situation is quite involved and it depends on the choices of the hierarchy parameter $sign(\Delta m^2_{23})$ and of θ_{13}, as discussed in 1.3.1. For the sake of definiteness, we choose the pattern of Normal Hierarchy Δm^2_{23}. In this case, essentially, the $e\tau$ resonance (governed by the "atmospheric" parameters), as well as the $e\mu$ resonance (governed by the "solar" parameters) lie in the neutrino sector and have no role for our purposes. The value of θ_{13} also has no impact on the antineutrinos.

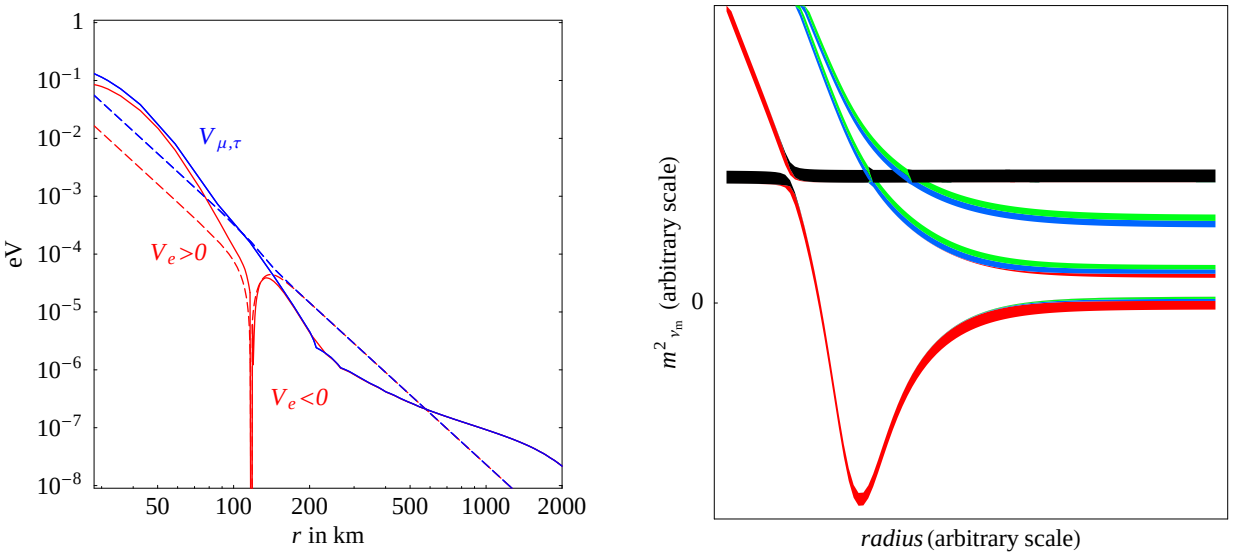

Figure 2.5: Left: matter potentials in the SN environment, for electron antineutrinos (red) and for muon and tau antineutrinos (blue). As in fig. 2.4, the analytic approximations are plotted as dashed lines. Right: matter eigenstates in the SN mantle. Colors indicate the flavor composition. An extra sterile neutrino with small mixing is represented by an horizontal line with height equal to its mass.

As for the computation of the crossing probabilities at the active-sterile resonances, it is convenient to consider the basis of mass eigenstates in absence of active/sterile mixing (i.e. $\theta_{\rm s} \to 0$ or $\theta_{\rm s} \to \pi/2$, depending on which limit is closer to the value of $\theta_{\rm s}$ under examination). This limit allows to precisely define level-crossings. When $\nu_{\rm s}$ crosses one of the active eigenstates, ν_{ma} $(a = 1, 2, 3)$ (see fig. 2.1a for one example), the level crossing probability P_C is well approximated by

$$P = \frac{e^{\tilde{\gamma}\cos^2\theta^m_{as}} - 1}{e^{\tilde{\gamma}} - 1} \qquad \gamma = \frac{4\mathscr{H}^2_{as}}{dH_a/dr} \equiv \tilde{\gamma} \cdot \frac{\sin^2 2\theta^m_{as}}{2\pi|\cos 2\theta^m_{as}|} \quad \text{where} \quad \sin\theta^m_{as} = \vec{n} \cdot \vec{\nu}^m_a \sin\theta_{\rm s}. \tag{2.27}$$

where $\mathscr{H}$ is the 4×4 complete Hamiltonian in matter, while H_a stands for the a matter eigenstate of the 3×3 matrix. The above equation looks similar to the well known expression for P_C valid in the simpler 2ν case, but there is one important difference. Our γ and θ^m_{as} must be computed around the resonance where $\mathscr{H}_{aa} = \mathscr{H}_{ss}$ (or around the point where adiabaticity is maximally violated, in cases where there is no resonance) and are in general different from their vacuum values, that are instead conveniently used to parameterize the 2ν expression. In order to elucidate its physical meaning, we emphasize that the crossing angle θ^m_{as} can also be extracted from the scalar product between the flavour vectors of the two matter eigenstates i and $i+1$ that cross: $\sin\theta^m_{as} = \nu^*_{m_i}(r \lesssim r_n) \cdot \nu_{m_i}(r \gtrsim r_n)$ and $\cos\theta^m_{as} = \nu^*_{m_i}(r \lesssim r_n) \cdot \nu_{m_{i+1}}(r \gtrsim r_n)$.

We emphasize that reducing the full 4×4 Hamiltonian to the effective 2×2 Hamiltonian of the 2 states that cross and computing $\mathscr{H}_{as}$ is non trivial, since sterile mixing sometimes redefines the flavour

of the active neutrino involved in the crossing.[14] In these situations it is useful to know the physical meaning of $2\mathscr{H}_{as}$: it is the minimal difference between the eigenvalues of the two states that cross.

With the matter eigenstates pattern of fig. 2.5 in mind, one can easily reconstruct the shape of the matrix $\mathcal{P}$ introduced in eq. (2.22). As an explicit example: a ν_e produced at the neutrinosphere coincides almost totally with a ν_2, due to the dominant matter potential; in order to come out of the SN as a ν_1 matter eigenstate, therefore, it must jump at the deep resonance among the states ν_2 and ν_1. The same can be done with the other states, so that

$$\mathcal{P} = \begin{pmatrix} P_{12} & 0 & 0 & (1-P_{12}) \\ (1-P_{12})(1-P_{23}) & 0 & P_{23} & (1-P_{12})(1-P_{23}) \\ (1-P_{12})P_{23}P_{34} & (1-P_{34}) & (1-P_{23})(1-P_{34}) & P_{12}P_{23}(1-P_{34}) \\ (1-P_{12})P_{23}P_{34} & (1-P_{34}) & (1-P_{23})P_{34} & P_{12}P_{23}P_{34} \end{pmatrix} \tag{2.28}$$

where P_{ij} stands for the crossing probability at the resonance between the i-th and j-th states, computed case by case with the formula described in eq. (2.27). In the end, the fluxes of the flavors eigenstates interacting on Earth are obtained via eq. (2.23).

2.3.2 Results

For every choice of the oscillation parameters Δm^2_{14} and $\theta_{\rm s}$ and for every case of mixing, the above formalism allows to compute the final $\bar{\nu}_e$ flux on Earth surface. Let us single out, for the purposes of illustration, only one example: the case of $\nu_e/\nu_{\rm s}$ mixing in the region of small mixing angle ($\theta_{\rm s} \ll \pi/4$). A complete discussion can be found in Ref. [1].

Let us begin with the null hypothesis: if no oscillation in any sterile state occurs ($\theta_{\rm s} \equiv 0$), no resonance is relevant ($P_{12} = P_{23} = P_{34} \equiv 1$) so that one obtains

$$F^{\rm null}_{\bar{\nu}_e} = \left[c^2\right] F^0_{\bar{\nu}_e} + \left[s^2\right] F^0_{\bar{\nu}_\tau} \tag{2.29}$$

where $c = \cos\theta_{12}$, $s = \sin\theta_{12}$.

In the case of $\nu_e/\nu_{\rm s}$ mixing, the $\bar{\nu}_e$ meet a resonance so that in general $P_{12} \neq 1$. Of course $\bar{\nu}_\mu$ and $\bar{\nu}_\tau$ do not meet any resonance (P_{23}=P_{34}=1). One obtains

$$F_{\bar{\nu}_e} = \left[c^2\ \cos^2\theta_{\rm s} P_{12} + \sin^2\theta_{\rm s}(1-P_{12})\right] F^0_{\bar{\nu}_e} + \left[s^2\ \cos^2\theta_{\rm s}\right] F^0_{\bar{\nu}_\tau} \tag{2.30}$$

Imposing the final $\bar{\nu}_e$ flux to be reduced by no more than 60% (40%) with respect to the flux of the null hypothesis, in the light of accounting for the signal of SN1987a (see the discussion in 1.3.2), produces the contours in fig. 2.6. For small mixing angles, the bound is an oblique line in the $\Delta m^2 - \tan^2\theta$ plain, due to the disappearance of (part of) the original $\bar{\nu}_e$ flux at the P_{12} resonance. However, the contribution of $F^0_{\bar{\nu}_\tau}$ is not affected, so that a non negligible portion of $\bar{\nu}_e$ (that converted from $\bar{\nu}_\tau$) always manages to reach Earth surface, with the consequence that an overall cut larger than $\sim 70\%$ can never occur.

[14] Neglecting this subtelty would give a qualitatively wrong result e.g. in the following situation: $\nu_{\rm s}$ is mixed with ν_e and is quasi degenerate to ν_1.

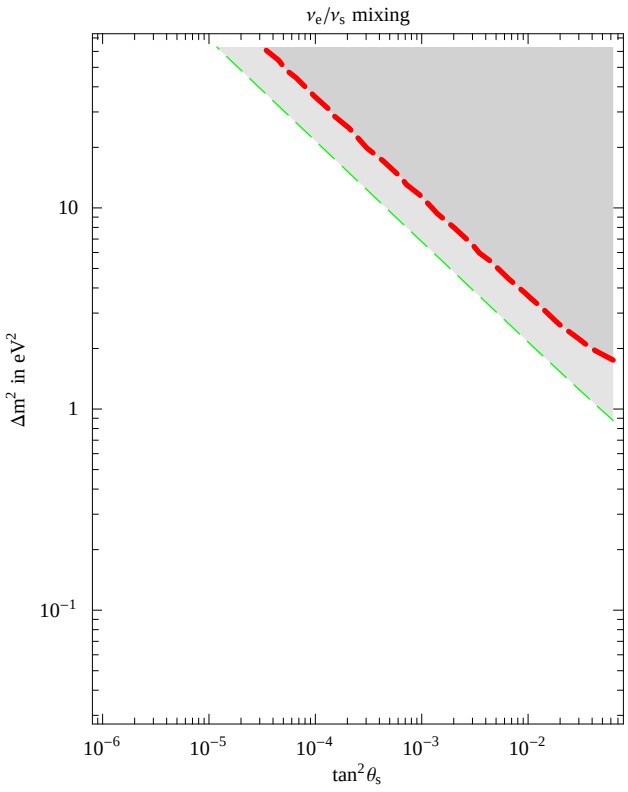

Figure 2.6: Excluded regions from the reduction of the SN1987a $\bar{\nu}_e$ flux. Contours enclose and rule out the regions where the cut of events in the detector is more than 40% (green), 60% (red).

Chapter 3

Neutrinos in Extra Dimensions

In this chapter (based on ref. [2, 3]) I focus on models with Gravitational Extra Dimensions, of which the general features have been described in Section 1.1.2.

The firm points are the following: (i) the fundamental scale M_* is set at ~ 1 TeV, (ii) I consider a single compact extra dimension (with flat metric), (iii) the Standard Model fields are confined on a brane while (iv) the graviton propagates in the bulk.

On top of this, the fundamental observation is that it is very natural to allow also the propagation of **fermionic fields in the extra dimension**. Indeed, for instance ("bottom-up" approach), once the existence of the extra dimension has been postulated, any field which is sterile under the SM gauge group (not only the graviton) has no good reason to be confined on the brane; the most natural candidate is the right handed neutrino, a fermion. Also ("top-down" approach), if extra dimensions are inspired and implied by string/M theory, then several scalars are inevitably present in the bulk (e.g. the moduli that fix the internal radii) and so are their fermionic superpartners, since SuperSymmetry is also part of string theory. With an obvious extension of terminology, we will call these fermions "bulk neutrinos" or "neutrinos in extra dimensions". As we will see, these fields appear as light, dense KK towers of sterile neutrinos in 4 dimensions, possibly mixed with the Standard Model ones. Due to this mixing (superimposed to the traditional flavor mixing that accounts for the solar and atmospheric oscillation signals in the usual way), the bulk provides an example of an alternative channel of energy loss in the supernova core, that must pass the test of the constraint discussed in Section 1.3.2. The bounds that follow on the parameter space of bulk neutrino models indeed look at first sight quite severe. However, we will see that those bounds are relaxed by interesting feedback mechanisms that prevent an unacceptable energy loss, requiring a revisitation of the limits in the literature, and affect the protoneutron star deleptonization and cooling through a non trivial interplay with diffusion, giving rise to an interesting and peculiar phenomenology. In other words, we will mainly address two questions: What are the actual limits on the parameters of the extra dimensions set by SN evolution? What will be the signatures of the presence of extra dimensions in the neutrino signal from a SN detectable on Earth?

The necessary basic notions of SN have already been presented in Section 1.3.

3.1 The extra dimensional setup

We will only consider the single *largest* compact extra dimension, of radius R, on which the only request comes from direct tests of the Newton's law at small distances:

$$1/R \gtrsim 10^{-3}\,\mathrm{eV} \quad \text{i.e.} \quad R \lesssim 100\mu m\ . \tag{3.1}$$

Additional smaller dimensions will be in general present. What we consider is therefore an effective theory valid up to scales below the inverse scales of the smaller dimensions. The physics we are interested in involves bulk neutrinos with masses within $\sim 100\,\mathrm{keV}$. We therefore assume that the inverse scale of the additional smaller dimension is larger than 100 keV and neglect them in the following.

Let us first discuss the simplest paradigm of a neutrino in extra dimensions [157] and then move to the general features of these models.

Consider a sterile 5D Dirac fermion

$$\Psi(x^\mu, y) = (\overline{\xi}(x^\mu, y), \eta(x^\mu, y))^T. \tag{3.2}$$

The simplest allowed lagrangian terms include of course the 5D kinetic term and a general brane-bulk interaction

$$\int d^4x\, dy \frac{h}{\sqrt{M_*}} L(x^\mu) H(x^\mu) \xi(x^\mu, y) \delta(y=0) + \mathrm{h.c.}\,, \tag{3.3}$$

where h is a Yukawa coupling assumed to be naturally of order 1, $L = (\nu_\ell, \ell)$ is the SM lepton doublet and H the Higgs field. In terms of a 4D description, the extra dimensional fermion is reduced to a tower of sterile fields ψ_n via the expansion in Kaluza-Klein (KK) modes: $\Psi(x^\mu, y) = \frac{1}{\sqrt{2\pi R}} \sum_{n\in\mathbb{Z}} \psi_n(x^\mu) e^{in\frac{y}{R}}$. The above lagrangian terms then compose a mass matrix that involves the SM neutrino and the KK fields. The SM neutrino ends up mixed with the sterile eigenstates with a mixing angle θ_n, smaller and smaller as n increases, and with mass gaps $(\Delta M^2)_n$, given by

$$\theta_n \simeq \sqrt{2}\frac{mR}{n} \qquad (\Delta M^2)_n \simeq n^2/R^2\,. \tag{3.4}$$

Here $m \simeq \frac{hv}{\sqrt{2\pi R M_*}} = \frac{hvM_*}{M_{Pl}} \simeq 10^{-4}\,\mathrm{eV}$ is a Dirac mass acquired by the neutrino.

In order to include a larger set of models in the literature [158, 159, 161], we can be more general than the direct example above: what we only need to assume is that the mixing angle θ_n of the SM neutrino with the n-th mass eigenstate be parametrized as

$$\theta_n \simeq \frac{m}{\sqrt{2}M_n} \tag{3.5}$$

where now m is a free parameter, not forcely related to the physical ν mass; the exact dependence of M_n on $1/R$ can be a model dependent feature provided that the density of KK states is proportional to R. We allow for a separate mixing with a KK tower for each SM flavour, superimposed to the traditional flavour mixing and parametrized by the three (unrelated) quantities m_e, m_μ and m_τ.

We require to be working in a regime of small mixing angles, to ensure the smallness of the transition probabilities and to keep under control other oscillation effects (see the Appendix 3.5 to this Chapter). This corresponds to

$$m_e R \lesssim 10^{-5} \qquad m_{\mu,\tau} R \lesssim 10^{-4}\,. \tag{3.6}$$

Equations (3.1) and (3.6) define the parameter space on the plane m–R that we want to probe.

3.2 Cosmological safety (or irrelevance)

The framework defined above ($M_* \sim$ TeV and one single extra dimension under consideration) is compatible with all known constraints from astrophysics and cosmology [162]. Indeed, most bounds on the minimum number of extra dimensions probed by the gravitons given a certain M_* (or, conversely, on the lowest possible M_* given the number of extra dimensions) can be easily avoided if one relaxes the equality of all compactification radii. Or one could postulate that the single extra dimension probed by sterile neutrinos is a subspace of the gravitational bulk. On the other hand, the assumed smallness of the mixing angles is enough to protect from any undesidered drawback on BBN, CMB and so on, essentially because KK sterile neutrinos are produced through the mixing with the SM ones at a very suppressed rate in the early universe.

3.3 Supernova core evolution

What are the modifications to the SN cooling phase described in Section 1.3 in presence of the mixing introduced in Section 3.1?

Let us consider a flavour eigenstate neutrino (ν_e, ν_μ or ν_τ) produced with energy E_ν in the matter of the core by some interaction. It immediately experiences a large MSW potential $V_{e,\mu,\tau}$ (of order of several eV) that is proportional to the local matter density and composition and it acquires an effective squared mass $m^2_{\rm eff} = 2E_\nu V_{e,\mu,\tau}$. The effective mass changes along the neutrino path as the density and composition change: whenever $m_{\rm eff}$ equals the mass of one of the KK sterile states, a resonance occurs and the neutrino has a certain probability to *oscillate into a bulk sterile state, escape from the core and go lost*, carrying his energy away with him. The same argument applies to the escape of antineutrinos if the MSW potential is negative. The escape probability at each ($n^{\rm th}$) resonance is given by

$$P_n \simeq e^{-\pi\gamma_n/2} \tag{3.7}$$

where the adiabaticity factor

$$\gamma = \frac{\Delta M^2 \sin^2 2\theta}{2E_\nu \cos 2\theta \frac{dV}{dr}/V} \ll 1 \tag{3.8}$$

is computable in terms of the vacuum mixing angles and ΔM^2 discussed in Section 3.1. The disappearance probability along a distance L then reads

$$P\left(\overset{(-)}{\nu}_{e,\mu,\tau} \to \text{bulk}\right) \simeq L\,\frac{\pi}{2\sqrt{2}} m^2_{e,\mu,\tau} R \left(\frac{|V_{e,\mu,\tau}|}{E_\nu}\right)^{1/2} \qquad \left(\nu \text{ if } V_{e,\mu,\tau} > 0\,,\ \bar\nu \text{ if } V_{e,\mu,\tau} < 0\right). \tag{3.9}$$

The crucial parameter m^2R (with $m = m_{e,\mu,\tau}$) sets the magnitude of the escape effect and will be the subject of our analysis from now on. The parameter space boundaries eq. (3.1) and eq. (3.6) imply the general limits

$$m_e^2 R < 10^{-8}\,\mathrm{eV}\,, \qquad m_{\mu,\tau}^2 R < 10^{-5}\,\mathrm{eV}\,. \tag{3.10}$$

The escape into extra dimensions constitutes an unconventional channel for (anti)neutrino and energy loss [1] that has to pass the test of the energy loss argument discussed in Section 1.3.
How dangerous is this channel? Estimates in the literature, essentially based on the assumption of a matter potential which is constant in time, imply the very stringent bound

$$m^2 R \lesssim 10^{-12}\,\mathrm{eV}, \tag{3.11}$$

cutting a large portion of the ranges in (3.10).[161] Within such a limit, the escape process is too small to have any effect and the SN evolution is completely untouched. We want to reconsider this conclusion in more details.

3.3.1 The feedback mechanisms

The matter potentials probed by electron and non-electron neutrinos are respectively [2]

$$V_e = \sqrt{2} G_{\mathrm{F}} n_B \left(\frac{3}{2} Y_e + 2 Y_{\nu_e} - \frac{1}{2} \right) \qquad V_{\mu,\tau} = \sqrt{2} G_{\mathrm{F}} n_B \left(\frac{1}{2} Y_e + 2 Y_{\nu_{\mu,\tau}} + Y_{\nu_e} - \frac{1}{2} \right) . \tag{3.12}$$

Their initial configurations are the thickest curves depicted in fig. 3.1. Let us first consider the case where the extra dimension is open for the electron flavour and focus on the potential V_e. In the region where $V_e > 0$, ν_e quickly escape into the bulk, thus reducing their contribution Y_{L_e} to the potential, that is then pushed to zero.[159, 160] Since the escape probability is proportional to V_e, this stops the escape itself. Similarly, in the region where $V_e < 0$, $\bar{\nu}_e$ escape, thus increasing Y_{L_e} and forcing the potential towards zero. Subsequently, neutrino diffusion starts to deplete the relative fractions Y_x and pulls V_e below zero. Again, then, $\bar{\nu}_e$ escape tends to pull V_e back to zero. A non trivial feedback mechanism on the escape process is thus at work.

In the case that the extra dimension is seen by the muon (or tau) flavour, the potential $V_{\mu,(\tau)}$ is negative everywhere so that $\bar{\nu}_{\mu,(\tau)}$ escape into the bulk. This generates a positive $Y_{\nu_{\mu,(\tau)}}$, the balance ν–$\bar{\nu}$ is broken and a positive chemical potential arises. This in turn inhibits the escape itself, both

[1] Notice, in passing, that matter effects play a crucial role: independently on how small the vacuum mixing angle with the $n-$th state is, the SM neutrino runs the risk of oscillating into that sterile state if the corresponding resonance is met. It would be not appropriate to restrict to a mixing with the lowest lying sterile states.

Also, notice that the fact that the SN core is so hot (implying $E_\nu \sim 100\,\mathrm{MeV}$) and so dense (implying $V_{e,\mu,\tau} \sim$ several eV) means a large effective mass for the neutrino so that many resonances with the KK states are met. On the contrary, in the Sun the same mechanism is uneffective since not even the lowest resonances are met, for $1/R$ in a large portion of the range (3.1). The same is true in the case of atmospheric neutrinos. This protects from undesired effects due to sterile KK neutrinos in the solar and atmospheric contexts.

[2] In general, a $Y_{\nu_{\mu,\tau}}$ term could be present in V_e, but it never moves significantly from zero in the case of extra dimension open only to electron neutrinos considered below.

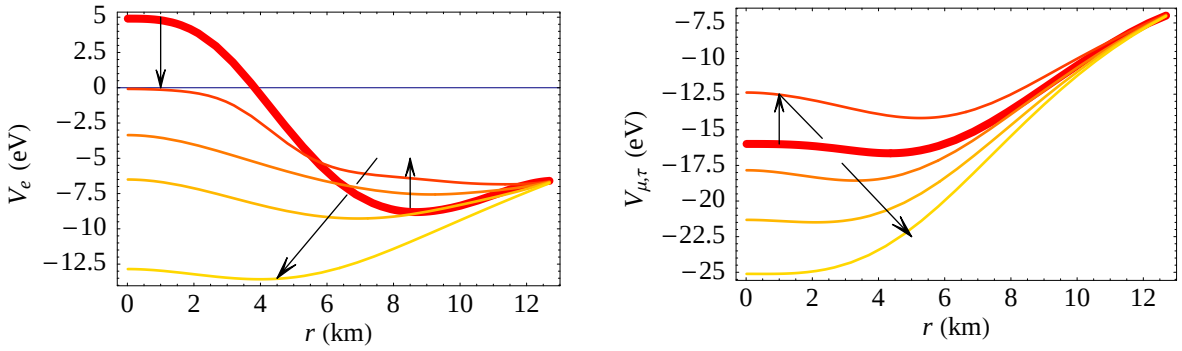

Figure 3.1: Profile of the MSW potentials experienced by electron neutrinos (left) and muon and tau neutrinos (right). The thick line is a typical initial configuration that we adopt; the thin lines are snapshots at 1, 5, 10 and 20 secs, in presence of the escape effect, for $m_e^2 R = 10^{-9}\,\mathrm{eV}$ on the left and $m_{\mu,\tau}^2 R = 10^{-7}\,\mathrm{eV}$ on the right.

because $V_{\mu,(\tau)}$ is lifted towards zero by the term $Y_{\nu_{\mu,(\tau)}}$ in eq. (3.12) and, more important, because the $\bar{\nu}_{\mu,(\tau)}$ abundance is suppressed in presence of the chemical potential. A feedback mechanism on the escape process is again at work.

To study the above picture quantitatively, we need a (simplified) model of the SN core dynamics that essentially superimposes to the usual neutrino diffusion the escape effect. We will discuss such a model in detail in the next section.

3.3.2 Details of the model of core evolution

We now discuss the equations we use to model the evolution of the inner core. We concentrate on the inner core because the bulk of energy and lepton number is stored there. Moreover, the loss rates and the effectiveness of the feedback on the MSW potential are highest in the core. That is because the neutrino densities are large and because the transition probability in eq. (3.9) grows with the potential, which is proportional to the baryon density[3]. Focusing on the inner core has also practical advantages. Unlike the mantle, the core settles into local thermodynamic equilibrium very quickly after the collapse. The hydrodynamics is also much simpler, with the mass profile becoming essentially constant in a few hundreds milliseconds [75, 76]. The mantle of the protoneutron star, on the other hand, accretes matter for the first 0.5–1 sec and then slowly contracts.

We will consider three different cases: namely, the extra dimension open to either ν_e or ν_μ or ν_τ, one at a time, each for several values of the corresponding extra dimensional parameter $m_{e,\mu,\tau}^2 R$. We will comment on the possibility that all species are involved in the energy loss only in the end. The analysis presents interesting differences among the cases, since, in the standard picture of collapse and

[3]The transition probability goes with $(V/E_\nu)^{1/2}$, where E_ν also grows with the baryon density n_B. However, $V \propto n_B$, whereas $E_\nu \propto n_B^{1/3}$.

cooling of the SN core, the role of muon and tau neutrinos is rather different from the electron ones. In fact, while electron neutrinos are copiously produced by the neutronization process during collapse and build up a degenerate ν_e sea with large chemical potential μ_{ν_e} (therefore electron antineutrinos are a negligible fraction in these conditions), muon and tau neutrinos and antineutrinos are produced in pairs and have almost vanishing chemical potential. Moreover, lacking in charged current interactions, they have a faster diffusion and give an important contribution to the transport of thermal energy out of the core. Also, muon and tau lepton number does not play a significant role in the diffusion dynamics. On the other hand, the case of muon neutrino escaping into the bulk would in principle be quite more complicated than the case of tau neutrinos. Indeed: the oscillations of ν_μ or ν_τ into bulk neutrinos build up a non-zero tau or muon lepton number, but, while the tau neutrino abundance is simply determined by the tau lepton number (since tau leptons are not thermally produced, as their mass is large with respect to the energies involved ($T \sim 30\,\mathrm{MeV}$)), on the contrary the muon neutrino abundance would also depend on a small $\mu^\pm$ fraction through the β-equilibrium processes $\mu^- p \leftrightarrow n\,\nu_\mu$ and $\mu^+ n \leftrightarrow p\,\bar{\nu}_\mu$. We prefer to neglect this complication since we do not expect a qualitatively different behaviour in the presence of muons, so we adopt the same equations for the ν_μ and ν_τ escape cases. One can also wonder whether the conventional ν_e–ν_μ–ν_τ mixing could introduce a significant fraction of the other flavors in the problem (i.e. ν_μ in the case of ν_τ escape (or viceversa) and therefore maybe a non negligible presence of muon leptons). This is not the case, since that mixing is largely suppressed by the differences in the matter potentials (at one loop in the case of the muon and tau potential [163]) and by an even larger difference originating from the new effect. In fact, as soon as the resonant conversion into the bulk begins, a non-vanishing lepton number of the escaping flavor is generated and thus the matter interactions produce different effective masses for (anti)neutrinos of that flavor. For sufficiently large mixing with the extra dimension fields, as is our case, the oscillations are suppressed before they significantly influence the neutrino fractions.

3.3.2.a Standard evolution

Let us start from the standard case of no mixing with bulk neutrinos. Assuming thermodynamic equilibrium and neglecting general relativity effects, the basic equations of neutrino transport in absence of mixing are [164]

$$n_B \frac{\partial Y_{L_i}}{\partial t} = -\vec{\nabla} \cdot \vec{F}_{L_i} \tag{3.13a}$$

$$n_B T \frac{\partial s}{\partial t} = \sum_i \left(-\vec{\nabla} \cdot \vec{F}_{\epsilon_i} + \mu_{\nu_i} \vec{\nabla} \cdot \vec{F}_{L_i} \right) , \tag{3.13b}$$

where $i = e, \mu, \tau$ so that the first equation (for the leptonic fractions Y_L) is actually intended replicated for each species. The second equation ("for energy") contains contributions from all families and in principle couples the three sectors. s is the entropy per baryon and $\vec{F}_{L_i} = \vec{F}_{\nu_i} - \vec{F}_{\bar{\nu}_i}$, $\vec{F}_{\epsilon_i} = \vec{F}_{\epsilon_{\nu_i}} + \vec{F}_{\epsilon_{\bar{\nu}_i}}$

are the lepton number and lepton energy density currents respectively. The neutrino currents are

$$\vec{F}_{\nu_i} = -\frac{1}{3}\int \frac{d\vec{p}}{(2\pi)^3}\lambda_{\nu_i}(E_\nu)\vec{\nabla} f_{\nu_i}(E_\nu) \tag{3.14a}$$

$$\vec{F}_{\epsilon_{\nu_i}} = -\frac{1}{3}\int \frac{d\vec{p}}{(2\pi)^3}\, E_\nu\, \lambda_{\nu_i}(E_\nu)\vec{\nabla} f_{\nu_i}(E_\nu)\,, \tag{3.14b}$$

where $\vec{p}$ is the neutrino momentum, $E_\nu = p$ is the neutrino energy, λ_{ν_i} is the neutrino mean free path (mfp), which also depends on the local thermodynamic variables, and f_{ν_i} is the Fermi-Dirac distribution, $f_{\nu_i}(E_\nu) = (e^{(E_\nu - \mu_{\nu_i})/T}+1)^{-1}$, which depends on the temperature T and the neutrino chemical potential μ_{ν_i}. Analogous expressions hold for antineutrinos with $\mu_{\nu-i} \to -\mu_{\nu_i}$. We assume, for this case with no new physics effect, that muon and tau neutrinos have vanishing chemical potential[4]. As a consequence, they do not contribute to the lepton number current and only give a thermal contribution to the energy current. The neutrino chemical potential, as the electron, neutron and proton ones, μ_e, μ_n and μ_p, can be obtained in terms of the thermodynamic variables T, Y_L and ρ (ρ is the mass density), by solving the equilibrium equation $\mu_e - \mu_\nu = \mu_n - \mu_p$. Since we do not solve the whole protoneutron star evolution, we also have to specify boundary conditions for eqs. (3.13). We approximate them by imposing that the lepton number and energy fluxes at the border are proportional to the neutrino number and energy density. We assume spherical symmetry.

The transport equations (3.13) for Y_L and T incorporate all the physics we are interested in before inclusion of non-standard effects. Their solution however requires (i) the knowledge of the mean free paths, (ii) the knowledge of the equation of state, which enters the equilibrium condition and the entropy, and (iii) the determination of the density $\rho(r,t)$. We consider a typical SN core characterized by a mass of $1.5\,M_\odot$ and a radius of 12.7 km. For the matter density, we use a static profile $\rho(r)$, justified by the relative hydrodynamical stability of the inner core in which we are interested. Explicitly $\rho(r) = \rho_c/(1+(r/\bar{r})^3)$, with $\rho_c = 7.5\times 10^{14}$ g/cm^3 and $4/3\ \pi\ \bar{r}^3\ \rho_c = 1.1\,M_\odot$. As for the equation of state, we consider a core made only of n, p, $e^\pm$, $\nu_{e,\mu,\tau}$, $\bar{\nu}_{e,\mu,\tau}$ and γ. The effective nucleon mass is expressed as $m_N^* = \frac{m_N}{1+\beta_0\ \rho/\rho_0}$, where $m_N = 939$ MeV is the vacuum value, β_0 is chosen to be 0.5 and $\rho_0 = 3\times 10^{14}$ g/cm^3 is the reference nuclear density. As for the mean free paths λ_{ν_e} and $\lambda_{\nu_\mu,\nu_\tau}$, in general they would exhibit a non-trivial dependence on the neutrino energy E_ν and the evolution variables (ρ, T, Y_{L_e}, Y_{L_μ}, Y_{L_τ}), besides on several other aspects related to the medium in which the neutrinos diffuse. However, the essential features can be grasped by assuming a simple inverse quadratic dependence on the neutrino energy for all species and incorporating an inverse dependence on matter density for muon and tau neutrinos, while keeping constant with density the mean free path of electron neutrinos. We checked these simplified assumptions versus the more complete modellings of [165]. Moreover, the above choices allow us to obtain an evolution whose main features and timescales agree with the results of more sophisticated analyses. The expressions we use are the following:

$$\lambda_{\nu_e}(E_\nu) = \lambda^0_{\nu_e}\frac{E^2_{\nu,0}}{E^2_\nu}\,, \qquad \lambda_{\nu_\mu,\nu_\tau}(E_\nu, r) = \lambda^0_{\nu_\mu,\nu_\tau}\frac{\rho_c}{\rho(r)}\frac{E^2_{\nu,0}}{E^2_\nu}\,, \tag{3.15}$$

[4]Given the high energies involved, a non-vanishing number of muons could participate to the inner core life, giving a non-vanishing chemical potential.

taking $\lambda^0_{\nu_e} = 1.2$ cm and $\lambda^0_{\nu_\mu,\nu_\tau} = 2.8$ cm at the reference energy $E_{\nu,0} = 260\,\mathrm{MeV}$ and reference density $\rho_c = 7.5 \times 10^{14}$ g/cm^3. With the choice above on the energy dependence of the mean free paths and setting $\lambda_{\bar\nu} = \lambda_\nu$ in the antineutrino contribution, one finds the simple expressions

$$-\vec{F}_{L_i} = a_i \vec{\nabla}\mu_{\nu_i}\,, \tag{3.16a}$$

$$-\vec{F}_{\epsilon_i} = \frac{a_e}{2}\vec{\nabla}\mu^2_{\nu_e} + \frac{a_\mu}{2}\vec{\nabla}\mu^2_{\nu_\mu} + \frac{a_\tau}{2}\vec{\nabla}\mu^2_{\nu_\tau} + (a_e + a_\mu + a_\tau)\frac{\pi^2}{6}\vec{\nabla}T^2\,, \tag{3.16b}$$

where $a_i = \lambda^0_{\nu_i}\,(\rho_c/\rho(r))^{\delta_{i,(\mu,\tau)}}\,E^2_{\nu,0}/(6\pi^2)$, $i = e, \mu, \tau$.

The initial profiles for T and Y_{L_e} are shown in fig. 3.2 (the thick dashed lines). Their main features follow from models of core collapse [166]. The detailed structure of those profiles is not important for our purposes. Diffusion will in fact soon smooth them. Moreover, the mixing with bulk neutrinos, when important, also affects the early stages of SN evolution. This point will be discussed in more detail below. Of course, the profile for Y_{L_μ} and Y_{L_τ} is zero in all the core at the beginning.

3.3.2.b Adding neutrino (and antineutrino) escape into the bulk

Let us now incorporate the effect of neutrino and antineutrino escape in the bulk. A neutrino with energy E_ν contribute to the lepton number loss rate by $\langle P\rangle/\lambda$ each, where $P = P(\nu_i \to \text{bulk})$ and "$\langle\rangle$" indicates an average over the distance traveled L.[5] Since in our case the probability is linear in L, we simply have $\langle P\rangle/\lambda = P/L = \theta(V_i)\pi/(2\sqrt{2})m_i^2 R(|V_i|/E_\nu)^{1/2}$. The total neutrino number loss rate Γ_{ν_i} follows from integration over neutrino momenta and can be written by means of the Fermi integrals F_α as

$$\Gamma_{\nu_i} = \frac{\theta(V_i)}{4\sqrt{2}\pi} m_i^2 R\sqrt{|V_i|}T^{5/2}F_{3/2}\left(\frac{\mu_{\nu_i}}{T}\right)\,, \quad \Gamma_{\epsilon_{\nu_i}} = \frac{\theta(V_i)}{4\sqrt{2}\pi} m_i^2 R\sqrt{|V_i|}T^{7/2}F_{5/2}\left(\frac{\mu_{\nu_i}}{T}\right)\,,$$
$$F_\alpha(y) = \int_0^\infty dx \frac{x^\alpha}{e^{x-y}+1}\,. \tag{3.17}$$

Analogously for antineutrinos. Putting all together, we find the following modified evolution equations for Y_{L_e}, Y_{L_μ}, Y_{L_τ} and T:

$$n_B\frac{\partial Y_{L_e}}{\partial t} = \vec{\nabla}\cdot(a_e\ \vec{\nabla}\mu_{\nu_e}) + \frac{\sigma}{4\sqrt{2}\pi} m_e^2 R\sqrt{|V_e|}\ T^{5/2}F_{3/2}\left(\sigma\frac{\mu_{\nu_e}}{T}\right) \tag{3.18a}$$

$$n_B\frac{\partial Y_{L_\mu}}{\partial t} = \vec{\nabla}\cdot(a_\mu\ \vec{\nabla}\mu_{\nu_\mu}) + \frac{1}{4\sqrt{2}\pi} m_\mu^2 R\sqrt{|V_\mu|}\ T^{5/2}F_{3/2}\left(-\frac{\mu_{\nu_\mu}}{T}\right) \tag{3.18b}$$

$$n_B\frac{\partial Y_{L_\tau}}{\partial t} = \vec{\nabla}\cdot(a_\tau\ \vec{\nabla}\mu_{\nu_\tau}) + \frac{1}{4\sqrt{2}\pi} m_\tau^2 R\sqrt{|V_\tau|}\ T^{5/2}F_{3/2}\left(-\frac{\mu_{\nu_\tau}}{T}\right) \tag{3.18c}$$

[5] Note the difference between $\langle P\rangle/\lambda$ and $\langle P/L\rangle$. While the latter expression looks at first sight more correct, it actually does not take into account, as the former does, the variation of the number densities in the time necessary to travel the distance L.

$$
\begin{aligned}
n_B T \frac{\partial s}{\partial t} = & a_e \left(\vec{\nabla}\mu_{\nu_e}\right)^2 + a_\mu \left(\vec{\nabla}\mu_{\nu_\mu}\right)^2 + a_\tau \left(\vec{\nabla}\mu_{\nu_\tau}\right)^2 + \vec{\nabla}\cdot\left((a_e + a_\mu + a_\tau)\frac{\pi^2}{6}\vec{\nabla}T^2\right) \\
& - \frac{1}{4\sqrt{2}\pi} m_e^2 R \sqrt{|V_e|}\, T^{7/2} \left(F_{5/2}\left(\sigma\frac{\mu_{\nu_e}}{T}\right) - \sigma\frac{\mu_{\nu_e}}{T} F_{3/2}\left(\sigma\frac{\mu_{\nu_e}}{T}\right)\right) \\
& - \frac{1}{4\sqrt{2}\pi} m_\mu^2 R \sqrt{|V_\mu|}\, T^{7/2} \left(F_{5/2}\left(-\frac{\mu_{\nu_\mu}}{T}\right) + \frac{\mu_{\nu_\mu}}{T} F_{3/2}\left(-\frac{\mu_{\nu_\mu}}{T}\right)\right) \\
& - \frac{1}{4\sqrt{2}\pi} m_\tau^2 R \sqrt{|V_\tau|}\, T^{7/2} \left(F_{5/2}\left(-\frac{\mu_{\nu_\tau}}{T}\right) + \frac{\mu_{\nu_\tau}}{T} F_{3/2}\left(-\frac{\mu_{\nu_\tau}}{T}\right)\right) ,
\end{aligned}
\tag{3.19a}
$$

where $\sigma = \mathrm{sgn}(V_e)$. Recall that V_e can have both signs in the core, implying that neutrinos or antineutrinos convert into bulk depending on the condition, while $V_{\mu,\tau}$ are always negative, implying that only antineutrinos do convert. The equations for the Y_L feature the standard transport term $\vec{\nabla}\cdot(a_i\ \vec{\nabla}\mu_{\nu_i})$ plus the escape term eq.3.16. The equation for temperature features the heating terms $a_i\left(\vec{\nabla}\mu_{\nu_i}\right)^2$ $(i = e, \mu, \tau)$ associated to the degradation of the degeneracy energy of neutrinos reaching regions with lower chemical potential. After the standard temperature diffusion term $\vec{\nabla}\cdot(\vec{\nabla}T^2)$, last come the contributions from neutrinos or antineutrinos escape. In the part that refers to electron neutrinos, there is a heating term proportional to $F_{3/2}$ that can overcome the cooling term proportional to $F_{5/2}$. In this case the temperature increases because of the degradation of the degeneracy energy of neutrinos at the Fermi surface that downscatter to replace neutrinos inside the Fermi sphere escaped in the bulk. In the part of muon and tau neutrinos, there are cooling terms: their first addend is related to the energy flux into bulk when an antineutrino is lost, the second one is associated with the (negative) muon/tau lepton number flux into the bulk and thus with the storing of energy in the muon/tau neutrino degenerate sea.

Although these equations are completely general, remember that we will consider separately the case of extra dimension open to one family at a time.

3.3.3.c In case of escape of electron neutrinos

Let us first discuss the case of extra dimension open to electron neutrinos, i.e. $m_e^2 R \neq 0$, $m_\mu^2 R \equiv m_\tau^2 R \equiv 0$. In this case, the equations for Y_{L_μ} and Y_{L_τ} are trivial, their right hand side is identically zero and they don't move from the vanishing initial profile. In the temperature equation, they only show in the standard diffusion term.

Three processes contribute to the variation of the electron lepton fraction: diffusion, neutrino and antineutrino conversion into bulk neutrinos. Each of them has a characteristic time scale, t_{diff}, t_ν and $t_{\bar{\nu}}$ respectively, defined e.g. as the elapsed time per fraction of Y_{L_e} variation. While t_ν turns out to be finite and roughly the same in all the region where $V_e > 0$, $t_{\bar{\nu}}$ strongly depends on the position in the $V_e < 0$ region and may become infinite, as we will see. In any case, $t_\nu \ll t_{\bar{\nu}}$. In most of the inner core, in fact, the beta equilibrium forces μ_{ν_e} to be positive and the neutrinos to be degenerate, $\mu_{\nu_e} \gg T$. As a consequence, the antineutrino number is strongly suppressed and so is the lepton number variation due to antineutrino escape.

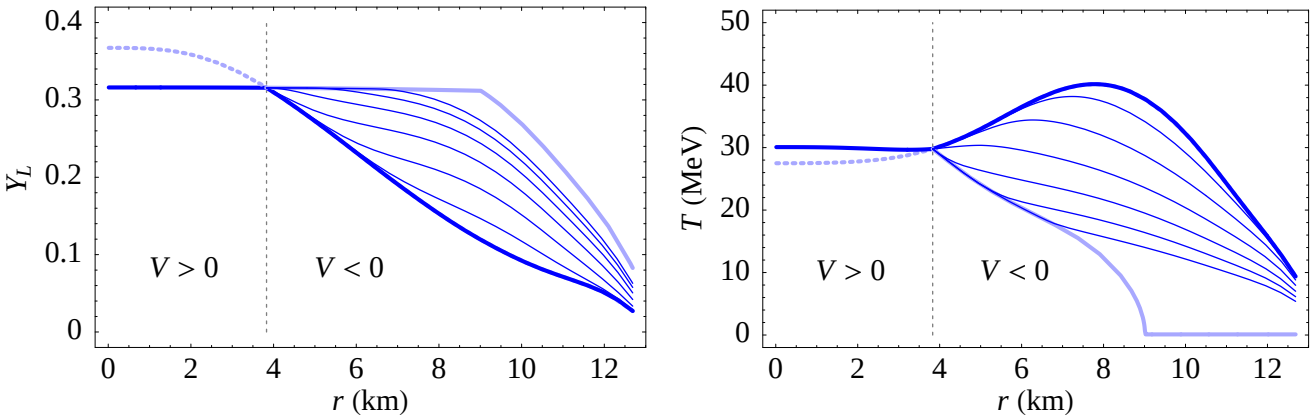

Figure 3.2: Electron lepton fraction and temperature profiles in the initial phase of the evolution. The thick dashed lines (dark solid in the $V_e < 0$ region) represent the initial profiles. The dark thick lines show the profiles at the end of the neutrino escape phase. The thin lines show the effect of antineutrino escape 1 second later for $m_e^2 R = 10^{-(10,\,9,\,8,\,7,\,6,\,5)}$ eV. They can also be considered as the profiles at times $t = 10^{-(5,\,4,\,3,\,2,\,1,\,0)}\,\mathrm{sec}\,(m_e^2 R/(10^{-5}\,\mathrm{eV}))$ provided that $t \lesssim 1\,\mathrm{sec}$. Finally, the light thick lines show the values that would be asymptotically approached if diffusion could be indefinitely neglected.

While the time scale for diffusion is typically $\sim 10\,\mathrm{sec}$, the escape time scale depends on $m_e^2 R$. Moreover, neglecting diffusion, the evolution due to the escape depends on $m_e^2 R$ only through an overall scale factor, $Y_{L_e}(r, t; k\, m_e^2 R) = Y_{L_e}(r, k\, t; m_e^2 R)$, $T(r, t; k\, m_e^2 R) = T(r, k\, t; m_e^2 R)$. The larger $m_e^2 R$, the faster the variation of Y_{L_e}:[6]

$$t_\nu \sim 10\,\mathrm{sec}\,\frac{10^{-12}\,\mathrm{eV}}{m_e^2 R}\left(\frac{\rho}{\rho_0}\right)^{1/2}\left(\frac{Y_{L_e}}{0.3}\right)^{1/3}. \tag{3.20}$$

We therefore distinguish two regimes:

- $m_e^2 R \ll 10^{-12}\,\mathrm{eV}$, or $t_\nu \gg t_{\mathrm{diff}}$. Neutrino and antineutrino escape are too slow to affect significantly the evolution of the protoneutron star. Consistency with the observed neutrino signal from SN 1987A is ensured.

- $m_e^2 R \gg 10^{-12}\,\mathrm{eV}$, or $t_\nu \ll t_{\mathrm{diff}}$. Neutrino escape changes Y_{L_e} faster than diffusion. The consistency with the SN 1987A signal would be in question if the feedback were not taken into account. Deleptonization and cooling are affected.

In the remaining of this subsection, we will concentrate on the case of fast escape, say $m_e^2 R \gtrsim 10^{-11}\,\mathrm{eV}$.

We can distinguish two phases in the evolution. In the first one neutrino escape dominates and diffusion can be neglected. The second is a mixed phase where antineutrino escape dominates in some region and for some time and is comparable to diffusion elsewhere.

[6] For $m_e^2 R \gtrsim 10^{-7}$ the thermal processes would not be fast enough to maintain equilibrium. The time scale above would be affected, but the results below would not.

The first phase (**neutrino escape**) takes place in the $V_e > 0$ region, corresponding to $Y_{L_e} \gtrsim 3/10$, on the left of the vertical lines in fig. 3.2. The change of Y_{L_e} and T due to antineutrino conversion (where $V_e < 0$) and diffusion is negligible, since the time scales are slower. Due to neutrino disappearance, both Y_{L_e} and the energy density start decreasing. The essential point is whether the value of Y_{L_e} that stops the MSW conversion is reached before all the energy has been lost. This turns out to be the case in all the region where $V_e > 0$. In fact, by neglecting the diffusion terms in eqs. (3.18) we find the following relation between lepton fraction and the entropy variation:

$$\frac{\partial s}{\partial Y_{L_e}} = \left(\frac{F_{5/2}(\mu_{\nu_e}/T)}{F_{3/2}(\mu_{\nu_e}/T)} - \frac{\mu_{\nu_e}}{T} \right) \sim -\frac{2}{7} \frac{\mu_{\nu_e}}{T} \,, \tag{3.21}$$

where the partial derivative is taken at a fixed position and the approximation $\partial s/\partial Y_{L_e} \sim -2/7\, \mu_{\nu_e}/T$ holds for degenerate neutrinos. Since such an approximation does hold for $Y_{L_e} \gtrsim 0.3$ and $T \gtrsim 30\,\mathrm{MeV}$, eq. (3.21) shows that the temperature in the $V_e > 0$ region actually grows while it deleptonizes. In turn, that means that the $V_e = 0$ condition is comfortably attained spending only a fraction of the available energy. Within a time $t = 0.5$–$1\,\mathrm{sec}(10^{-11}\,\mathrm{eV}/m_e^2 R)$, Y_{L_e} has reached $\sim 3/10$ in all the $V_e > 0$ region and the fastest phase of evolution has ended. The profiles are now shown as solid thick lines in fig. 3.2. The temperature has increased as a consequence of the conversion of degeneracy energy into thermal energy. Such a conversion takes place when states deep inside the neutrino Fermi sphere are emptied by neutrinos escaping in the bulk. In summary, after the initially dramatic energy leak into the bulk, most of the energy in the $V_e > 0$ region gets locked as Y_{L_e} reaches $\sim 3/10$, which happens on the t_ν time scale. The thick lines in fig. 3.2 can therefore be considered as the initial condition for the subsequent evolution.

Before discussing the next phase, a comment on the initial condition we used is in order. As mentioned at the beginning of the subsection, for $m_e^2 R \gg 10^{-12}\,\mathrm{eV}$ the initial profiles are likely to be affected by the neutrino escape. For $m_e^2 R = 10^{-8}\,\mathrm{eV}$, for example, moving from the initial to the $Y_{L_e} \simeq 3/10$ profile only takes about a millisecond. Therefore, the initial profiles in fig. 3.2, following from analysis that do not take into account the new effect, cannot be trusted hundreds milliseconds after core bounce. On the other hand, given the fixed point character of the evolution in the fast phase, we can be confident that the thick solid profile is indeed reached as soon as the core settles. We are therefore entitled to use that profile in the subsequent evolution. Why not to use it in the first place and ignore the fast phase of evolution, then? Because the simulation based on eq. (3.21), although it does not take into account the conditions met in the early stages of the SN, still gives a conservative estimate of the temperature variation and of the amount of the energy loss, a key piece of information for what follows. In summary, the thick profiles in fig. 3.2 can be considered realistic initial profiles for the next phase within the approximations and uncertainties associated to our approach and to core collapse models. Needless to say, the original initial profiles are suitable as initial conditions for the standard diffusive regime ($m_e^2 R \lesssim 10^{-12}$ case) within the same uncertainties.

After neutrinos in what was initially the $V_e > 0$ region have been locked, **antineutrinos escape** begins to be significant in the $V_e < 0$ region. This happens on the slower time scale $t_{\bar{\nu}}$, which depends

on the position in the core. Since antineutrinos are lost, the lepton fraction Y_{L_e}, initially smaller than $\sim 3/10$, grows and V_e becomes less and less negative. Again, the essential point is whether the $V_e = 0$ condition, or $Y_{L_e} =\sim 3/10$, is reached before all the available energy is lost. The relevant equation is in this case

$$\frac{\partial s}{\partial Y_{L_e}} = -\left(\frac{F_{5/2}(-\mu_{\nu_e}/T)}{F_{3/2}(-\mu_{\nu_e}/T)} + \frac{\mu_{\nu_e}}{T}\right) \sim -\left(\frac{\mu_{\nu_e}}{T} + \frac{5}{2}\right) . \tag{3.22}$$

The loss turns out to be more pronounced than in the previous phase. Actually, the energy loss per unit of lepton number change is smaller, since the average antineutrino energy is $5/2\,T$ whereas the average neutrino energy was $5/7\mu_{\nu_e}$. However, the entropy variation is larger since the increase of Y_{L_e} leads to an increase of the energy stored in the degenerate neutrino or electron sea at the expenses of the temperature and entropy. That is why the RHS in eq. (3.22) is larger than in eq. (3.21). Furthermore, the change in Y_{L_e} needed to reach $\sim 3/10$ is larger in the external part of the inner core, where Y_{L_e} is lower. In order to clarify the situation, we need to numerically solve eq. (3.22). The result is that $V_e = 0$ is reached before all the local energy is gone only in the inner part of the $V_e < 0$ region. The outer part cools completely while Y_{L_e} is still lower than $\sim 3/10$, as it is apparent from Figs. 3.2. There, the light thick lines represent the asymptotic lepton fraction and temperature profiles that would be reached if the antineutrino escape phase continued indefinitely without diffusion. In the $r \gtrsim 9\,\mathrm{km}$ region, the asymptotic temperature profile reaches zero. Correspondingly, the maximum value of Y_{L_e} attainable before complete cooling is not $\sim 3/10$ anymore. In practice, complete cooling does not occur. The profiles reached after one second, before diffusion becomes essential, are shown by the thin lines in the $V_e < 0$ regions of figs. 3.2. The lines correspond to $m_e^2 R = 10^{-(10,\,9,\,8,\,7,\,6,\,5)}\,\mathrm{eV}$. The three largest values, that are not in the parameter space we are interested in, illustrate the asymptotic behavior of the profiles. Alternatively, they can be considered as the profiles at times $t = 10^{-(5,\,4,\,3,\,2,\,1,\,0)}\,\mathrm{sec}\,(m_e^2 R/(10^{-5}\,\mathrm{eV}))$ for a given value of $m_e^2 R$ — as long as $t \lesssim 1\,\mathrm{sec}$, of course. The $V_e = 0$ condition is reached and antineutrinos are locked in a portion of the initially $V_e < 0$ region which is larger the larger is $m_e^2 R$. In a sufficiently large but finite time that would happen in all the region where the asymptotic Y_{L_e} profile is constant and the T one is non vanishing. In the outer part of the inner core, on the other hand, neither $\sim 3/10$ nor the asymptotic profile will ever be reached. However, the attraction of the fixed point on Y_{L_e} has the effect of raising the Y_{L_e} profile, with interesting implications that will be discussed in section 3.4. The total energy loss in this phase is again a small fraction of the total available energy.

After the first, fast phase of neutrino escape and the second slower phase of antineutrino escape, **diffusion** begins to play a significant role. This happens on the slowest time scale t_{diff}. Diffusion "unlocks" the energy stored in the $V_e = 0$ region. Some of it gets lost in the bulk, the rest diffuses out in the outer part and eventually is emitted mainly as active neutrinos. The diffusion regime however is different from the standard one that takes place in absence of transitions into the bulk. We have in this case a mixed regime in which the evolution is determined by an interplay of diffusion and escape. Let us consider first the inner part of the core, where $V_e = 0$. Due to diffusion, the densities change, thus spoiling the $V_e = 0$ condition. The lepton fraction decreases and V_e becomes slightly negative. As V_e becomes negative, though, antineutrinos start to escape in the bulk thus giving a positive contribution to V_e. At some point, the positive contribution to V_e from conversion into bulk neutrinos will balance

the negative contribution from diffusion. In this regime, some of the energy is lost in the bulk and some is diffused out. The amount of energy lost in the invisible channel turns out to be independent of $m_e^2 R$ as long as the conversion of antineutrinos (slower than the neutrino conversion) is efficient enough to keep $|V_e|$ small. The evolution in such a regime is well described by a single equation for the temperature. In fact, denoting $Y_{L_e} = 3/10 + \delta Y_{L_e}$, we have

$$V_e = V_e(\rho, T) \simeq \frac{\partial V_e}{\partial Y_{L_e}} \delta Y_{L_e} \ . \tag{3.23}$$

When inserted in eqs. (3.18), the previous expression allows to recover $\delta Y_{L_e}(\rho, T)$ from eq. (3.18a). Eq. (3.18b) then becomes

$$\begin{aligned} n_B T \frac{\partial s}{\partial t} = a_e \left(\vec{\nabla} \mu_{\nu_e} \right)^2 + \vec{\nabla} \cdot \left((a_e + a_\mu + a_\tau) \frac{\pi^2}{6} \vec{\nabla} T^2 \right) \\ + \left(\mu_{\nu_e} - \sigma T \frac{F_{5/2}(\sigma \mu_{\nu_e}/T)}{F_{3/2}(\sigma \mu_{\nu_e}/T)} \right) \left(\vec{\nabla} \cdot \left(a_e \ \vec{\nabla} \mu_{\nu_e} \right) - n_B \frac{\partial Y_{L_e}}{\partial t} \right) \ . \end{aligned} \tag{3.24}$$

Eq. (3.24) always holds. In the small $|V_e|$ limit, one can approximate $Y_{L_e} \simeq 3/10$ everywhere, in which case the equation becomes selfconsistent and the evolution becomes independent of $m_e^2 R$. This of course will not hold forever since the efficiency of antineutrino conversion decreases as the star cools. Moreover, it certainly does not hold in the outer region where V_e is well below zero in the first place.

The numerical counterpart of all the above discussion is shown in fig. 3.3, where we plot the evolution of the Y_{L_e} and T profiles that follows from eqs. (3.18) for three values of $m_e^2 R$: $10^{-10}\,\mathrm{eV}$, $10^{-9}\,\mathrm{eV}$ and $10^{-8}\,\mathrm{eV}$. The case of no new physics is also showed in each plot for comparison (dashed lines). We do not aim at reproducing the results of the most sophisticated analysis in the literature for the latter case. However, a comparison between the solid and dashed lines in figure well illustrates the effect of new physics on the evolution. Due to neutrino conversion, Y_{L_e} quickly drops to $\sim 3/10$ in the inner part of the core. Then, on a longer time scale, diffusion further lowers Y_{L_e}, thus starting antineutrino conversion. For large values of $m_e^2 R$, the latter is efficient enough to keep Y_{L_e} close to $\sim 3/10$ for a few seconds, until the region becomes too cool to sustain the necessary conversion. After the initial dramatic fall, the lepton fraction is higher than in the case of pure diffusion. The same happens in the outer part of the core, where the effect is more pronounced because neutrino loss never took place and $|V_e|$ is larger during antineutrino conversion. The lepton fraction even grows in the first second and then decreases slower than in the case of pure diffusion, at the expenses of a quicker cooling. For $m_e^2 R = 10^{-8}\,\mathrm{eV}$, the temperature in the inner core essentially never increases. The corresponding evolution of the matter potential V_e is shown in fig. 3.1.

3.3.3.d In case of escape of muon or tau neutrinos

Let us now discuss more concisely the case of extra dimension open to muon neutrinos or (alternatively) to tau neutrinos, i.e. $m_\mu^2 R \neq 0$ with $m_e^2 R \equiv 0, m_\tau^2 R \equiv 0$ or $m_\tau^2 R \neq 0$ with $m_e^2 R \equiv 0, m_\mu^2 R \equiv 0$. As already mentioned, in this cases the matter MSW potential is initially negative in the whole inner core so

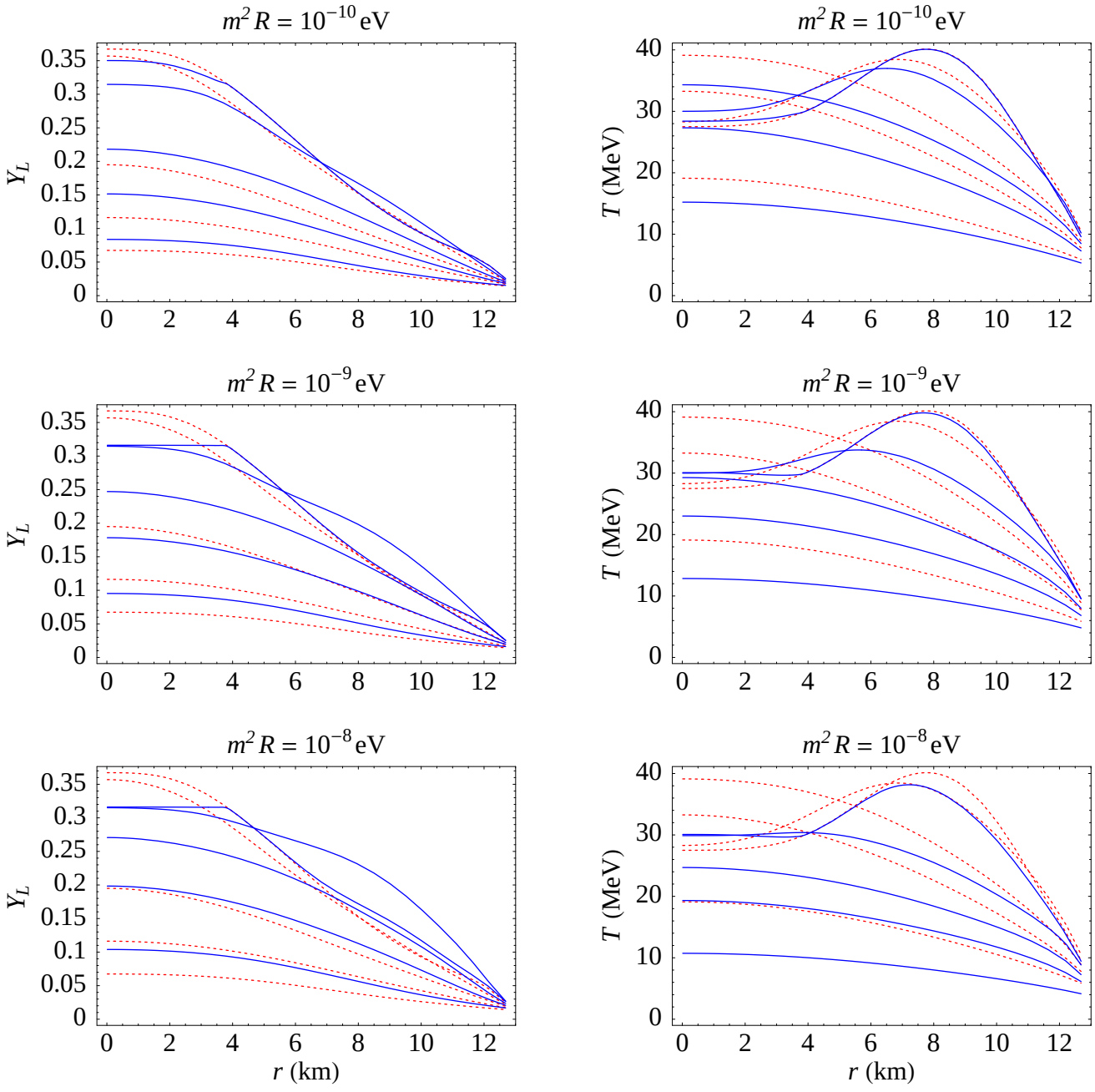

Figure 3.3: Electron lepton fraction and temperature profiles at $t = (0.01,\ 1,\ 10,\ 20,\ 40)$ sec for different values of $m_e^2 R$ (solid lines). The profiles for $m_e^2 R = 0$ are also shown for comparison (dashed lines).

that only $\bar{\nu}_{\mu,\tau}$ cross resonances. As conversions push $V_{\mu,\tau}$ towards zero and deleptonization pulls it down to its negative minimum value, a non-trivial interplay between diffusion and the new effect takes place. Nevertheless, the main features of the evolution can be easily understood. First of all, since the new physics is in the $\nu_{\mu,\tau}$ sector, the Y_{L_e} evolution is only indirectly affected, mainly via the modifications

to the temperature. As the ν_e's are almost degenerate, we expect their diffusion to be only slightly changed and in particular the deleptonization time scale to be unaffected. On the other hand, the $\bar{\nu}_{\mu,\tau}$ escape generates a positive Y_{ν_μ,ν_τ}, the balance $\nu_{\mu,\tau}$–$\bar{\nu}_{\mu,\tau}$ is broken and a positive chemical potential $\mu_{\nu_{\mu,\tau}}$ arises. This in turn inhibits the escape itself, both because $V_{\mu,\tau}$ is lifted towards zero by the term Y_{ν_μ,ν_τ} in eq. (3.12) and, more important, because the $\bar{\nu}_{\mu,\tau}$ abundance is suppressed in the presence of the chemical potential. In particular, $V_{\mu,\tau}$ has no chances to switch to positive values and only $\bar{\nu}_{\mu,\tau}$ do convert during all the evolution. Now, how do we expect the T evolution to be affected? In a first fast phase, as long as the conversion is dominant, a portion of the thermal energy is absorbed both by bulk neutrinos and by the sea of increasingly degenerate $\nu_{\mu,\tau}$'s. During all the following evolution, the thermal energy that the $\bar{\nu}_{\mu,\tau}$'s escape keeps on transferring to tau neutrinos is carried outside by their diffusion. Thus, we expect the T evolution to be sped up with respect to the standard case. Moreover, we expect the $\bar{\nu}_{\mu,\tau}$ escape cooling channel to be more effective than in the case of electron neutrinos as the $\nu_{\mu,\tau}$ diffusion time scale is shorter than for ν_e's.

The numerical solutions of the equations (3.18), for several choices of the parameter $m_\mu^2 R$ or $m_\tau^2 R$ in the range of eq. (3.10), confirm the above expectations. Essentially, the electron neutrino density follows the standard evolution while the temperature fall is faster. The muon/tau leptonic fraction $Y_{L_{\mu,\tau}}$ rapidly grows from zero up to a certain profile (the higher the larger $m_\mu^2 R$ or $m_\tau^2 R$, but always below about 0.1) and then lowers on typical diffusion timescales. In parallel, the chemical potential $\mu_{\nu_{\mu,\tau}}$ quickly grows up to values as large as those of μ_{ν_e} (of order 200 MeV) and then clears out with diffusion. A typical evolution of the matter potential is shown in fig. 3.1: at the beginning it is pushed towards zero by the rising of $Y_{L_{\mu,\tau}}$ but, the initial potential being well below zero, the available energy is not sufficient for a complete zeroing, and diffusion soon reverses the trend.

3.4 The outcome: bounds and signals

Let us analyse the relevant outputs of the modified core evolutions as a function of m^2R.

Fig. 3.3 shows [7] that deleptonization and cooling do take place on the same time scale as in absence of new physics despite the time scale of neutrino disappearance can be orders of magnitude faster than the diffusion one. What we need to know in addition is the size of the portion of the available lepton number and energy that disappears in the bulk and the portions that is actually emitted from the SN. Is something left to give rise to the SN1987a neutrino signal and to revive the shock in the delayed explosion scenario? This issue is addressed in fig. 3.4, where the energy lost by the inner core in the first 10 seconds are plotted against m^2R and split in the component that goes into the observable neutrino flux and the component that is irremediably lost in the bulk. The first ten seconds are the most interesting interval since this is the lapse of time during which the relevant neutrino signal is produced.

One sees that a sizeable portion can be lost into the invisible channel, especially for high values of $m_{\mu,\tau}^2 R$. At the same time, however, the total amount of drained energy increases significantly with

[7] Although it is relative to the case of electron neutrino escape, very similar plots come out in the case of muon and tau neutrinos going into the extra dimension, since the Y_{L_e} and T evolution is only marginally affected in these cases as discussed above.

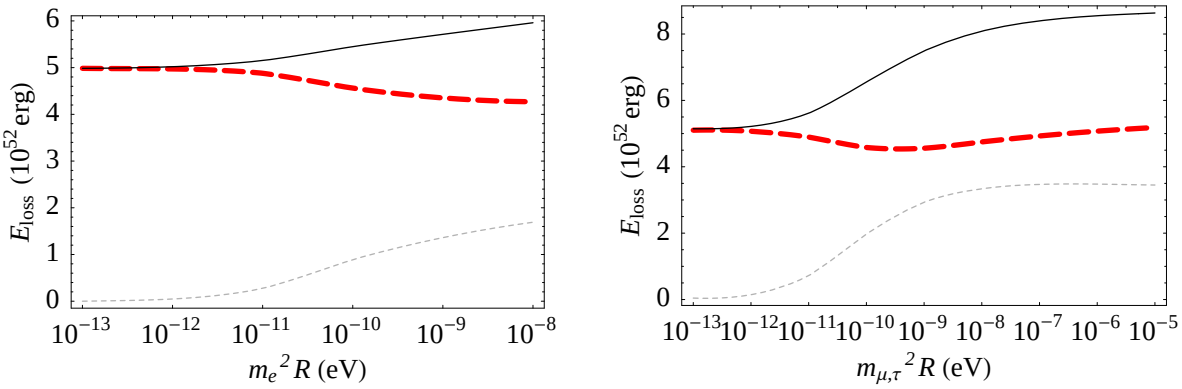

Figure 3.4: Energy that leaves the SN core in the first 10 secs as a function of the parameter m^2R, for the case of extra dimension open to electron neutrinos (left) or muon or tau neutrinos (right). The portion emitted in usual visible neutrinos is highlighted (red dashed line). See also shown the total energy (black solid line) and the portion carried into the bulk by sterile neutrinos (lower dotted line).

m^2R, as a consequence of the faster cooling of the core. Balancing the two effects, what is important is that the reduction of the portion emitted into the visible channel is always limited to $\sim 20\%$ of the standard case, which is well acceptable in the light of the need of accounting for the SN1987a signal.

We can therefore conclude that the **energy loss constraint** discussed in section 1.3.2 is **passed**: no direct upper bounds on the parameters $m^2_{e,\mu,\tau}R$ need to be imposed. They only remain subject to the generic bounds in (3.10), as represented in fig. 3.5.

The other significant result (see fig. 3.6) is the **emission of an excess of net lepton number** from the core with respect to the standard case, counterbalancing the antineutrinos that have escaped into the bulk. Fig. 3.7 also shows, for the case of $\nu_{\mu,\tau}$ neutrinos into extra dimensions, that the time distribution of the $\nu_{\mu,\tau}$ emission is concentrated in the very first seconds. An analogous behaviour is exhibited by the total energy emission, so that we can foresee a peculiar time dependence of the final neutrino number flux on Earth, more peaked at earlier times. Letting aside this general expectation, we focus in the following on time-integrated quantities.

The excesses of emitted lepton numbers can have interesting phenomenological consequences on SN physics and on the ν signal observable on Earth. In order to address them, one has to follow the vicissitudes and the ultimate fate of the neutrinos, from their way out of the core to their arrival on Earth: we have discussed these steps in 1.3.1, so we limit here to present the results.

First of all, coming out from the neutrino spheres, the flux displays a peculiar composition (see fig. 3.8). (Recall that the total luminosity in all neutrino species is not significantly affected, as the left panel of fig. 3.4 shows (integrated over 10 sec, but the same holds for the luminosity itself), therefore the effect of new physics that we are discussing is essentially a redistribution among the flavors.)

In the case of electron neutrinos escaping into the bulk, the electron neutrino flux can be significantly larger than the case without new physics. Since the electron neutrinos are much more effective

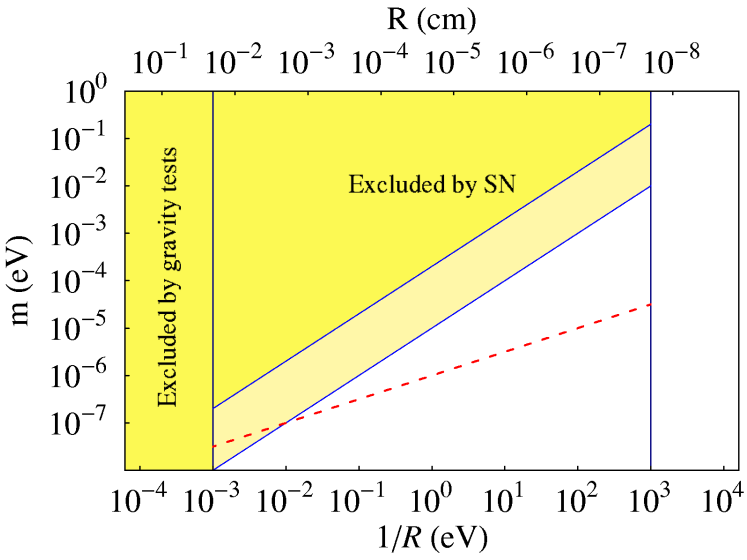

Figure 3.5: Excluded regions (on the plane $m - R$) in the case of electron neutrino escape (all the shaded region) or in the case of muon or tau neutrino escape (only the darker shaded area). The parameter m is to be intended as m_e, m_μ or m_τ depending on the case. The red dashed line marks the border of the region that would be erroneously excluded adopting the stringent bound in 3.11. The region above $1/R \simeq 10^3$ eV is allowed by the fact that the neutrinos do not cross enough resonances so the effect is not active.

than muon or tau neutrinos in depositing energy in the matter outside the neutrinosphere, a larger ν_e component might help a stalling shock in ejecting the SN envelope. In fact, the heating rate of matter irradiated by a hotter ν_e flux is proportional to T_ν^2, which we expect not to be significantly affected by a large $m_e^2 R$, and to the ν_e luminosity. An increase of the ν_e component has the effect of increasing the ν_e luminosity and, in turn, the heating rate.

On the other hand, in the case of muon and tau neutrinos escaping into the bulk, for large values of $m_{\mu,\tau}^2 R$, the $\nu_{\mu,\tau}$'s are ~ 5 times more than in the case without new physics, at the expense of the ν_e's and of all flavours of antineutrinos (all reduced by up to $\sim 60\%$). These reductions, although not so large, go into the direction opposite to the need of rejuvenating the stalling shock wave and thus helping the explosion, since muon and tau neutrinos are much less efficient than the electron ones in transferring their energy to the lingering matter. On the other hand, this qualitative argument does not imply a strong drawback. The actual explosion mechanism may be hidden in the complexity of the system, whose simulation is still a non-trivial task.

Following, then, the fluxes during all their way to the Earth, the indicative percentual composition of the neutrino signal as a function of $m^2 R$ is represented in fig. 3.9, assuming present global best fit values for θ_{12}, θ_{23}, ΔM_{12}^2 and $|\Delta M_{23}^2|$, taking into account the current upper bound on θ_{13} and choosing e.g. the case of normal hierarchy. Although the compositions are quite case-dependent, some structures can be observed.

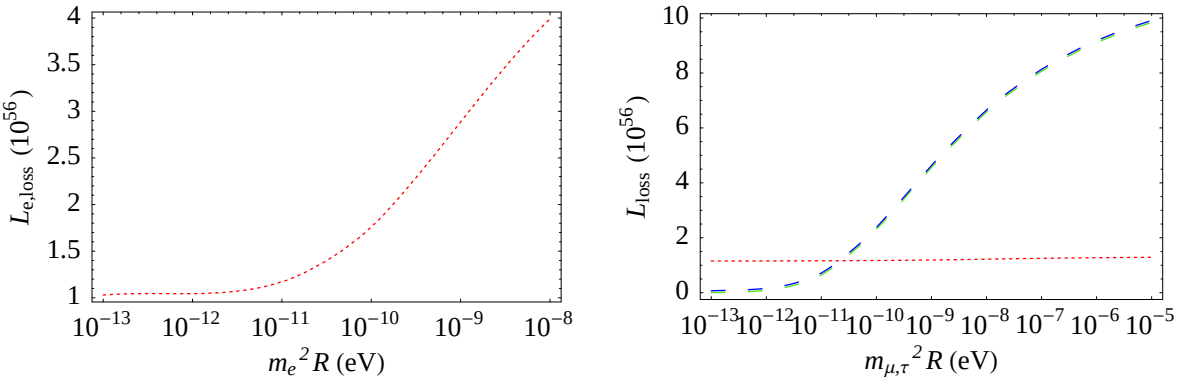

Figure 3.6: Lepton numbers emitted from the SN core in the first 10 secs as a function of m^2R. Left: the electron lepton number emitted in the case of extra dimension open to electron neutrinos. Right: the muon or tau lepton number emitted in the case of extra dimension open to muon or tau neutrinos (blue-green dashed line) and electron lepton number simultaneously emitted (red dotted line).

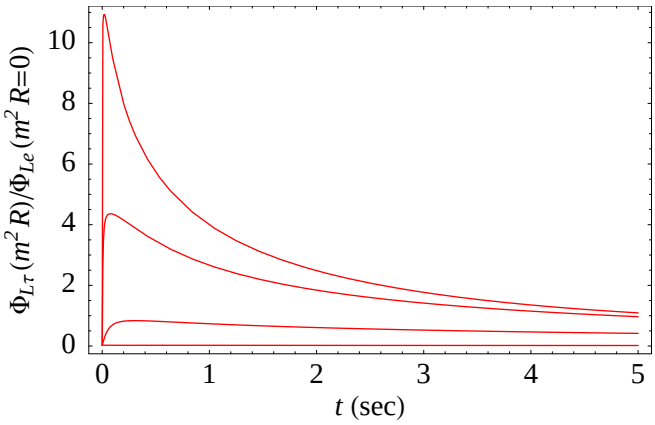

Figure 3.7: The tau lepton number flux versus time during the first 5 secs, for increasing values of $m_\tau^2 R = 10^{-(12,\ 10,\ 8,\ 6)}$, from bottom to top. The normalization is given by the value of the electron lepton number flux in absence of new physics.

First of all, a general important feature is the $\bar{\nu}_e$ flux reduction that can amount to up to $\sim 60\%$. Given the limited statistics of the 1987 event, the overall uncertainties on the expected neutrino fluxes (as predicted by full simulations, also based on assumptions on the progenitor star) and finally the approximate nature of the supernova core evolution adopted here, such a reduction is still compatible with present observations. Nevertheless, this feature is an interesting and potentially challenging one, and deserves to be addressed more closely in case of a future SN event with higher statistics. A similar remark also holds for the time structure of the neutrino signal mentioned above.

Moreover, as the net effect is always an increase in the total emitted lepton number, a crucial signature is the enhanced ratio between neutrinos and antineutrinos. This is a general feature of supernova neutrino oscillations into extra dimensions that does not depend on which flavour has a

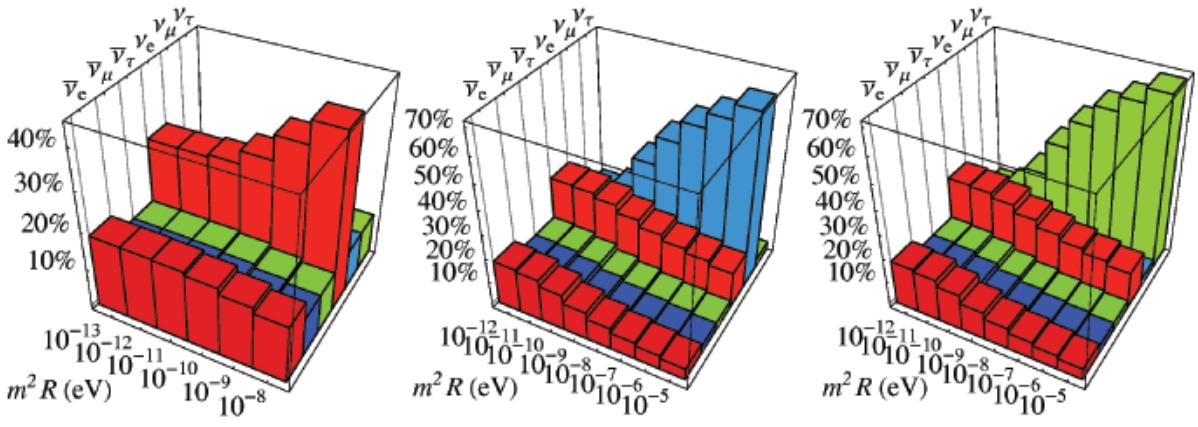

Figure 3.8: Indicative composition of the neutrino flux out of the neutrino spheres as a function of m^2R for the three different cases.

significant mixing with bulk neutrinos. What is case-dependent is which channel the enhancement shows up in. First one can focus on the electron channel, which will have high statistics in the future supernova events. Indeed, $\bar{\nu}_e$ are the dominant signal in the present and in most of the future detectors, while ν_e can be efficiently collected by large Čerenkov detectors, already existing (SK, SNO) or proposed (UNO), and liquid-argon detectors (Icarus, LANNDD) (see the discussion in 1.3.3). For several cases in fig. 3.9 the $\nu_e/\bar{\nu}_e$ ratio is significantly enlarged. However, it is also clear from fig. 3.9 that, depending on the value of P_H (i.e. of θ_{13}), the effect of ν_e or ν_τ conversion into the bulk could turn out to be irrelevant for the $\nu_e/\bar{\nu}_e$ channel in some cases, so that it would be necessary to measure the ν_μ or ν_τ fluxes. This is a harder task, which is however feasible at SNO, future detectors (UNO, LANNDD, OMNIS) or even at large scintillator detectors (KamLAND, Borexino). On the other hand, once an anomalous neutrino/antineutrino ratio is measured, how is it possible to distinguish which flavour does mix with the bulk? The answer lies in the energy spectrum. In fact, since the electron neutrinos are less energetic than the muon and tau ones when they leave the neutrino spheres, the effect of the $\nu_e \leftrightarrow \nu_{\mu,\tau}$ oscillation is to harden the ν_e spectrum on the Earth. The conversion into the bulk of the electron flavour, increasing the ν_e component flowing in the SN mantle, reduces this hardness, while the muon or tau conversion enhances it.

We have illustrated our results for a specific point in the parameter space of the standard neutrino oscillations. The residual dependence on θ_{12} (and θ_{23}) is mild. On the other hand, the distribution of the neutrino flux enhancement in the three flavours depends significantly on the neutrino mass pattern. Disentangling the flavour structure of the mixing with bulk neutrinos would therefore require the knowledge of sign(Δm^2_{23}) [167].

As already mentioned, another source of uncertainty is the precise value of the mean energies of the neutrinos coming out from their neutrino spheres. We checked that the adoption of a $\langle E_{\nu_{\mu,\tau},\bar{\nu}_{\mu,\tau}} \rangle$ closer to $\langle E_{\bar{\nu}_e} \rangle$, as suggested in [82], yields only minor modifications of our result. Namely, each column in fig. 3.8

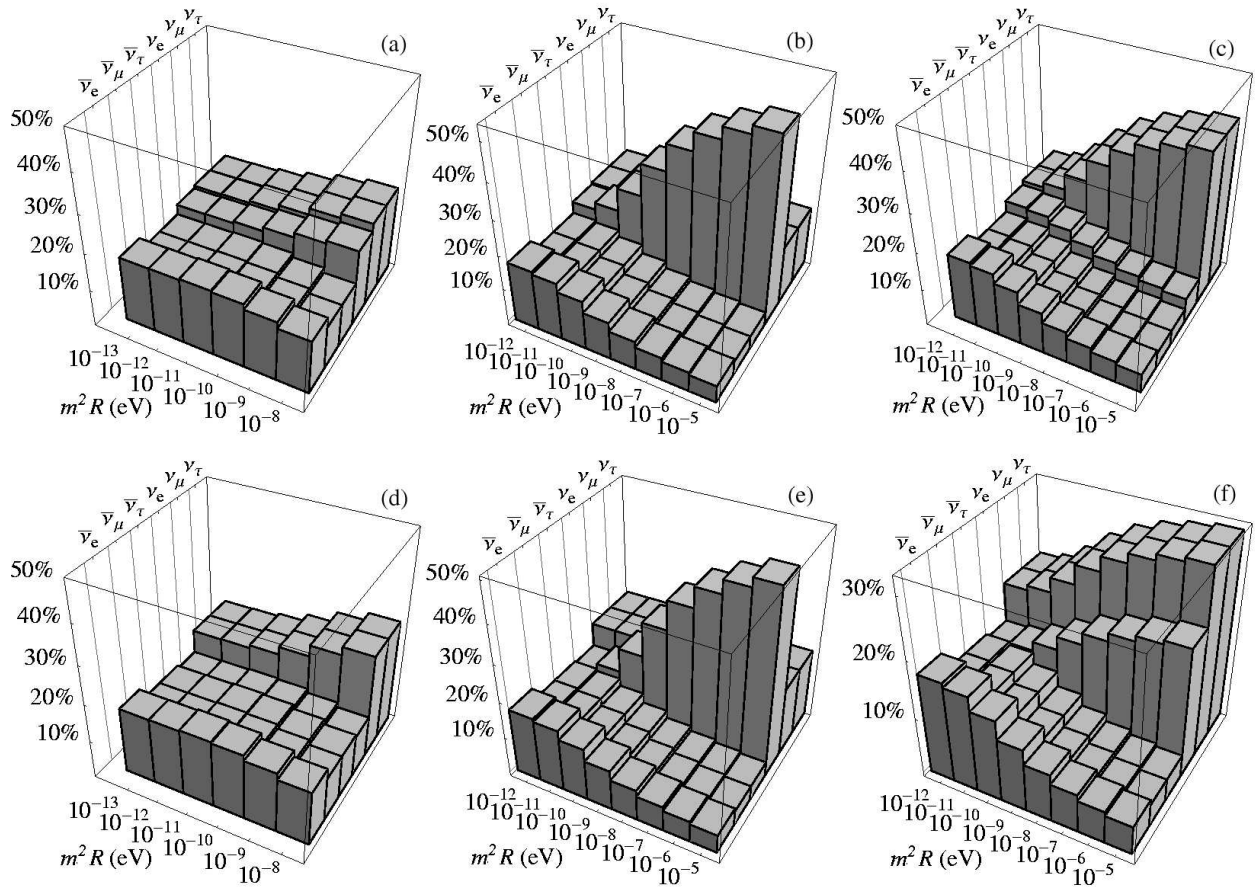

Figure 3.9: Indicative composition of the neutrino flux reaching the Earth's surface, as a function of m^2R, for the different cases of escape into the bulk: ν_e (first column), ν_μ (second column), ν_τ (third column); for $\sin^2\theta_{13} < 10^{-5}$ (first line) and for $\sin^2\theta_{13} > 10^{-3}$ (second line).

and figs. 3.9 is affected at most by a variation of $5 - 10\%$ in composition, within the uncertainties of our simplified model. Thus, the analysis is unchanged and the general trend confirmed: we only remark that the closer the mean energies, the smaller the differences among the channels, although preserving the features described above.

While we have so far considered the case in which the neutrino escape is dominated by the oscillations in the bulk of one of the three neutrinos, it is also possible that all SM neutrinos are involved in the energy loss. In this case, the neutrino flux on the Earth would still be enhanced over the antineutrino one. However, the neutrino flux composition would also be determined by the relative size of the three mixing parameters m_e, m_μ, m_τ. The evolutions of the three neutrino abundances in the core would be coupled through the temperature and the matter potential. The feedback mechanisms would however still take place, but we expect the m_i–R parameter space for the three channels to be slightly reduced.

3.5 Appendix: subleading invisible channels

In this Appendix, we discuss the limits on conventional (non self-limiting) invisible cooling channels. This simple application of the formalism set up in the present Chapter is relevant to our discussion because it provides the condition under which subleading contribution to the disappearance probability are under control and therefore sets the limits we have used in eq. (3.6).

Let $P_\nu(L,E)$ be the probability that a neutrino of type $\nu = \nu_e, \nu_\mu, \nu_\tau, \bar\nu_e, \bar\nu_\mu, \bar\nu_\tau$ with energy E disappears in an invisible channel while traveling a distance L and let us assume that there is no reappearance[8]. In order to obtain a limit on P_ν, we compare the consequent lepton number loss rate with the diffusion one. The simplest case is that of a power-law disappearance probability $P_\nu(L,E) = P_0(L/L_0)^\alpha(E/E_0)^\beta$. For example, the mixing with a tower of KK states gives rise to a contribution to the escape probability which is essentially constant in the relevant range for L, E: $P_{\nu,\bar\nu} \sim (mR)^2$.

The neutrino number density loss rate is

$$\Gamma_\nu = \int \frac{d\vec p}{(2\pi)^3} \frac{\langle P\rangle_E}{\lambda_\nu(E)} f_\nu(E)\,, \tag{3.25}$$

where $\langle P\rangle = \int_0^\infty dx P(x\lambda_\nu(E),E)e^{-x}$ is the average over the distance traveled of the disappearance probability. In the case of a power law probability and within the approximations discussed in Section 3.3.2, one has

$$\Gamma_\nu = \frac{\Gamma(\alpha+1)}{12\pi^4 a_\nu}\, T^5 F_{4+\beta-2\alpha}\left(\frac{\mu_\nu}{T}\right)\,, \tag{3.26}$$

where $a_\nu = \lambda_\nu E^2/(6\pi^2)$. By definition of $t_{\rm diff}$, the diffusion rate is $\Gamma_{\rm diff} = n_B \partial Y_L/\partial t = n_B Y_L/t_{\rm diff}$. The limit on the probability following from $\Gamma_\nu < \Gamma_{\rm diff}$ reflects the abundance of the neutrino type considered,

$$P_\nu(\lambda(\mu_\nu),\mu_\nu) < 2\cdot 10^{-11} a_{\alpha\beta}\left(\frac{200\,\text{MeV}}{\mu_\nu}\right)^5 \frac{\rho}{\rho_0}\frac{Y_L}{0.3}\frac{10\,\text{sec}}{t_{\rm diff}} \qquad \text{for } \nu=\nu_e \tag{3.27a}$$

$$P_\nu(\lambda(T),T) < 1.5\cdot 10^{-8} b_{\alpha\beta}\left(\frac{30\,\text{MeV}}{T}\right)^5 \frac{\rho}{\rho_0}\frac{Y_L}{0.3}\frac{10\,\text{sec}}{t_{\rm diff}} \qquad \text{for } \nu=\nu_{\mu,\tau} \text{ or } \bar\nu_{\mu,\tau} \tag{3.27b}$$

$$P_\nu(\lambda(T),T) < 3\cdot 10^{-6} b_{\alpha\beta}\, e^{(\mu_\nu/T-20/3)}\left(\frac{30\,\text{MeV}}{T}\right)^5 \frac{\rho}{\rho_0}\frac{Y_L}{0.3}\frac{10\,\text{sec}}{t_{\rm diff}} \quad \text{for } \nu=\bar\nu_e\,, \tag{3.27c}$$

where $a_{\alpha\beta} = (5+\beta-2\alpha)/(5\Gamma(\alpha+1))$, $b_{\alpha\beta} = 24/(\Gamma(5+\beta-2\alpha)\Gamma(\alpha+1))$ are numerical coefficients normalized to $a_{00} = b_{00} = 1$. In particular, in the case of a constant electron neutrino disappearance probability $P_{\nu_e} = (mR)^2$ we get the limit $mR \lesssim 0.5\cdot 10^{-5}(200\,\text{MeV}/\mu_\nu)^{5/2}(10\,\text{sec}/t_{\rm diff})$ that we used to determine the conservative upper bound $m^2R \lesssim 10^{-8}\,\text{eV}$.

[8] In the case of oscillations, reappearance can be neglected when $P \ll 1$. The case of large mixing is not covered here.

Chapter 4

Conclusions

In this thesis I discussed the bounds and the possible signals for sterile neutrinos (under the form of a 4D additional state or of an infinite tower of states motivated by extra dimensional models) that come from astrophysical and cosmological processes.

In Chapter 1 I set the stage (presenting the status of the SM, the status of neutrino oscillations and the open directions) and I introduced the main characteristics of the relevant cosmological and astrophysical tools (BBN, LSS, CMB and the supernovæ).

Chapter 2 was devoted to the case of a single (4D) sterile neutrino mixed with the active neutrinos. The (now consolidated) mixing among active neutrinos themselves was included in the game and the analysis that I presented addresses every possible mixing pattern in all the available range of the oscillation parameters. First I described the parametrization of the full 4 neutrino mixing that is employed. Then I discussed and followed in detail the neutrino evolution in the Early Universe. The resulting bounds in the oscillation parameter space that come from BBN (considering Helium and Deuterium), LSS and CMB were summarized in the plots of fig. 2.3. Concerning the BBN constraint, the new modifications due to the inclusion of the active-active mixing can be appreciated via the comparison with the plots in the simplified cases of fig. 2.2. Concerning the LSS limit, the plots show its more detailed structure, missing in previous analysis that did not follow the time evolution of the neutrino densities. Moreover, those plots show the sensitivity that the future measurements (of the primordial abundances, of the neutrino contribution to Ω and of the CMB spectrum) might reach. The bounds that come from SN1987a were discussed in Section 2.3 and an example is shown in fig. 2.6.

Chapter 3 was devoted to the case of sterile 5D fermions in models with extra space dimensions, which translate in infinite towers of 4D sterile neutrinos, mixed with the active ones. While the cosmological implications of such a scenario are shown to be negligible, it on the contrary opens a potentially dangerous channel of energy loss in the supernova core. However, it is shown that a careful study of the SN physics can allow a relaxation of the previous bounds on the extra dimensional parameters in the literature by several orders of magnitude, thanks to feedback mechanisms that prevent an excessive loss. In particular, the compatibility with the SN1987a signal is assured. The constraints that survive (eq. (3.10)) come from subleading effects. The re-opened and excluded regions are shown in fig. 3.5. An interesting modified phenomenology, however, is also obtained. For the three cases of electron, muon

and tau neutrinos mixed with the extra dimensional states, the possible signatures of extra dimensional states in the neutrino signal from the next SN are considered: fig. 3.9 presents the indicative composition of the flux reaching the Earth surface for every case. The dominance of neutrinos over antineutrinos of all flavors, which can be traced back to the escape of antineutrinos into the bulk, is the most distinctive feature. Other possible signatures include a modified time structure of the signal (in the case of muon or tau neutrino mixed with the bulk fermions) and peculiar hardening or softening of the neutrino spectra. Finally, the general case of all neutrinos mixed with extra dimensional sterile states is briefly addressed.

Needless to say, the discussed topics cover only a small part of the large amount of work that has been done and is to be done yet at the intersection of Astrophysics, Cosmology, Neutrino Physics and High Energy Physics, not to speak of the possible surprises coming from these very active fields. The fascinating study of Supernovæ and of the Early Universe encourages now more than ever to explore the open prospectives of the Physics which is beyond the Standard.

Bibliography

[1] M. Cirelli, G. Marandella, A. Strumia, F. Vissani, "Probing oscillations into sterile neutrinos with cosmology, astrophysics and experiments," to appear soon.

[2] G. Cacciapaglia, M. Cirelli, Y. Lin and A. Romanino, "Bulk neutrinos and core collapse supernovae," Phys. Rev. D **67** (2003) 053001 [arXiv:hep-ph/0209063].

[3] G. Cacciapaglia, M. Cirelli and A. Romanino, "Signatures of supernova neutrino oscillations into extra dimensions," Phys. Rev. D **68** (2003) 033013 [arXiv:hep-ph/0302246].

[4] G. Cacciapaglia, M. Cirelli and G. Cristadoro, "Gluon fusion production of the Higgs boson in a calculable model with one extra dimension," Phys. Lett. B **531** (2002) 105 [arXiv:hep-ph/0111287].

[5] G. Cacciapaglia, M. Cirelli and G. Cristadoro, "Muon anomalous magnetic moment in a calculable model with one extra dimension," Nucl. Phys. B **634** (2002) 230 [arXiv:hep-ph/0111288].

Bibliography for introductory sections:
1.1: The Standard Model and why to go beyond

[6] J. L. Rosner, "Resource letter: The standard model and beyond," arXiv:hep-ph/0206176;

S. Willenbrock, "The standard model and the top quark," arXiv:hep-ph/0211067, Chapter 1 only;

J. R. Ellis, "Beyond the standard model for hillwalkers," arXiv:hep-ph/9812235;

Z. Kunszt, "Bread and butter standard model", arXiv:hep-ph/0004103;

C. Quigg, "The state of the standard model", arXiv:hep-ph/0001145;

J. Womersley, "Physics beyond the standard model," J. Phys. G **26** (2000) 505 [arXiv:hep-ex/0001039].

[7] The Lep ElectroWeak Working Group, results presented at 2003 summer conferences, http://www.cern.ch/LEPEWWG/

[8] H. E. Montgomery, "XXXVIIieme Rencontres de Moriond: Electroweak 2002 conference summary," arXiv:hep-ex/0207002.

P. Langacker, "Recent developments in precision electroweak physics," arXiv:hep-ph/0211065.

[9] http://www.g-2.bnl.gov/

[10] S. Davidson, S. Forte, P. Gambino, N. Rius and A. Strumia, "Old and new physics interpretations of the NuTeV anomaly," JHEP **0202** (2002) 037 [arXiv:hep-ph/0112302].

R. H. Bernstein [NuTeV Collaboration], "Standard model explanations for the NuTeV electroweak measurements," J. Phys. G **29** (2003) 1919 [arXiv:hep-ex/0210061].

B. A. Dobrescu and R. K. Ellis, "Analytic estimates of the QCD corrections to neutrino nucleus scattering," arXiv:hep-ph/0310154.

S. Kretzer, F. Olness, J. Pumplin, D. Stump, W. K. Tung and M. H. Reno, "The parton structure of the nucleon and precision determination of the Weinberg angle in neutrino scattering," arXiv:hep-ph/0312322.

[11] F. Wilczek, "Beyond the standard model: This time for real," Nucl. Phys. Proc. Suppl. **77** (1999) 511 [arXiv:hep-ph/9809509].

[12] T. Hambye and K. Riesselmann, "Matching conditions and Higgs mass upper bounds revisited," Phys. Rev. D **55** (1997) 7255 [arXiv:hep-ph/9610272], and references inside.

See also the Lep Higgs Working Group, http://lephiggs.web.cern.ch/LEPHIGGS/www/Welcome.html.

[13] R. Barbieri and A. Strumia, "The 'LEP paradox'," arXiv:hep-ph/0007265.

[14] V. A. Rubakov, "Large and infinite extra dimensions: An introduction," Phys. Usp. **44** (2001) 871 [Usp. Fiz. Nauk **171** (2001) 913] [arXiv:hep-ph/0104152].

M. Besancon, "Experimental introduction to extra dimensions," arXiv:hep-ph/0106165.

A. Perez-Lorenzana, "Theories in more than four dimensions," AIP Conf. Proc. **562** (2001) 53 [arXiv:hep-ph/0008333].

R. Tabbash, "Physics of extra dimensions: Higher-dimensional virtual environments," arXiv:hep-ph/0111334.

[15] N. Arkani-Hamed, S. Dimopoulos and G. R. Dvali, "The hierarchy problem and new dimensions at a millimeter," Phys. Lett. B **429** (1998) 263 [arXiv:hep-ph/9803315].

See also:

I. Antoniadis, "A Possible New Dimension At A Few Tev," Phys. Lett. B **246** (1990) 377;

J. D. Lykken, "Weak Scale Superstrings," Phys. Rev. D **54** (1996) 3693 [arXiv:hep-th/9603133];

[16] J. C. Long, H. W. Chan, A. B. Churnside, E. A. Gulbis, M. C. Varney and J. C. Price, "New experimental limits on macroscopic forces below 100-microns," arXiv:hep-ph/0210004.

[17] N. Arkani-Hamed, S. Dimopoulos and G. R. Dvali, "Phenomenology, astrophysics and cosmology of theories with sub-millimeter dimensions and TeV scale quantum gravity," Phys. Rev. D **59** (1999) 086004 [arXiv:hep-ph/9807344].

[18] I. Antoniadis, N. Arkani-Hamed, S. Dimopoulos and G. R. Dvali, "New dimensions at a millimeter to a Fermi and superstrings at a TeV," Phys. Lett. B **436** (1998) 257 [arXiv:hep-ph/9804398].

[19] G. F. Giudice, R. Rattazzi and J. D. Wells, "Quantum gravity and extra dimensions at high-energy colliders," Nucl. Phys. B **544** (1999) 3 [arXiv:hep-ph/9811291].

See also:

G. F. Giudice, R. Rattazzi and J. D. Wells, "Graviscalars from higher-dimensional metrics and curvature-Higgs mixing," Nucl. Phys. B **595** (2001) 250 [arXiv:hep-ph/0002178].

[20] G. F. Giudice, R. Rattazzi and J. D. Wells, "Transplanckian collisions at the LHC and beyond," Nucl. Phys. B **630** (2002) 293 [arXiv:hep-ph/0112161].

[21] L. Anchordoqui, T. Paul, S. Reucroft and J. Swain, "Ultrahigh energy cosmic rays: The state of the art before the Auger observatory," arXiv:hep-ph/0206072, sections VII and IX

R. Emparan, M. Masip and R. Rattazzi, "Cosmic rays as probes of large extra dimensions and TeV gravity," Phys. Rev. D **65** (2002) 064023 [arXiv:hep-ph/0109287].

[22] R. Brandenberger, invited seminar at Scuola Normale Superiore, Pisa, Italy, 14 February 2002; based on

S. Alexander, R. H. Brandenberger and D. Easson, "Brane gases in the early universe," Phys. Rev. D **62** (2000) 103509 [arXiv:hep-th/0005212].

[23] A. Pomarol and M. Quiros, "The standard model from extra dimensions," Phys. Lett. B **438** (1998) 255 [arXiv:hep-ph/9806263].

A. Delgado, A. Pomarol and M. Quiros, "Supersymmetry and electroweak breaking from extra dimensions at the TeV-scale," Phys. Rev. D **60** (1999) 095008 [arXiv:hep-ph/9812489].

A. Delgado, A. Pomarol and M. Quiros, "Electroweak and flavor physics in extensions of the standard model with large extra dimensions," JHEP **0001** (2000) 030 [arXiv:hep-ph/9911252].

[24] T. Appelquist, H. C. Cheng and B. A. Dobrescu, "Bounds on universal extra dimensions," Phys. Rev. D **64** (2001) 035002 [arXiv:hep-ph/0012100].

[25] Y. Kawamura, "Triplet-doublet splitting, proton stability and extra dimension," Prog. Theor. Phys. **105** (2001) 999 [arXiv:hep-ph/0012125].

[26] G. Altarelli and F. Feruglio, "SU(5) grand unification in extra dimensions and proton decay," Phys. Lett. B **511** (2001) 257 [arXiv:hep-ph/0102301].

[27] R. Ruckl, Lectures at Corfu Summer Institute, September 2001; based on

A. Muck, A. Pilaftsis and R. Ruckl, "An introduction to 5-dimensional extensions of the standard model," arXiv:hep-ph/0209371.

[28] J. Lykken and S. Nandi, "Asymmetrical large extra dimensions," Phys. Lett. B **485** (2000) 224 [arXiv:hep-ph/9908505].

[29] R. Barbieri, L. J. Hall and Y. Nomura, "A constrained standard model from a compact extra dimension," Phys. Rev. D **63** (2001) 105007 [arXiv:hep-ph/0011311].

[30] L. Randall and R. Sundrum, "A large mass hierarchy from a small extra dimension," Phys. Rev. Lett. **83** (1999) 3370 [arXiv:hep-ph/9905221].

[31] W. D. Goldberger and M. B. Wise, "Modulus stabilization with bulk fields," Phys. Rev. Lett. **83** (1999) 4922 [arXiv:hep-ph/9907447].

[32] L. Randall and R. Sundrum, "An alternative to compactification," Phys. Rev. Lett. **83** (1999) 4690 [arXiv:hep-th/9906064].

1.2: "Standard" neutrino physics and why to go beyond

[33] There are ktons of reviews on neutrino physics, especially oscillations. Among them:

M. C. Gonzalez-Garcia and Y. Nir, "Developments in neutrino physics," Rev. Mod. Phys. **75** (2003) 345 [arXiv:hep-ph/0202058].

E. K. Akhmedov, "Neutrino physics," arXiv:hep-ph/0001264.

S. M. Bilenky, C. Giunti, J. A. Grifols and E. Masso, "Absolute values of neutrino masses: Status and prospects," Phys. Rept. **379** (2003) 69 [arXiv:hep-ph/0211462].

T. K. Kuo and J. Pantaleone, "Neutrino Oscillations In Matter," Rev. Mod. Phys. **61** (1989) 937.

[34] One can also see the very accessible and nice reviews (and references therein):

N. Schmitz, "The discovery of neutrino masses," arXiv:hep-ex/0211041.

H. Pas, "Neutrino masses and particle physics beyond the standard model," Annalen Phys. **11** (2002) 551 [arXiv:hep-ph/0209018].

[35] A. de Gouvea, A. Friedland and H. Murayama, "The dark side of the solar neutrino parameter space," Phys. Lett. B **490** (2000) 125 [arXiv:hep-ph/0002064].

[36] J. N. Bahcall, M. C. Gonzalez-Garcia and C. Pena-Garay, "Before and after: How has the SNO neutral current measurement changed things?," JHEP **0207** (2002) 054 [arXiv:hep-ph/0204314].

[37] G. L. Fogli, E. Lisi, A. Marrone, D. Montanino, A. Palazzo and A. M. Rotunno, "Solar neutrino oscillation parameters after first KamLAND results," Phys. Rev. D **67** (2003) 073002 [arXiv:hep-ph/0212127].

[38] P. Creminelli, G. Signorelli and A. Strumia in [40]

[39] KamLAND Collaboration, "First results from KamLAND: Evidence for reactor anti-neutrino disappearance," Phys. Rev. Lett. **90** (2003) 021802 [arXiv:hep-ex/0212021];

V. Barger and D. Marfatia, "KamLAND and solar neutrino data eliminate the LOW solution," Phys. Lett. B **555** (2003) 144 [arXiv:hep-ph/0212126];

G. L. Fogli, E. Lisi, A. Marrone, D. Montanino, A. Palazzo and A. M. Rotunno, "Solar neutrino oscillation parameters after first KamLAND results," Phys. Rev. D **67** (2003) 073002 [arXiv:hep-ph/0212127];

M. Maltoni, T. Schwetz and J. W. Valle, "Combining first KamLAND results with solar neutrino data," Phys. Rev. D **67** (2003) 093003 [arXiv:hep-ph/0212129];

P. Creminelli, G. Signorelli and A. Strumia, "Frequentist analyses of solar neutrino data," JHEP **0105** (2001) 052, see addendum in arXiv:hep-ph/0102234v4;

A. Bandyopadhyay, S. Choubey, R. Gandhi, S. Goswami and D. P. Roy, "The solar neutrino problem after the first results from KamLAND," Phys. Lett. B **559** (2003) 121 [arXiv:hep-ph/0212146];

J. N. Bahcall, M. C. Gonzalez-Garcia and C. Peña-Garay, "Solar neutrinos before and after KamLAND," JHEP **0302** (2003) 009 [arXiv:hep-ph/0212147];

H. Nunokawa, W. J. Teves and R. Zukanovich Funchal, "Determining the oscillation parameters by solar neutrinos and KamLAND," Phys. Lett. B **562** (2003) 28 [arXiv:hep-ph/0212202];

P. Aliani, V. Antonelli, M. Picariello and E. Torrente-Lujan, "Neutrino mass parameters from Kamland, SNO and other solar evidence," arXiv:hep-ph/0212212;

P. C. de Holanda and A. Y. Smirnov, "LMA MSW solution of the solar neutrino problem and first KamLAND results," JCAP **0302** (2003) 001 [arXiv:hep-ph/0212270].

[40] P. Creminelli, G. Signorelli and A. Strumia, "Frequentist analyses of solar neutrino data," JHEP **0105** (2001) 052, see addendum in arXiv:hep-ph/0102234v5;

A. Bandyopadhyay, S. Choubey, S. Goswami, S. T. Petcov and D. P. Roy, "Constraints on neutrino oscillation parameters from the SNO salt phase data," arXiv:hep-ph/0309174.

P. Aliani, V. Antonelli, M. Picariello and E. Torrente-Lujan, "The neutrino mass matrix after Kamland and SNO salt enhanced results," arXiv:hep-ph/0309156.

P. C. de Holanda and A. Y. Smirnov, "Solar neutrinos: The SNO salt phase results and physics of conversion," arXiv:hep-ph/0309299.

A. B. Balantekin and H. Yuksel, "Constraints on neutrino parameters from neutral-current solar neutrino measurements," Phys. Rev. D **68** (2003) 113002 [arXiv:hep-ph/0309079].

S. N. Ahmed *et al.* [SNO Collaboration], "Measurement of the total active B-8 solar neutrino flux at the Sudbury Neutrino Observatory with enhanced neutral current sensitivity," arXiv:nucl-ex/0309004.

[41] G. L. Fogli, E. Lisi, A. Marrone and D. Montanino, "Status of atmospheric nu/mu → nu/tau oscillations and decoherence after the first K2K spectral data," Phys. Rev. D **67** (2003) 093006 [arXiv:hep-ph/0303064].

[42] M. H. Ahn *et al.* [K2K Collaboration], "Indications of neutrino oscillation in a 250-km long-baseline experiment," Phys. Rev. Lett. **90** (2003) 041801 [arXiv:hep-ex/0212007].

[43] E. T. Kearns, "Atmospheric neutrinos in 2002," Frascati Phys. Ser. **28** (2002) 413 [arXiv:hep-ex/0210019].

[44] M. C. Gonzalez-Garcia and C. Pena-Garay, "Three-neutrino mixing after the first results from K2K and KamLAND," Phys. Rev. D **68** (2003) 093003 [arXiv:hep-ph/0306001].

M. Maltoni, T. Schwetz, M. A. Tortola and J. W. F. Valle, "Status of three-neutrino oscillations after the SNO-salt data," Phys. Rev. D **68** (2003) 113010 [arXiv:hep-ph/0309130].

[45] A. Y. Smirnov, "Neutrino physics after KamLAND," arXiv:hep-ph/0306075.

A. Y. Smirnov, "Neutrino physics: Open theoretical questions," arXiv:hep-ph/0311259.

[46] G. L. Fogli, E. Lisi, A. Marrone and A. Palazzo, "Evidence for Mikheyev-Smirnov-Wolfenstein effects in solar neutrino flavor transitions," arXiv:hep-ph/0309100.

[47] O. G. Miranda, T. I. Rashba, A. I. Rez and J. W. F. Valle, "Constraining the neutrino magnetic moment with anti-neutrinos from the sun," arXiv:hep-ph/0311014.

[48] S. Davidson, C. Pena-Garay, N. Rius and A. Santamaria, "Present and future bounds on non-standard neutrino interactions," JHEP **0303** (2003) 011 [arXiv:hep-ph/0302093].

[49] O. L. G. Peres and A. Y. Smirnov, "Atmospheric neutrinos: LMA oscillations, U(e3) induced interference and CP-violation," arXiv:hep-ph/0309312.

[50] M. Lindner, "The physics potential of future long-baseline neutrino oscillation experiments," arXiv:hep-ph/0209083.

[51] A. Aguilar *et al.* [LSND Collaboration], "Evidence for neutrino oscillations from the observation of anti-nu/e appearance in a anti-nu/mu beam," Phys. Rev. D **64** (2001) 112007 [arXiv:hep-ex/0104049].

[52] C. Athanassopoulos *et al.* [LSND Collaboration], "Evidence for nu/mu → nu/e neutrino oscillations from LSND," Phys. Rev. Lett. **81** (1998) 1774 [arXiv:nucl-ex/9709006].

[53] K.Hagiwara et al., Phys. Rev. D66, 010001 (2002) or http://lepewwg.web.cern.ch/LEPEWWG/

[54] H. Murayama and T. Yanagida, "LSND, SN1987A, and CPT violation," Phys. Lett. B **520** (2001) 263 [arXiv:hep-ph/0010178].

G. Barenboim, L. Borissov and J. Lykken, "CPT violating neutrinos in the light of KamLAND. ((U))," arXiv:hep-ph/0212116.

[55] A. Strumia, "Interpreting the LSND anomaly: Sterile neutrinos or CPT-violation or...?," Phys. Lett. B **539** (2002) 91 [arXiv:hep-ph/0201134].

[56] M. C. Gonzalez-Garcia, M. Maltoni and T. Schwetz, "Status of the CPT violating interpretations of the LSND signal," Phys. Rev. D **68** (2003) 053007 [arXiv:hep-ph/0306226].

[57] K. S. Babu and S. Pakvasa, "Lepton number violating muon decay and the LSND neutrino anomaly," arXiv:hep-ph/0204236.

[58] V. Barger, D. Marfatia and K. Whisnant, "LSND anomaly from CPT violation in four-neutrino models," Phys. Lett. B **576** (2003) 303 [arXiv:hep-ph/0308299].

[59] O. L. G. Peres and A. Y. Smirnov, "(3+1) spectrum of neutrino masses: A chance for LSND?," Nucl. Phys. B **599** (2001) 3 [arXiv:hep-ph/0011054].

M. Sorel, J. Conrad and M. Shaevitz, "A combined analysis of short-baseline neutrino experiments in the (3+1) and (3+2) sterile neutrino oscillation hypotheses," arXiv:hep-ph/0305255.

. S. Babu and G. Seidl, "Simple model for (3+2) neutrino oscillations," arXiv:hep-ph/0312285.

[60] D. B. Kaplan, A. E. Nelson and N. Weiner, "Neutrino oscillations as a probe of dark energy," arXiv:hep-ph/0401099.

[61] E. D. Zimmerman [BooNE Collaboration], "BooNE has begun," eConf **C0209101** (2002) TH05 [Nucl. Phys. Proc. Suppl. **123** (2003) 267] [arXiv:hep-ex/0211039].

[62] J. N. Bahcall, "Solar models: An historical overview," AAPPS Bull. **12N4** (2002) 12 [Nucl. Phys. Proc. Suppl. **118** (2003 IMPAE,A18,3761-3776.2003) 77] [arXiv:astro-ph/0209080].

[63] S. Mohanty, "Determination of the age of the earth from KamLAND measurement of geo-neutrinos," arXiv:hep-ph/0302060.

[64] G. Fiorentini, T. Lasserre, M. Lissia, B. Ricci and S. Schonert, "KamLAND, terrestrial heat sources and neutrino oscillations," Phys. Lett. B **558** (2003) 15 [arXiv:hep-ph/0301042].

H. Nunokawa, W. J. C. Teves and R. Zukanovich Funchal, "Discriminating among earth composition models using geo-antineutrinos," JHEP **0311** (2003) 020 [arXiv:hep-ph/0308175].

G. Fiorentini, M. Lissia, F. Mantovani and R. Vannucci, "Geo-neutrinos, mantle circulation and silicate earth," arXiv:hep-ph/0401085.

[65] P. Jain, J. P. Ralston and G. M. Frichter, "Neutrino absorption tomography of the Earth's interior using isotropic ultra-high energy flux," Astropart. Phys. **12** (1999) 193 [arXiv:hep-ph/9902206].

M. Lindner, T. Ohlsson, R. Tomas and W. Winter, "Tomography of the earth's core using supernova neutrinos," Astropart. Phys. **19** (2003) 755 [arXiv:hep-ph/0207238].

T. Ohlsson and W. Winter, "Reconstruction of the earth's matter density profile using a single neutrino baseline," Phys. Lett. B **512** (2001) 357 [arXiv:hep-ph/0105293].

M. M. Reynoso and O. A. Sampayo, "On neutrino absorption tomography of the earth," arXiv:hep-ph/0401102.

[66] A. Datta, R. Gandhi, P. Mehta and S. U. Sankar, "Atmospheric neutrinos as a probe of CPT and Lorentz violation," arXiv:hep-ph/0312027.

S. Choubey and S. F. King, "Electrophobic Lorentz invariance violation for neutrinos and the see-saw mechanism," arXiv:hep-ph/0311326.

V. A. Kostelecky and M. Mewes, "Lorentz and CPT violation in neutrinos," arXiv:hep-ph/0309025.

[67] For introductions and specific points, see:

S. M. Bilenky and C. Giunti, "Sterile neutrinos?," arXiv:hep-ph/9905246.

M. Patel and G. M. Fuller, "What are sterile neutrinos good for?," arXiv:hep-ph/0003034.

R. R. Volkas, "Introduction to sterile neutrinos," Prog. Part. Nucl. Phys. **48** (2002) 161 [arXiv:hep-ph/0111326].

[68] B. Pontecorvo, "Neutrino Experiments And The Question Of Leptonic-Charge Conservation," Sov. Phys. JETP **26** (1968) 984 [Zh. Eksp. Teor. Fiz. **53** (1967) 1717].

[69] A. Kusenko, "Explanations of pulsar velocities," arXiv:astro-ph/9903167.

[70] See for instance: X. d. Shi and G. M. Fuller, "A new dark matter candidate: Non-thermal sterile neutrinos," Phys. Rev. Lett. **82** (1999) 2832 [arXiv:astro-ph/9810076].

[71] R. N. Mohapatra and D. W. Sciama, "Diffuse ionization in the Milky Way and sterile neutrinos," arXiv:hep-ph/9811446.

[72] G. C. McLaughlin, J. M. Fetter, A. B. Balantekin and G. M. Fuller, "An Active-Sterile Neutrino Transformation Solution for r-Process Nucleosynthesis," Phys. Rev. C **59** (1999) 2873 [arXiv:astro-ph/9902106].

[73] P. C. de Holanda and A. Y. Smirnov, "Homestake result, sterile neutrinos and low energy solar neutrino experiments," arXiv:hep-ph/0307266.

[74] C. Giunti, "Last CPT-invariant hope for LSND neutrino oscillations," Mod. Phys. Lett. A **18** (2003) 1179 [arXiv:hep-ph/0302173].

1.3: The role of Supernovæ

[75] For general reviews and extensive references, see for instance:

G.G.Raffelt, " Stars and as laboratories for fundamental physics", Chicago Univ.Press, Chicago, 1996;

[76] See also:

H.A.Bethe, "Supernova Mechanisms," Rev. Mod. Phys. **62** (1990) 801;

J.M.Lattimer, in "Nuclear Equation of State", ed. A. Ansari and L. Satpathy (World Scientific, Singapore), pp. 83-208 (1996);

M.Prakash, J.M.Lattimer, J.A.Pons, A.W.Steiner and S.Reddy, "Evolution of a Neutron Star From its Birth to Old Age," Lect. Notes Phys. **578** (2001) 364 [arXiv:astro-ph/0012136];

H.T.Janka, K.Kifonidis and M.Rampp, "Supernova explosions and neutron star formation," Lect. Notes Phys. **578** (2001) 333 [arXiv:astro-ph/0103015];

G.G.Raffelt, "Particle physics from stars," Ann. Rev. Nucl. Part. Sci. **49** (1999) 163 [arXiv:hep-ph/9903472].

G. G. Raffelt, "Physics with supernovae," Nucl. Phys. Proc. Suppl. **110** (2002) 254 [arXiv:hep-ph/0201099].

[77] S. Yamada, H-Th. Janka and H. Suzuki, " Neutrino transport in type II supernovae: Boltzmann solver vs. Monte Carlo method", A.& A. **344** (1999) 533-550 [arXiv:astro-ph/9809009];

M. Rampp and H. T. Janka, "Spherically symmetric simulation with Boltzmann neutrino transport of core collapse and post-bounce evolution of a 15 solar mass star," Astrophys. J. **539** (2000) L33 [arXiv:astro-ph/0005438];

A. Mezzacappa, M. Liebendorfer, O. E. Messer, W. R. Hix, F. K. Thielemann and S. W. Bruenn, "The Simulation of a Spherically Symmetric Supernova of a 13 Solar Mass Star with Boltzmann Neutrino Transport, and Its Implications for the Supernova Mechanism," Phys. Rev. Lett. **86** (2001) 1935 [arXiv:astro-ph/0005366];

M. Liebendorfer, A. Mezzacappa, F. K. Thielemann, O. E. Messer, W. R. Hix and S. W. Bruenn, "Probing the gravitational well: No supernova explosion in spherical symmetry with general relativistic Boltzmann neutrino transport," Phys. Rev. D **63** (2001) 103004 [arXiv:astro-ph/0006418].

[78] M. Rampp, E. Mueller and M. Ruffert, "Simulations of non-axisymmetric rotational core collapse," A.& A. **332** (1998) 969-983 [arXiv:astro-ph/9711122].

[79] For example, convective motions have been considered in M. Herant, W. Benz, W. R. Hix, C. L. Fryer and S. A. Colgate, "Inside the supernova: A Powerful convective engine," Astrophys. J. **435** (1994) 339 [arXiv:astro-ph/9404024];

A. Burrows, J. Hayes and B. A. Fryxell, "On the nature of core collapse supernova explosions," Astrophys. J. **450** (1995) 830 [arXiv:astro-ph/9506061];

rotation in R. Mönchmeyer, G. Schaefer, E. Mueller and R. E. Kates, "Gravitational waves from the collapse of rotating stellar cores", A.& A. **246** (1991) 417-440;

rotation and magnetic fields in J. M. Leblanc and J. R. Wilson, "A Numerical Example of the Collapse of a Rotating Magnetized Star", Astrophys. J. **450** (1995) 830.

[80] See, for example, polarization spectrometry results in D. C. Leonard, A. V. Filippenko, D. R. Ardila and M. S. Brotherton, "Is it Round? Spectropolarimetry of the Type II-P Supernova 1999em," Astrophys. J. **553** (2001) 861 [arXiv:astro-ph/0009285];

L. Wang, D. A. Howell, P. Höflich, and J. C. Wheeler, "Bipolar Supernova Explosion," Astrophys. J. **550** (2001) 1030.

[81] A. Mezzacappa, M. Liebendorfer, O. E. Messer, W. R. Hix, F. K. Thielemann and S. W. Bruenn, "The Simulation of a Spherically Symmetric Supernova of a 13 Solar Mass Star with Boltzmann Neutrino Transport, and Its Implications for the Supernova Mechanism," Phys. Rev. Lett. **86** (2001) 1935 [arXiv:astro-ph/0005366];

A. Burrows, T. Young, P. Pinto, R. Eastman and T. Thompson, "Supernova neutrinos and a new algorithm for neutrino transport," arXiv:astro-ph/9905132;

G. G. Raffelt, "Mu- And Tau-Neutrino Spectra Formation In Supernovae," Astrophys. J. **561** (2001) 890;

M. T. Keil, G. G. Raffelt and H. T. Janka, "Monte Carlo study of supernova neutrino spectra formation," arXiv:astro-ph/0208035.

[82] see M. T. Keil, G. G. Raffelt and H. T. Janka in [81].

[83] A. Y. Smirnov, D. N. Spergel and J. N. Bahcall, "Is Large Lepton Mixing Excluded?," Phys. Rev. D **49** (1994) 1389 [arXiv:hep-ph/9305204];

B. Jegerlehner, F. Neubig and G. Raffelt, "Neutrino Oscillations and the Supernova 1987A Signal," Phys. Rev. D **54** (1996) 1194 [arXiv:astro-ph/9601111];

A. S. Dighe and A. Y. Smirnov, "Identifying the neutrino mass spectrum from the neutrino burst from a supernova," Phys. Rev. D **62** (2000) 033007 [arXiv:hep-ph/9907423];

M. Kachelriess, R. Tomas and J. W. Valle, "Large lepton mixing and supernova 1987A," JHEP **0101** (2001) 030 [arXiv:hep-ph/0012134];

M. Kachelriess, A. Strumia, R. Tomas and J. W. Valle, "SN1987A and the status of oscillation solutions to the solar neutrino problem," Phys. Rev. D **65** (2002) 073016 [arXiv:hep-ph/0108100];

C. Lunardini and A. Y. Smirnov, "Supernova neutrinos: Earth matter effects and neutrino mass spectrum," Nucl. Phys. B **616** (2001) 307 [arXiv:hep-ph/0106149].

[84] E. K. Akhmedov, C. Lunardini and A. Y. Smirnov, "Supernova neutrinos: Difference of nu/mu - nu/tau fluxes and conversion effects," Nucl. Phys. B **643** (2002) 339 [arXiv:hep-ph/0204091].

[85] K. Hirata *et al.* [KAMIOKANDE-II Collaboration], "Observation Of A Neutrino Burst From The Supernova Sn1987a," Phys. Rev. Lett. **58** (1987) 1490;

R. M. Bionta *et al.*, "Observation Of A Neutrino Burst In Coincidence With Supernova Sn1987a In The Large Magellanic Cloud," Phys. Rev. Lett. **58** (1987) 1494.

[86] G. G. Raffelt, see the last reference of [76];

E. Cappellaro, R. Barbon and M. Turatto, "Supernova Statistics," arXiv:astro-ph/0310859, and references therein.

[87] E. N. Alekseev and L. N. Alekseeva, "Twenty Years Of Galactic Observations In Searching For Bursts Of Collapse Neutrinos With The Baksan Underground Scintillation Telescope," J. Exp. Theor. Phys. **95** (2002) 5 [Zh. Eksp. Teor. Fiz. **95** (2002) 10] [arXiv:astro-ph/0212499].

[88] M. Malek *et al.* [Super-Kamiokande Collaboration], "Search for supernova relic neutrinos at Super-Kamiokande," Phys. Rev. Lett. **90** (2003) 061101 [arXiv:hep-ex/0209028].

[89] L. E. Strigari, M. Kaplinghat, G. Steigman and T. P. Walker, "The supernova Relic neutrino backgrounds at KamLAND and Super-Kamiokande," arXiv:astro-ph/0312346.

[90] J. F. Beacom, W. M. Farr and P. Vogel, "Detection of supernova neutrinos by neutrino proton elastic scattering," Phys. Rev. D **66** (2002) 033001 [arXiv:hep-ph/0205220].

See also: J. F. Beacom, "Supernovae and neutrinos," Nucl. Phys. Proc. Suppl. **118** (2003) 307 [arXiv:astro-ph/0209136], and references therein.

[91] F. Cei, "Neutrinos from supernovae: Experimental status and perspectives," Int. J. Mod. Phys. A **17** (2002) 1765 [arXiv:hep-ex/0202043], and all references therein.

[92] J. F. Beacom and P. Vogel, "Mass signature of supernova nu/mu and nu/tau neutrinos in SuperKamiokande," Phys. Rev. D **58** (1998) 053010 [arXiv:hep-ph/9802424].

[93] A. Bandyopadhyay, S. Choubey, S. Goswami and K. Kar, "Prospects of probing theta(13) and neutrino mass hierarchy by supernova neutrinos in KamLAND," arXiv:hep-ph/0312315.

[94] J. F. Beacom and P. Vogel, "Mass signature of supernova nu/mu and nu/tau neutrinos in the Sudbury neutrino observatory," Phys. Rev. D **58** (1998) 093012 [arXiv:hep-ph/9806311].

[95] M. Aglietta *et al.*, "Effects of neutrino oscillations on the supernova signal in LVD," Nucl. Phys. Proc. Suppl. **110** (2002) 410 [arXiv:astro-ph/0112312].

M. Aglietta *et al.* [LVD Collaboration], "Study of the effect of neutrino oscillation on the supernova neutrino signal with the LVD detector," arXiv:hep-ph/0307287.

[96] L. Cadonati, F. P. Calaprice and M. C. Chen, "Supernova neutrino detection in Borexino," Astropart. Phys. **16** (2002) 361 [arXiv:hep-ph/0012082].

[97] See: http://www.physics.ohio-state.edu/OMNIS .

P. F. Smith, "Omnis: An Improved Low Cost Detector To Measure Mass And Mixing Of Mu Tau Neutrinos From A Galactic Supernova," Astropart. Phys. **8** (1997) 27.

P. F. Smith, "Further Studies Of The Omnis Supernova Neutrino Observatory: Optimisation Of Detector Configuration And Possible Extension To Solar Neutrinos," Astropart. Phys. **16** (2001) 75.

R. N. Boyd, A. S. J. Murphy and R. L. Talaga, "OMNIS, The Observatory for multiflavor neutrinos from supernovae," Nucl. Phys. A **718** (2003) 222.

[98] . Arneodo *et al.* [ICARUS collaboration], "The ICARUS experiment, a second-generation proton decay experiment and neutrino observatory at the Gran Sasso Laboratory," arXiv:hep-ex/0103008.

F. Cavanna, M. L. Costantini, O. Palamara and F. Vissani, "Neutrinos as astrophysical probes," arXiv:astro-ph/0311256.

[99] D. B. Cline, F. Sergiampietri, J. G. Learned and K. McDonald, "LANNDD: A massive liquid argon detector for proton decay, supernova and solar neutrino studies, and a neutrino factory detector," Nucl. Instrum. Meth. A **503** (2003) 136 [arXiv:astro-ph/0105442].

[100] C. J. Horowitz, K. J. Coakley and D. N. McKinsey, "Supernova observation via neutrino nucleus elastic scattering in the CLEAN detector," Phys. Rev. D **68** (2003) 023005 [arXiv:astro-ph/0302071].

[101] F. Halzen, J. E. Jacobsen and E. Zas, "Possibility That High-Energy Neutrino Telescopes Could Detect Supernovae," Phys. Rev. D **49** (1994) 1758.

[102] A. S. Dighe, M. T. Keil and G. G. Raffelt, "Detecting the neutrino mass hierarchy with a supernova at IceCube," JCAP **0306** (2003) 005 [arXiv:hep-ph/0303210].

[103] R. Tomas, D. Semikoz, G. G. Raffelt, M. Kachelriess and A. S. Dighe, "Supernova pointing with low- and high-energy neutrino detectors," Phys. Rev. D **68** (2003) 093013 [arXiv:hep-ph/0307050].

[104] M. K. Sharp, J. F. Beacom and J. A. Formaggio, Phys. Rev. D **66** (2002) 013012 [arXiv:hep-ph/0205035].

[105] E. K. Akhmedov and T. Fukuyama, "Supernova prompt neutronization neutrinos and neutrino magnetic moments," JCAP **0312** (2003) 007 [arXiv:hep-ph/0310119].

[106] C. Lunardini and A. Y. Smirnov, "Probing the neutrino mass hierarchy and the 13-mixing with supernovae," JCAP **0306** (2003) 009 [arXiv:hep-ph/0302033].

[107] A. S. Dighe, M. T. Keil and G. G. Raffelt, "Detecting the neutrino mass hierarchy with a supernova at IceCube," JCAP **0306** (2003) 005 [arXiv:hep-ph/0303210].

[108] A. S. Dighe, M. T. Keil and G. G. Raffelt, "Identifying earth matter effects on supernova neutrinos at a single detector," JCAP **0306** (2003) 006 [arXiv:hep-ph/0304150].

[109] A. S. Dighe, M. Kachelriess, G. G. Raffelt and R. Tomas, "Signatures of supernova neutrino oscillations in the earth mantle and core," arXiv:hep-ph/0311172.

[110] R. C. Schirato, G. M. Fuller, (. U. (. LANL), UCSD and LANL), "Connection between supernova shocks, flavor transformation, and the neutrino signal," arXiv:astro-ph/0205390.

1.4: The role of the Early Universe

[111] For general reviews and extensive references on the role of neutrinos in cosmology see for instance [112, 113, 114]

[112] A. D. Dolgov, "Neutrinos in cosmology," Phys. Rept. **370** (2002) 333 [arXiv:hep-ph/0202122].

[113] S. Sarkar, "Neutrinos from the big bang," arXiv:hep-ph/0302175.

[114] E. W. Kolb and M. S. Turner, "The Early Universe," Addison-Wesley Publishing Company, Chicago, 1994

[115] For general reviews of BBN see for instance [114, 116].

[116] V. Mukhanov, "Nucleosynthesis Without a Computer," arXiv:astro-ph/0303073.

[117] L. Kawano, "Let's go: Early universe. 2. Primordial nucleosynthesis: The Computer way," FERMILAB-PUB-92-004-A

[118] A. Cuoco, F. Iocco, G. Mangano, G. Miele, O. Pisanti and P. D. Serpico, "Present status of primordial nucleosynthesis after WMAP: results from a new BBN code," arXiv:astro-ph/0307213.

[119] P. Di Bari, "Update on neutrino mixing in the early universe," Phys. Rev. D **65** (2002) 043509 [Addendum-ibid. D **67** (2003) 127301] [arXiv:hep-ph/0108182].

P. Di Bari, "Addendum to: Update on neutrino mixing in the early universe," Phys. Rev. D **67** (2003) 127301 [arXiv:astro-ph/0302433].

[120] G. Mangano, G. Miele, S. Pastor and M. Peloso, "A precision calculation of the effective number of cosmological neutrinos," Phys. Lett. B **534** (2002) 8 [arXiv:astro-ph/0111408].

[121] R. E. Lopez and M. S. Turner, "An accurate calculation of the big-bang prediction for the abundance of primordial helium," Phys. Rev. D **59** (1999) 103502 [arXiv:astro-ph/9807279].

[122] B. E. J. Pagel, E. A. Simonson, R. J. Terlevich and M. G. Edmunds, "The Primordial Helium Abundance From Observations Of Extragalactic H-Ii Regions," Mon. Not. Roy. Astron. Soc. **255** (1992) 325.

[123] K. A. Olive and G. Steigman, "On the abundance of primordial helium," Astrophys. J. Suppl. **97** (1995) 49 [arXiv:astro-ph/9405022].

[124] Y. I. Izotov and T. X. Thuan, "The Primordial Abundance Of 4-He Revisited," Astrophys. J. **500** (1998) 188.

[125] K. A. Olive, E. Skillman and G. Steigman, "The Primordial Abundance of He4: An Update," Astrophys. J. **483** (1997) 788 [arXiv:astro-ph/9611166].

[126] Y. I. Izotov, F. H. Chaffee, C. B. Foltz, R. F. Green, N. G. Guseva and T. X. Thuan, "Helium abundance in the most metal-deficient blue compact galaxies: I Zw 18 and SBS 0335-052," arXiv:astro-ph/9907228.

[127] T. X. Thuan and Y. I. Izotov, "Blue compact galaxies and the primordial 4Helium abundance," arXiv:astro-ph/0003234.

[128] M. Peimbert, A. Peimbert and M. T. Ruiz, "The Chemical Composition of the Small Magellanic Cloud H II Region NGC 346 and the Primordial Helium Abundance," arXiv:astro-ph/0003154.

[129] A. Peimbert, M. Peimbert and V. Luridiana, "Temperature Bias and the Primordial Helium Abundance Determination," arXiv:astro-ph/0107189.

[130] Y. I. Izotov and T. X. Thuan, "Systematic effects and a new determination of the primordial abundance of 4He and dY/dZ from observations of blue compact galaxies," arXiv:astro-ph/0310421.

[131] R. Trotta and S. H. Hansen, "Observing the helium abundance with CMB," arXiv:astro-ph/0306588.

[132] G. Huey, R. H. Cyburt and B. D. Wandelt, "Precision Primordial ^{4}He Measurement with CMB Experiments," arXiv:astro-ph/0307080.

[133] C. L. Bennett *et al.*, "First Year Wilkinson Microwave Anisotropy Probe (WMAP) Observations: Preliminary Maps and Basic Results," Astrophys. J. Suppl. **148** (2003) 1 [arXiv:astro-ph/0302207].

D. N. Spergel *et al.*, "First Year Wilkinson Microwave Anisotropy Probe (WMAP) Observations: Determination of Cosmological Parameters," Astrophys. J. Suppl. **148** (2003) 175 [arXiv:astro-ph/0302209].

[134] W. Hu, D. J. Eisenstein and M. Tegmark, "Weighing neutrinos with galaxy surveys," Phys. Rev. Lett. **80** (1998) 5255 [arXiv:astro-ph/9712057].

[135] O. Elgaroy and O. Lahav, "The role of priors in deriving upper limits on neutrino masses from the 2dFGRS and WMAP," JCAP **0304** (2003) 004 [arXiv:astro-ph/0303089].

[136] D. J. Eisenstein, W. Hu and M. Tegmark, Astrophys. J. **518** (1998) 2 [arXiv:astro-ph/9807130].

[137] O. Elgaroy *et al.*, "A new limit on the total neutrino mass from the 2dF galaxy redshift survey," Phys. Rev. Lett. **89** (2002) 061301 [arXiv:astro-ph/0204152].

[138] S. Hannestad, "Cosmological limit on the neutrino mass," Phys. Rev. D **66** (2002) 125011 [arXiv:astro-ph/0205223].

[139] M. Tegmark *et al.* [SDSS Collaboration], "Cosmological parameters from SDSS and WMAP," arXiv:astro-ph/0310723.

[140] V. Barger, D. Marfatia and A. Tregre, "Neutrino mass limits from SDSS, 2dFGRS and WMAP," arXiv:hep-ph/0312065.

[141] R. A. C. Croft, W. Hu and R. Dave, "Cosmological limits on the neutrino mass from the Ly alpha forest," Phys. Rev. Lett. **83** (1999) 1092 [arXiv:astro-ph/9903335].

[142] V. Barger, J. P. Kneller, H. S. Lee, D. Marfatia and G. Steigman, "Effective number of neutrinos and baryon asymmetry from BBN and WMAP," Phys. Lett. B **566** (2003) 8 [arXiv:hep-ph/0305075].

[143] P. Crotty, J. Lesgourgues and S. Pastor, "Measuring the cosmological background of relativistic particles with WMAP," Phys. Rev. D **67** (2003) 123005 [arXiv:astro-ph/0302337].

S. Hannestad, "Neutrino masses and the number of neutrino species from WMAP and 2dFGRS," JCAP **0305** (2003) 004 [arXiv:astro-ph/0303076].

E. Pierpaoli, "Constraints on the cosmic neutrino background," Mon. Not. Roy. Astron. Soc. **342** (2003) L63 [arXiv:astro-ph/0302465].

V. Barger *et al.* in [142]

[144] S. Hannestad in [143]

[145] A. Pierce and H. Murayama, "WMAPping out neutrino masses," Phys. Lett. B **581** (2004) 218 [arXiv:hep-ph/0302131].

[146] R. H. Cyburt, B. D. Fields and K. A. Olive, "Primordial Nucleosynthesis in Light of WMAP," Phys. Lett. B **567** (2003) 227 [arXiv:astro-ph/0302431].

Bibliography for Chapter 2: A (4D) sterile neutrino

[147] A. Strumia in [55]. Other authors finally agree that '2+2' oscillations are no longer viable, see e.g. M. Maltoni, T. Schwetz, M. A. Tortola and J. W. F. Valle, "Ruling out four-neutrino oscillation interpretations of the LSND anomaly?," Nucl. Phys. B **643** (2002) 321 [arXiv:hep-ph/0207157]. However some controversy remains, see e.g. R. Foot, "Are four neutrino models ruled out?," Mod. Phys. Lett. A **18** (2003) 2079 [arXiv:hep-ph/0210393]. and H. Paes, L. g. Song and T. J. Weiler, "The hidden sterile neutrino and the (2+2) sum rule," Phys. Rev. D **67** (2003) 073019 [arXiv:hep-ph/0209373]. Exclusion of '2+2' oscillations follows from global fits, not directly from a few simple measurements.

[148] The original studies on the subject are

R. Barbieri and A. Dolgov, "Bounds On Sterile-Neutrinos From Nucleosynthesis," Phys. Lett. B **237** (1990) 440.

R. Barbieri and A. Dolgov, "Neutrino Oscillations In The Early Universe," Nucl. Phys. B **349** (1991) 743.

X. Shi, D. N. Schramm and B. D. Fields, "Constraints on neutrino oscillations from big bang nucleosynthesis," Phys. Rev. D **48** (1993) 2563 [arXiv:astro-ph/9307027].

and [150]

[149] B. H. J. McKellar and M. J. Thomson, "Oscillating Doublet Neutrinos In The Early Universe," Phys. Rev. D **49** (1994) 2710.

[150] K. Enqvist, K. Kainulainen and M. J. Thomson, "Stringent Cosmological Bounds On Inert Neutrino Mixing," Nucl. Phys. B **373** (1992) 498.

[151] D. Notzold and G. Raffelt, "Neutrino Dispersion At Finite Temperature And Density," Nucl. Phys. B **307** (1988) 924.

[152] S. Weinberg, "Gravitation and Cosmology, Principles and Applications of the General Theory of Relativity", Wiley Text Books; July 1972

[153] S. Esposito, G. Mangano, G. Miele and O. Pisanti, "Precision rates for nucleon weak interactions in primordial nucleosynthesis and He-4 abundance," Nucl. Phys. B **540** (1999) 3 [arXiv:astro-ph/9808196].

[154] T. A. Thompson, A. Burrows and P. A. Pinto, "Shock breakout in core-collapse supernovae and its neutrino signature," Astrophys. J. **592** (2003) 434 [arXiv:astro-ph/0211194].

[155] K. Takahashi, K. Sato, A. Burrows and T. A. Thompson, "Supernova neutrinos, neutrino oscillations, and the mass of the progenitor star," Phys. Rev. D **68** (2003) 113009 [arXiv:hep-ph/0306056].

[156] An original study of the subject is in

H. Nunokawa, J. T. Peltoniemi, A. Rossi and J. W. Valle, "Supernova bounds on resonant active-sterile neutrino conversions," Phys. Rev. D **56** (1997) 1704 [arXiv:hep-ph/9702372].

See also

A. D. Dolgov, S. H. Hansen, G. Raffelt and D. V. Semikoz, "Cosmological and astrophysical bounds on a heavy sterile neutrino and the KARMEN anomaly," Nucl. Phys. B **580** (2000) 331 [arXiv:hep-ph/0002223].

Bibliography for Chapter 3: Neutrinos in Extra Dimensions

[157] K.R.Dienes, E.Dudas and T.Gherghetta, "Light neutrinos without heavy mass scales: A higher-dimensional seesaw mechanism," Nucl. Phys. B **557** (1999) 25 [arXiv:hep-ph/9811428];

N.Arkani-Hamed, S.Dimopoulos, G.R.Dvali and J.March-Russell, "Neutrino masses from large extra dimensions," Phys. Rev. D **65** (2002) 024032 [arXiv:hep-ph/9811448];

G.R.Dvali and A.Y.Smirnov, "Probing large extra dimensions with neutrinos," Nucl. Phys. B **563** (1999) 63 [arXiv:hep-ph/9904211].

[158] A.Lukas, P.Ramond, A.Romanino and G.G.Ross, "Solar neutrino oscillation from large extra dimensions," Phys. Lett. B **495** (2000) 136 [arXiv:hep-ph/0008049].

A.E.Faraggi and M.Pospelov, "Phenomenological issues in TeV scale gravity with light neutrino masses," Phys. Lett. B **458** (1999) 237 [arXiv:hep-ph/9901299];

A.K.Das and O.C.Kong, "On neutrino masses and mixings from extra dimensions," Phys. Lett. B **470** (1999) 149 [arXiv:hep-ph/9907272].

R.N.Mohapatra, S.Nandi and A.Perez-Lorenzana, "Neutrino masses and oscillations in models with large extra dimensions," Phys. Lett. B **466** (1999) 115 [arXiv:hep-ph/9907520];

A.Ioannisian and A.Pilaftsis, "Cumulative non-decoupling effects of Kaluza-Klein neutrinos in electroweak processes," Phys. Rev. D **62** (2000) 066001 [arXiv:hep-ph/9907522];

A.Lukas and A.Romanino, "A brane-world explanation of the KARMEN anomaly," arXiv:hep-ph/0004130;

K.R.Dienes and I.Sarcevic, "Neutrino flavor oscillations without flavor mixing angles," Phys. Lett. B **500** (2001) 133 [arXiv:hep-ph/0008144];

A.Lukas, P.Ramond, A.Romanino and G.G.Ross, "Brane-Bulk Neutrino Oscillations," Int. J. Mod. Phys. A **16S1C** (2001) 934;

N.Cosme, J.M.Frere, Y.Gouverneur, F.S.Ling, D.Monderen and V.Van Elewyck, "Neutrino suppression and extra dimensions: A minimal model," Phys. Rev. D **63** (2001) 113018 [arXiv:hep-ph/0010192].

D.O.Caldwell, R.N.Mohapatra and S.J.Yellin, "Large extra dimensions, sterile neutrinos and solar neutrino data," Phys. Rev. Lett. **87** (2001) 041601 [arXiv:hep-ph/0010353];

C.S.Lam and J.N.Ng, "Neutrino oscillations via the bulk," Phys. Rev. D **64** (2001) 113006 [arXiv:hep-ph/0104129].

A.S.Dighe and A.S.Joshipura, "Neutrino anomalies and large extra dimensions," Phys. Rev. D **64** (2001) 073012 [arXiv:hep-ph/0105288];

A.De Gouvea, G.F.Giudice, A.Strumia and K.Tobe, "Phenomenological implications of neutrinos in extra dimensions," Nucl. Phys. B **623** (2002) 395 [arXiv:hep-ph/0107156];

H.Davoudiasl, P.Langacker and M.Perelstein, "Constraints on large extra dimensions from neutrino oscillation experiments," Phys. Rev. D **65** (2002) 105015 [arXiv:hep-ph/0201128].

[159] A. Lukas, P. Ramond, A. Romanino and G. G. Ross, "Solar neutrino oscillation from large extra dimensions," Phys. Lett. B **495** (2000) 136 [arXiv:hep-ph/0008049].

[160] A. Lukas, P. Ramond, A. Romanino and G. G. Ross, "Neutrino masses and mixing in brane-world theories," JHEP **0104** (2001) 010 [arXiv:hep-ph/0011295].

[161] R. Barbieri, P. Creminelli and A. Strumia, "Neutrino oscillations from large extra dimensions," Nucl. Phys. B **585** (2000) 28 [arXiv:hep-ph/0002199].

[162] N.Arkani-Hamed, S.Dimopoulos and G.R.Dvali, "Phenomenology, astrophysics and cosmology of theories with sub-millimeter dimensions and TeV scale quantum gravity," Phys. Rev. D **59** (1999) 086004 [arXiv:hep-ph/9807344];

S.Cullen and M.Perelstein, "SN1987A constraints on large compact dimensions," Phys. Rev. Lett. **83** (1999) 268 [arXiv:hep-ph/9903422];

C.Hanhart, D.R.Phillips, S.Reddy and M.J.Savage, "Extra dimensions, SN1987a, and nucleon nucleon scattering data," Nucl. Phys. B **595** (2001) 335 [arXiv:nucl-th/0007016];

C.Hanhart, J.A.Pons, D.R.Phillips and S.Reddy, "The likelihood of GODs' existence: Improving the SN 1987a constraint on the size of large compact dimensions," Phys. Lett. B **509** (2001) 1 [arXiv:astro-ph/0102063];

L.J.Hall and D.R.Smith, "Cosmological constraints on theories with large extra dimensions," Phys. Rev. D **60** (1999) 085008 [arXiv:hep-ph/9904267];

S.Hannestad, "Strong constraint on large extra dimensions from cosmology," Phys. Rev. D **64** (2001) 023515 [arXiv:hep-ph/0102290];

S.Hannestad and G.Raffelt, "New supernova limit on large extra dimensions," Phys. Rev. Lett. **87** (2001) 051301 [arXiv:hep-ph/0103201];

S.Hannestad and G.G.Raffelt, "Stringent neutron-star limits on large extra dimensions," Phys. Rev. Lett. **88** (2002) 071301 [arXiv:hep-ph/0110067];

S.Hannestad and G.G.Raffelt, "Supernova and neutron-star limits on large extra dimensions reexamined," arXiv:hep-ph/0304029.

[163] F. J. Botella, C. S. Lim and W. J. Marciano, "Radiative Corrections To Neutrino Indices Of Refraction," Phys. Rev. D **35** (1987) 896.

S. Hannestad, H. T. Janka, G. G. Raffelt and G. Sigl, "Electron-, mu-, and tau-number conservation in a supernova core," Phys. Rev. D **62** (2000) 093021 [arXiv:astro-ph/9912242].

[164] A. Burrows, T. J. Mazurek, J. M. Lattimer, "The deleptonization and heating of proton-neutron stars," Astrophys. J. **251** (1981) 325;

A. Burrows and J. M. Lattimer, "The Birth Of Neutron Stars," Astrophys. J. **307** (1986) 178.

[165] S. Reddy, M. Prakash and J. M. Lattimer, "Neutrino interactions in hot and dense matter," Phys. Rev. D **58** (1998) 013009 [arXiv:astro-ph/9710115].

[166] W. Keil and H. T. Janka, "Hadronic Phase Transitions At Supranuclear Densities And The Delayed Collapse Of Newly Formed Neutron Stars," Astron. Astrophys. **296** (1995) 145;

K. Sumiyoshi, H. Suzuki and H. Toki, "Influence of the symmetry energy on the birth of neutron stars and supernova neutrinos," Astron. Astrophys. **303** (1995) 475 [arXiv:astro-ph/9506024];

J. A. Pons, S. Reddy, M. Prakash, J. M. Lattimer and J. A. Miralles, "Evolution of protoneutron stars," Astrophys. J. **513** (1999) 780 [arXiv:astro-ph/9807040].

[167] See, for instance: M. Apollonio *et al.*, arXiv:hep-ph/0210192.